Dissertation

submitted to the

Combined Faculty of Natural Sciences and Mathematics

of the Ruperto Carola University Heidelberg, Germany

for the degree of

Doctor of Natural Sciences

Presented by

M.Sc. Christiane Linda Ebelt

Born in: Dresden

Oral examination: 05.05.2020

Light-induced multi-site phosphorylation attenuates the activity of White Collar Complex

Referees: Prof. Dr. Michael Brunner

Prof. Dr. Walter Nickel

Zusammenfassung

Der White Collar Complex (WCC) ist ein Transkriptionsfaktor und Lichtrezeptor, bestehend aus zwei Untereinheiten. Nur White Collar-1 (WC-1) hat eine Lichtrezeptordomäne, aber sowohl WC-1 als auch White Collar-2 (WC-2) haben Zinkfinger-DNA-Bindungsdomänen. In der negativen Rückkopplungsschleife der circadianen Uhr von *Neurospora crassa* ist WCC das positive Element, welches die Uhr aktiviert und sie mit dem externen Tag-Nacht-Rhythmus synchronisiert. Entsprechend dieser beiden Funktionen gibt es zwei Gruppen von Zielgenen, die *clock-controlled genes* (ccgs) und die *light-inducible genes*. Die zweite Gruppe wird durch Bindung des Licht-aktivierten WCC (L-WCC) aktiviert. FREQUENCY (FRQ) ist ein Zielgen von WCC und ist das negative Element in der Rückkopplungsschleife der circadianen Uhr von *N. crassa*. FRQ rekrutiert Casein Kinase 1a (CK1a), um WCC durch Phosphorylierung zu inaktivieren. Diese circadiane Phosphorylierung stabilisiert WCC aber auch, so dass FRQ den WCC negativ und positiv beeinflusst. Die Licht-induzierte Aktivität von L-WCC wird auch durch Phosphorylierung reguliert, der Mechanismus dieser Licht-induzierten Phosphorylierung ist Gegenstand dieser Arbeit.

Es wurde gezeigt, dass L-WCC aus zwei Molekülen WC-1 und zwei Molekülen WC-2 besteht. In dieser Arbeit wurden 34 Phosphorylierungsstellen von WC-1 (27 neu) und 23 Stellen von WC-2 (22 neu) bestimmt. Weder in einer Proteindomäne, noch Licht- oder Dunkel-spezifisch wurde Phosphorylierung gefunden. Wahrscheinlich gibt es im Dunkeln eine Menge gering und verschieden phosphorylierter WCC Moleküle und Licht verstärkt die Phosphorylierung jedes Moleküls. Die Suche nach Kinasen ergab, dass FRQ die Licht-induzierte Phosphorylierung von WCC durch CK1a vermittelt, die Aktivität weiterer Kinasen wird vermutet. Die Mutation von Phosphorylierungsstellen von WC-2 zeigte eine graduelle Reduktion der transkriptionellen Aktivität von WCC, die regulatorische Kompensation von WC-1 und WC-2 und deutet die Gleichheit der circadianen und der Licht-aktivierten Phosphorylierung an. Von Prolin gefolgte Phosphorylierungsstellen sind auf WCC überrepräsentiert und wurden als ein Auslöser für FRQ-vermittelte Phosphorylierung identifiziert. Weitere Auslöser von Phosphorylierung sind DNA-Bindung und wahrscheinlich Licht-induzierte Dimerisierung von WCC. Die Bindung an die DNA bringt WCC in die Nähe der Prolin-gerichteten Kinasen der Transkriptionsmaschinerie (TM). Es wurde die Hypothese aufgestellt, dass die TM an aktivem WCC ein Signal für weitere, Aktivitäts-mindernde, FRQ-vermittelte Phosphorylierung setzt.
Eine kürzliche publizierte Studie der circadianen Phosphorylierung von WCC bestätigt größtenteils die hier gezeigten Ergebnisse und findet auch, aber thematisiert nicht, die Prolin-gerichtete Phosphorylierung. Diese ist auch auf CLOCK, dem WCC Ortholog in *Drosophila melanogaster*, überrepräsentiert, was die Hypothese eines Feedbacks der TM auf WCC weiter unterstützt.

Summary

The White Collar Complex (WCC) is a transcription factor and light receptor formed by two subunits. Only White Collar-1 (WC-1) has a light receptor domain but both WC-1 and White Collar-2 (WC-2) have zinc finger DNA binding domains. In the negative feedback loop of the circadian clock in *Neurospora crassa*, WCC is the positive element that drives the clock and synchronizes it with the external cycle of day and night. According to these two functions, there are two groups of target genes, the *clock-controlled genes* (*ccgs*) and the *light-inducible genes*. The latter subset is activated by binding of the light-activated WCC (L-WCC). FREQUENCY (FRQ) is a target of WCC and is the negative element in the feedback loop of the circadian clock in *N. crassa*. FRQ recruits Casein Kinase 1a (CK1a) to inactivate WCC by phosphorylation. This circadian phosphorylation also stabilizes WCC, so the feedback of FRQ on WCC is both negative and positive. The light-induced activity of L-WCC is regulated by phosphorylation as well, the mechanism of this light-induced phosphorylation is the subject of this study.

L-WCC was proven to consist of two molecules WC-1 and two molecules WC-2. In this work, 34 phosphorylation sites of WC-1 (27 new) and 23 sites of WC-2 (22 new) have been determined. Neither phosphorylation of a protein domain, nor light- or dark-specific phosphorylation were found. There seems to be a pool of poorly and differently phosphorylated WCC molecules in the dark, and light increases the phosphorylation of each molecule. The search for kinase(s) revealed that FRQ also mediates the light-induced phosphorylation of WCC by CK1a and the activity of other kinases is presumed. Phosphorylation site mutants of WC-2 revealed a gradual reduction of the transcriptional activity of WCC, a regulatory compensation of WC-1 and WC-2 and suggested identity of circadian and light-induced phosphorylation. Phosphorylation sites followed by proline are overrepresented on WCC and were shown to be a trigger for FRQ-mediated phosphorylation. Other triggers of phosphorylation of WCC are DNA-binding and most likely light-induced dimerization. DNA-binding brings WCC close to the proline-directed kinases of the transcriptional machinery (TM). It was hypothesized that the TM feeds back on the active WCC to mark it for subsequent, activity-attenuating, FRQ-mediated phosphorylation.

A recently published study of the circadian phosphorylation of WCC largely confirms these results but does not touch the topic of proline-directed phosphorylation although these sites are overrepresented in that study as well. Proline-directed phosphorylation is also overrepresented on CLOCK, the WCC ortholog in *Drosophila melanogaster*, further supporting the hypothesis of a feedback of the TM on WCC.

List of figures

List of tables

List of abbreviations

ΔFCD1+2	FRQ mutant that lacks the two FRQ-CK1a-interacting domains
6-PFK	6-Phosphofructokinase
acc. to	according to.
ADH	Alcohol Dehydrogenase
allA	WC-2 mutant, all phosphorylation sites found in this study mutated to Alanine (A)
allD	WC-2 mutant, all phosphorylation sites found in this study mutated to Aspartate (D)
approx.	approximately
APS	Ammonium persulfate
bHLH	basic helix-loop-helix, a DNA binding domain
BMAL1	Brain and Muscle ARNT-Like 1; ARNT = Aryl hydrocarbon receptor nuclear translocator; mammalian protein
CaM	Calmodulin
CAMK-1	Calcium/calmodulin-dependent protein kinase type 1
CDK7; 8; 9	Cyclin-dependent kinase 7; 8; 9
ChIP	Chromatin Immunoprecipitation
CK1a; ε	Casein Kinase 1a; ε
CK2	Casein kinase 2
CLK	CLOCK, Circadian locomotor output cycles kaput; *Drosophila melanogaster* protein
CLOCK	Circadian locomotor output cycles kaput; mammalian protein
CRY	Cryptochrome; mammalian protein
CTD	C-terminal domain of RNA Polymerase II
CYC	CYCLE; *Drosophila melanogaster* protein
DBD	defective in DNA binding, protein domain
DBT	DOUBLE-TIME, a homolog of mammalian CK1ε; *Drosophila melanogaster* protein
DD	Constant darkness, growth condition
Denat.	denaturing
D. melanogaster	*Drosophila melanogaster*
DOC	Sodium deoxycholate
DSIF	DRB sensitivity-inducing factor (DRB = 5,6-dichloro-1-β-D-ribofuranosylbenzimidazole, transcription elongation inhibitor)
DTT	Dithiothreitol
D-WCC	Dark-WCC, monomer, one WC-1 and one WC-2
E. coli	*Escherichia coli*
ESI	Electronspray injection
FFC	FRQ - FRH complex; *Neurospora crassa* protein

FGSC	Fungal genetics stock center
FRH	FRQ-interacting RNA Helicase; *Neurospora crassa* protein
frq, FRQ	Frequency; *Neurospora crassa* protein
GSK-3	Glycogen-synthase kinase 3
HAT	Histone Acetyl Transferase
HDAC	Histone Deacetylase
het	heterokaryon
HRP	horseradish peroxidase
IgG	Immunoglobulin G
IP	Immunoprecipitation
KO	Knock out
LDS	lithium dodecyl sulfate
LI	Light induction = switch on the light in the incubator after cultivation for defined duration in constant darkness
LL	Constant light, growth condition
LOV	Light-Oxygen-Voltage domain
LP	Light pulse = switch on the light for a short time (e.g. 1 min) in the incubator after cultivation for defined duration in constant darkness
LRE	light-responsive element
L-WCC	Light-activated White Collar Complex, dimer of two WC-1 and two WC-2
Lysine-5	Homocitrate synthase
MAPK-1; -2	Mitogen-activated protein kinase-1; -2
MDK-1	Mitotic division kinase-1
MS	Mass spectrometry
N. crassa	*Neurospora crassa*
NCU	Numbering system for *Neurospora crassa* genes
NELF	Negative elongation factor
NLS	Nuclear localization signal
N-Medium	Standard growth medium for *N. crassa*
o/n	Over night
ORF	Open reading frame
PAS	Per-Arnt-Sim; protein domain
PER	PERIOD; *D. melanogaster* and mammalian protein
PEX	Protein extraction
PKA	Protein kinase A
PKC	Protein kinase C
PMSF	Phenylmethylsulfonylfluorid
RNAP II S5-P	Phosphorylation at serine 5 residues in the CTD of RNAP II
polyQ	Glutamine-rich region of a protein
PP1, 2A; 4	Protein phosphatase 1; 2A; 4

PRD-4	*Neurospora* homolog of checkpoint kinase-2
prk-3	Serine-/Threonine protein kinase-3
P-TEFb	Positive transcription elongation factor b
qa	Quinic acid
qPCR	Real time quantitative PCR
qrf	Antisense *frq* mRNA
RACK1	Receptor for activated C kinase–1
RCM-1	Regulator of conidiation and morphology-1
RCO-1	Regulator of conidiation-1
RNAP II	RNA Polymerase II
rt	Room temperature
SDS-PAGE	Sodium dodecyl sulfate polyacrylamide gel electrophoresis
SDS-PAGE	sodium dodecyl sulfate–polyacrylamide gel electrophoresis
SGG	Shaggy, ortholog of GSK3; *Drosophila melanogaster* protein
ssi	single spore isolate
stk-1; 8	Serine/threonine protein kinase -1; -8
STPK47	Serine/threonine protein kinase-47
sWC-2	Short WC-2, N-terminally truncated protein due to a start codon within the ORF
SWI/SNF	SWItch/Sucrose Non-Fermentable
TAP	Tandem affinity purification
TCA	Trichloroacetic acid
TCA-DOC	Trichloroacetic acid, deoxycholate
TEV protease	Tobacco Etch Virus (TEV) Protease
TIM	Timeless, *Drosophila melanogaster* protein
TM	Transcriptional machinery
TX	Total protein extract
w/v	Weight per volume
wc-1 / WC-1; -2	White Collar 1, 2; gene and protein
WCC	White Collar Complex; *Neurospora crassa* protein
WT	Wild type
ZnF	Zinc finger DNA binding domain
λ	Lambda phosphatase

Content

1. Introduction

In this PhD project, the filamentous fungus *Neurospora crassa* is used to study the regulation of the synchronization of the intracellular circadian rhythm with the environmental rhythm of day and night. The following chapters highlight the importance of clock research, introduce to the circadian clock of *Neurospora crassa* and introduce the details required to describe the results of this research project.

1.1. Biological rhythms and the circadian clock

In 2017, the Nobel Prize in Physiology or Medicine was awarded to Jeffrey C. Hall, Michael Rosbash and Michael W. Young "for their discoveries of molecular mechanisms controlling the circadian rhythm" (The 2017 Nobel Prize in Physiology or Medicine Press Release). This highlights the importance of research on biological rhythms. “Circadian” is derived from “circa” and “dies”, the Latin words for “about a day”. The “circadian rhythm” or the “circadian clock” describes the rhythmic behavior and physiology of organisms that is observed over the course of a day (24 h). The research of the past decades has shown that organisms do not simply react to the environmental changes caused by the earth rotation. An internal rhythm with a period of approximately 24 h enables organisms to anticipate environmental changes. The advantage of a circadian clock is obvious because it has evolved across almost all kingdoms: in prokaryotic cyanobacteria, in plants, in fungi an in animals (Kondo *et al.*, 1993 (cyanobacteria), Buenning, 1935 (plants), Pittendrigh *et al.*, 1959 (fungi), Konopka and Benzer, 1971 (insects), Vitaterna *et al.*, 1994 (mouse), Aschoff, 1965 (human)).

Understanding the circadian clock is crucial since it is an important factor of human health. Defects of the human circadian clock as well as desynchrony of the internal rhythms of the human body caused by, for example, shift work, lead to severe injury to health (Dagan, 2002, Parry, 2002, Roenneberg and Merrow, 2016). Emerging from circadian clock research, the field of chronopharmaceutics makes drugs more effective and reduces side effects by taking the rhythm of physiological and pathophysiological processes into account (Ohdo *et al.*, 2011).

Understanding the circadian clock is also crucial since it helps to understand biological rhythms in general. Numerous natural processes are rhythmic in various shapes and sizes. Organisms have evolved strategies to anticipate various geophysical cycles like day and night, the seasons, the tides. Biological rhythms longer than one day (24 h) are called infradian rhythms. One example is the menstrual cycle in higher primates of about 25 to 35 days. Even longer are circannual cycles like hibernation and leaf fall in autumn. Biological rhythms shorter than one day are called ultradian rhythms. The sleep phases of humans are a prominent example for such short rhythms (Kishi *et al.*, 2018).

Among the various biological rhythms, the circadian clock ranges somewhere in between on the timescale and is characterized by three key features (Pittendrigh, 1960):

Maintenance of the internal oscillation in the absence of external cues. If an organism is kept under constant conditions without temporal information for several days, the internal rhythm keeps oscillating with an amplitude close to 24 h. Interestingly, the endogenous, self-sustaining rhythm generator oscillates with an amplitude larger or shorter, but not exactly 24h.

Synchronization with the environmental rhythms. The internal clock is synchronized with the environment by receiving external temporal information. Over the course of the day, light and temperature are changing. Thus, these two factors are called *zeitgebers* (German for "time giver") and can reset the circadian clock. Because the length of day and night are changing over the course of year, it is important for an organism to adjust the internal clock every day (Aschoff, 1954).

Temperature compensation. While (bio-)chemical processes are temperature-dependent, the circadian clock runs robustly and accurately over a wide range of physiological temperatures, in cold winter as well as very hot summer. Temperature changes over the course of a year as well as over the course of a day are compensated by the circadian clock.

1.2. *Neurospora crassa*, a model organism for the circadian clock

The filamentous fungus *Neurospora crassa* is a model organism used in various fields of biology, including circadian biology, because it is a simple eukaryote having a close evolutionary relatedness to animals (Stechmann and Cavalier-Smith, 2003). In contrast to model organisms like *Escherichia coli* and *Saccharomyces cerevisiae*, *N. crassa* allows the investigation of complex biological processes and the transfer of these findings on higher eukaryotic organisms (Roche *et al.*, 2014). The physiology and taxonomic description of *Neurospora* species is investigated since the 19th century (Perkins, 1992), and Beadle and Tatum demonstrated the one gene - one enzyme - hypothesis in *N. crassa* (Beadle and Tatum, 1941). In the 1950s, Pittendrigh and colleagues established *N. crassa* as model organism for clock research. It was shown that the developmental patterning of asexual conidiation seen when *N. crassa* grew over an agar surface (an observable change in morphology, see Figure 1.1) followed a rhythm that meets the criteria of a circadian clock (Pittendrigh *et al.*, 1959).

N. crassa is a haploid fungus that can grow and propagate asexually or via a sexual cycle. The heterothallic, haploid culture of *N. crassa* is not able to enter the sexual cycle. But *N. crassa* occurs as two mating types and crosses of the two opposing mating types can reproduce sexually. The asexual developmental cycle results in the production of macroconidiophores (conidia); the sexual cycle yields ascospores. Both processes are regulated by the circadian clock (Bobrowicz *et al.*, 2002). When *N. crassa* is grown in constant darkness, the rhythm of conidiation keeps running with an internal period of ~22,5 h that differs slightly from 24 h (Pittendrigh *et al.*, 1959; Ryan *et al.*, 1943). This finding met the first key feature of a circadian clock, the **internal oscillator**.

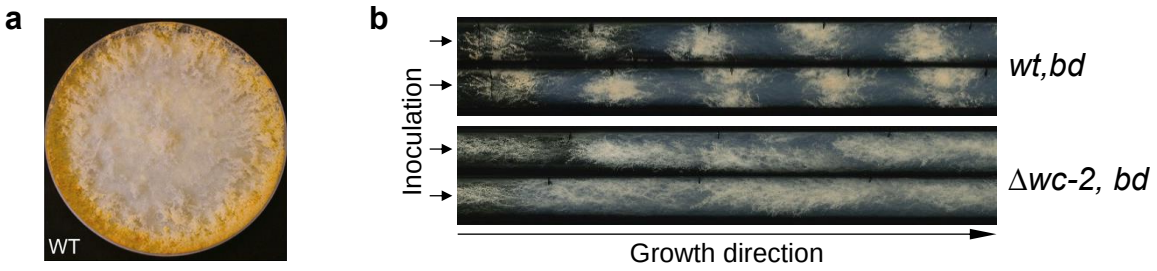

Figure 1.1: Growth pattern of *Neurospora crassa*.
1.1a: *N. crassa* wild type (*wt*) strain grown on a petri dish. The typical orange color origins from the synthesis of carotenoids (Roche *et al.*, 2014). **1.1b**: Patterning of the asexual conidiation when Neurospora crassa *bd* strains grow through a glass tube from left to right. The *bd* (*band*) genetic background of *N. crassa* refers to ras^{bd} mutation that allows growth of *N. crassa* strains under the conditions in small glass tubes (Belden, Larrondo *et al.*, 2007). The upper two lanes show the typical banding pattern of the *wt, bd* strain that is caused by the rhythmic change in morphology. In contrast to that, the clock mutant strain Δ*wc-2, bd* does not show a rhythmic banding pattern. (Experiment performed and picture taken by Linda Ebelt in 2016).

The first clock-mutant strains of *N. crassa* identified in the early 1970s the gene frequency (*frq*) as one of the main clock components in *N. crassa* (Feldman and Hoyle, 1973). Molecular analysis of the *Neurospora* clock was initiated shortly after that of *Drosophila* in the mid-1980s, and numerous clock-controlled genes (*ccgs*) were identified by global screening (Loros *et al.*, 1989). Later, a protein complex named White Collar Complex was discovered to be the blue light receptor that synchronizes the *N. crassa* circadian clock with the environment, meeting the second key feature of a circadian clock, the **synchronization with the environmental rhythms** (Ballario *et al.*, 1996; Ballario *et al.*, 1998; Linden and Macino, 1997). Besides being a blue light receptor, WCC is also required for the expression of *frq* in dark. The discovery of FRQ and of WCC with its light and its dark function revealed the basis of the molecular clock in *N. crassa* (Aronson *et al.*, 1994, Crosthwaite *et al.*, 1997).
The robustness of the *N. crassa* circadian clock over a wide range of physiological temperatures represents the third key feature of a circadian clock, the **temperature compensation** (Aronson *et al.*, 1994).

1.3. The circadian clock in *Neurospora crassa*

The basic structure of any molecular circadian clock comprises the input, the central oscillator and the output of the clock (see Figure 1.2). The input of the clock transfers information like light, temperature and also information about the metabolic status of the organism to the central oscillator to align (synchronize) the endogenous clock with the environment or other intracellular processes (reviewed in Baker *et al.*, 2012; Sancar and Brunner, 2014). The main input to the central oscillator of *N. crassa* is blue light sensed by WCC. A unique feature of the *N. crassa* circadian clock is that WCC represents both the blue light receptor and an element of the central oscillator (see Figure 1.2). In contrast to higher eukaryotes, there is no light input pathway feeding the light signal to the central

oscillator. In *N. crassa*, genes encoding for red light photoreceptors were found but these genes are not involved in any of the known photo responses of *N. crassa* (Borkovich *et al.*, 2004; Froehlich *et al.*, 2005; Galagan *et al.*, 2003). The function of these red light receptors remains unknown and WCC is so far the only known photoreceptor in *N. crassa* that has impact on the circadian clock.

Genes controlled by the circadian clock are referred to as clock-controlled genes (*ccgs*) and can be roughly clustered in primary *ccgs* that are direct targets of WCC and secondary *ccgs* that are indirectly regulated by WCC (see Figure 1.2; Loros *et al.*, 1989). Up to 40% of the *N. crassa* transcriptome were found to be under control of the circadian clock. The functional classification of primary and secondary *ccgs* revealed a clock-controlled temporal separation of physiological processes. The morning and the daytime are dominated by catabolic processes, the evening is dominated by anabolic processes (Hurley *et al.*, 2014; Sancar *et al.*, 2015). WCC was found to control ~20% of all annotated *N. crassa* transcription factors in response to light, revealing a flat hierarchical network (Smith *et al.*, 2010).

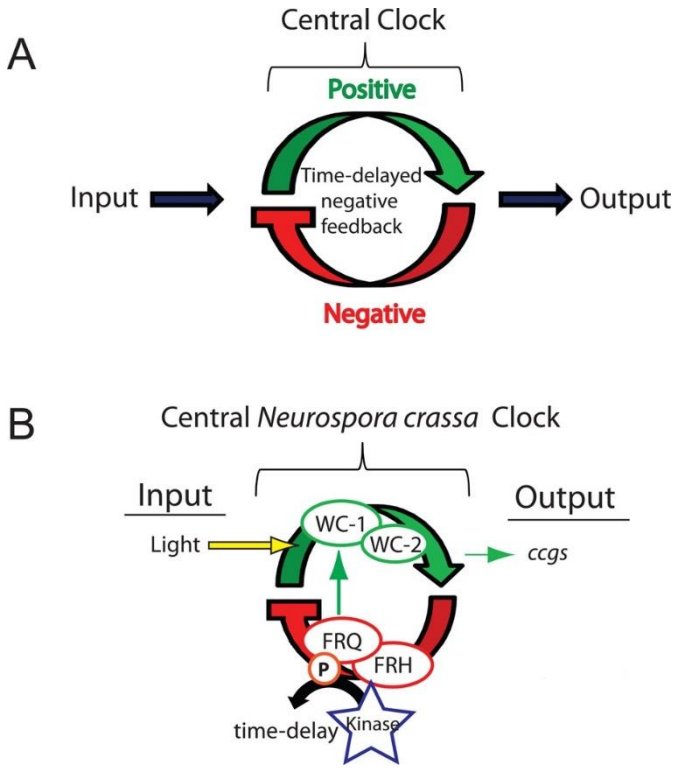

Figure 1.2: The circadian clock of *N. crassa*.
1.2A: The basic structure a molecular circadian clock comprises the input, the central oscillator and the output of the clock. The central oscillator (clock) is made up of a transcriptional / translational negative feedback loop. Together, the positive and the negative arm of the feedback loop create a time-delay that defines the circadian oscillation. **1.2B**: In *N. crassa*, the main input to the central oscillator is blue light. The positive element in the central clock of *N. crassa* is WCC, a transcription factor and blue light sensor. WCC also drives the output of the central oscillator, the expression of clock-controlled genes (*ccgs*). The negative element in the central clock of *N. crassa* is FRQ, whose expression is activated by WCC. FRQ forms a complex with FRH and Kinases and exerts both a negative and a positive feedback on WCC. The gradual phosphorylation of FRQ is the main pacemaker of the circadian clock of *N. crassa* (Figure modified acc. to Baker *et al.*, 2012).

As conserved principle of endogenous circadian clocks, the central oscillator in *N. crassa* is a transcriptional / translational negative feedback loop. In this feedback loop, a positive element drives the activation of the negative element that feeds back on the positive element to stop its own activation. The exciting question of clock research was (and still is) how interaction of molecules and biochemical reaction can create a defined time delay and a robust oscillation with a period of approximately 24 hrs. The positive element in *N. crassa* is WCC, the transcription factor that drives the expression of clock-controlled genes and especially the expression of *frq*. FRQ protein represents the negative element in the *N. crassa* central oscillator.

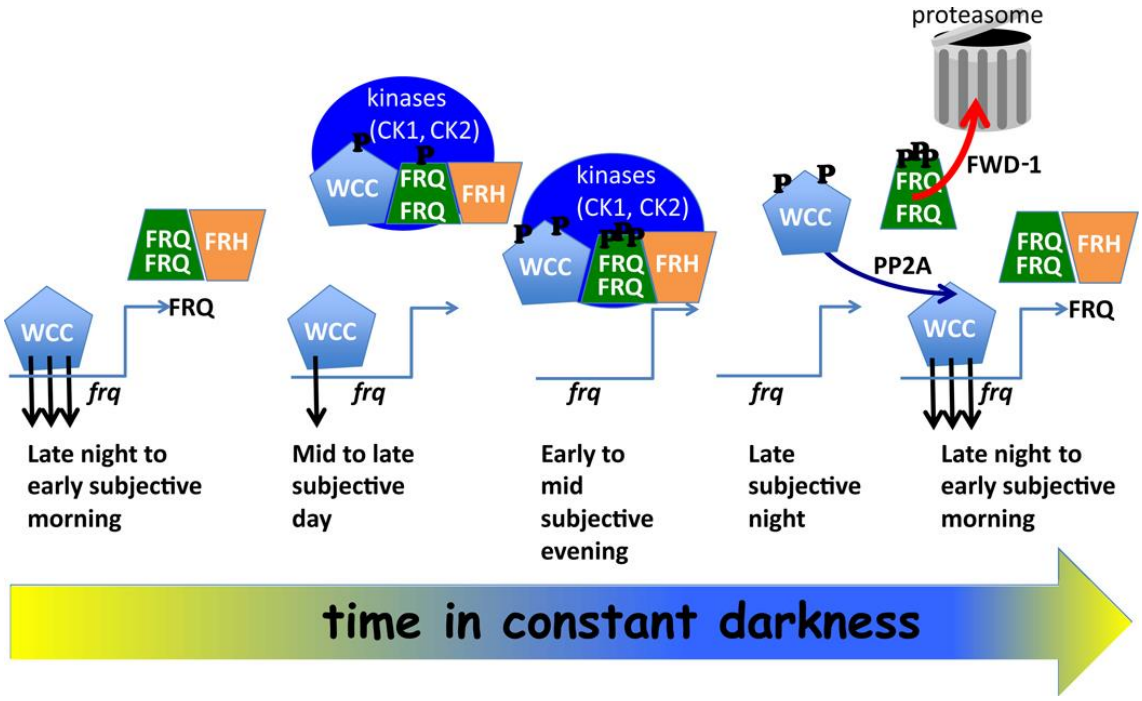

Figure 1.3: Molecular mechanism of the circadian clock in *N. crassa*.
When *N. crassa* is grown in constant darkness and in constant temperature, the intracellular clock keeps oscillating at an internal rhythm of about a day. The subjective daytime is illustrated by yellow and blue, representing the day and the night. WCC binds to the *frq* promoter and initiates the expression of FRQ. FRQ mediates the phosphorylation of both WCC and FRQ over the course of a circadian day. Phosphorylation inactivates but also stabilizes WCC. Phosphorylation of FRQ releases the negative feedback of FRQ on WCC and allows the start of the next cycle of transcription and translation (Figure from Baker *et al.*, 2012).

FRQ dimerizes and the FRQ-dimer forms a complex with the stabilizing FRQ-interacting RNA Helicase (FRH) and the kinase CK1a (see Figure 1.2). This FRQ/FRH complex (FFC) with CK1a interacts with WCC and inactivates it by phosphorylation to stop the expression of *frq* and subsequently the synthesis of FRQ. In the FFC complex, FRQ itself is phosphorylated successively and increasing phosphorylation of FRQ releases the negative feedback on WCC. Phosphorylation of FRQ leads to ubiquitination and degradation of FRQ (see Figure 1.3; reviewed in Baker *et al.*, 2012). However, the phosphorylation of FRQ is not just a simple tag for degradation, it is a complex mechanism that creates an hourglass-like, successive modulation of protein-protein interaction and protein conformation. There is evidence that degradation of

hyperphosphorylated FRQ is not required to maintain the circadian oscillation (Larrondo *et al.*, 2015). Furthermore, the cycles of WCC activation and inactivation, *frq* expression and FRQ synthesis alone do not set the period of approximately 24 hrs. The pacemaker of the *N. crassa* circadian clock, that determines the time constant of the feedback loop, is the time-of-day-specific phosphorylation of FRQ in the FRQ/FRH/CK1 complex on up to >85 phosphorylation sites (Baker *et al.*, 2009; Tang *et al.*, 2009; reviewed in Baker *et al.*, 2012).

Besides the negative feedback of FRQ on WCC, FRQ also exerts a positive feedback on WCC that is important for the restart of the transcription / translation cycle. Active, hypophosphorylated WCC is instable but the inactive, hyperphosphorylated WCC is not degraded and accumulates instead. Thus, FRQ-mediated, inactivating phosphorylation of WCC creates a pool of inactive WCC that can be dephosphorylated by phosphatases to become available for the next cycle of gene expression (reviewed in Baker *et al.*, 2012).

1.4. FRQ, the pacemaker of the circadian clock

The negative element and pacemaker of the circadian clock in *N. crassa*, FRQ, is an intrinsically disordered 108 kDa protein that requires the interaction with FRH to stabilize its conformation (FRQ/FRH complex, FFC). FRQ is highly regulated at the transcriptional, posttranscriptional, translational and posttranslational level, a glimpse on the complex regulation was outlined in the previous chapter (reviewed in Baker *et al.*, 2012). The most important and intensively investigated regulatory modification of FRQ is the phosphorylation. FRQ, embedded in FFC, is phosphorylated in clusters, there is no specific phosphorylation event acting as the switch that starts or stops any specific action (Baker *et al.*, 2009). Numerous kinases and phosphatases were found to have a direct effect on the phosphorylation status of FRQ: CK1a, CK2, PRD-4, CAMK-1, PKA, PP1, PP2a, PP4 (reviewed in Baker *et al.*, 2012; Diernfellner and Schafmeier, 2011). The most important kinase is CK1a that interacts tightly with FFC (Baker *et al.*, 2009; Gorl *et al.*, 2001; He *et al.*, 2006; Querfurth *et al.*, 2007). FRQ interacts with CK1a through the FRQ-CK1a-interacting domains (FCD1 and FCD2, see Figure 1.4). This interaction is required for the phosphorylation of FRQ by CK1a but it also brings CK1a close to WCC to mediate the phosphorylation of WCC by CK1a (He *et al.*, 2006; described in the following chapters).

The transcription of *frq* is activated by WCC and is a complex issue since *frq* represents one of the most complex loci known in microbes (see Figure 1.4; reviewed in Dunlap and Loros, 2006). There are binding sites for WCC both upstream and downstream of the *frq* ORF. To initiate transcription of *frq sense* mRNA, WCC binds in the *frq* promoter region to two distinct cis-acting sequences termed the clock box (c-box) and the proximal light-regulated element (PLRE) (Froehlich *et al.*, 2002; Froehlich *et al.*, 2003). The c-box is required for the rhythmic expression of FRQ over the course of a day. The PLRE is required for the light-induced expression of FRQ to synchronize the endogenous

oscillator with the environment. The molecular mechanisms of the circadian- and the light-activity of WCC are outlined in the following chapters.

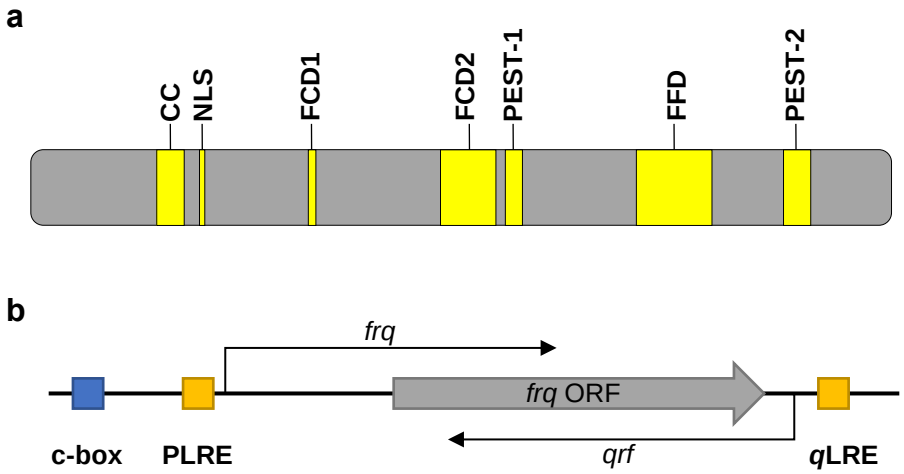

Figure 1.4: Protein structure of FRQ and gene locus of *frq*.
1.4a: Domain structure of the 989 aa protein FRQ (Figure acc. to Baker *et al.*, 2009; Querfurth *et al.*, 2011). **1.4b**: The frq locus and its regulatory elements. The clock box (c-box) and the proximal light-regulated element (PLRE) are binding sites of WCC to initiate *frq sense (frq)* transcription. The antisense light-regulated element (qLRE) is the binding site for WCC to initiate the transcription of *frq antisense (qrf)* (Figure acc. to Xue *et al.*, 2014; Cesbron *et al.*, 2015).

The *frq* expression is also regulated by the transcription of the long non-coding *frq* antisense RNA termed *qrf* (see Figure 1.4). The transcription of *qrf* is initiated by WCC in a light-dependent manner from an LRE (another than PLRE) in the *qrf* antisense promoter and comprises the full *frq* ORF in reverse direction. The levels of *frq* and *qrf* oscillate in antiphase and the expression of *frq* inhibits the expression of *qrf* and vice versa. This mutual inhibition is most likely mediated by chromatin modifications and premature termination of transcription and it forms a double-negative feedback loop that is interlocked with the core feedback loop. The expression of *qrf* is required for robust and sustained circadian rhythmicity (Xue *et al.*, 2014).

1.5. WCC, the activator of the circadian clock

The White Collar Complex (WCC) is a heterodimer of the two proteins White Collar 1 (127 kDa) and White Collar 2 (57 kDa). Both proteins were identified as key elements of the *Neurospora* clock in the early 1980s (Degli-Innocenti and Russo, 1984; Harding and Turner, 1981). WC-1, the larger subunit of WCC, is characterized by two glutamine-riche regions, the blue-light sensing LOV (light-oxygen-voltage) domain, two PAS (Per-Arnt-Sim) domains, a DBD (defective in DNA binding) domain and a GATA-type zinc finger DNA binding domain (ZnF) (see Figure 1.5; see detailed description of the LOV domain in chapter 1.7; (Ballario *et al.*, 1996; Ballario *et al.*, 1998; Linden and Macino, 1997). WC-2, the smaller subunit of WCC, is characterized by a single PAS domain and a GATA-type zinc finger DNA binding domain (ZnF) but lacks a LOV domain for light-sensing (see Figure 1.5; Linden and Macino, 1997).

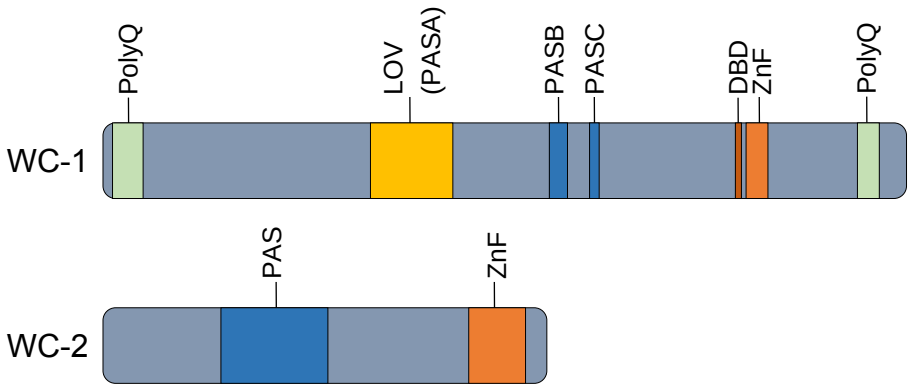

Figure 1.5: Domain structure of WC-1 and WC-2.
PolyQ = glutamine rich region. LOV (PASA) = light, oxygen, voltage domain. PASB, C = Per-Arnt-Sim domain. DBD = defective in binding DNA. ZnF = GATA-type zinc finger DNA binding domain. (acc. to Castro *et al.*, 2006; Liu *et al.*, 2003; Wang *et al.*, 2015)

WC-1 and WC-2 are transcriptional activators and localize to the nucleus. But to date, a transactivation domain and a nuclear localization signal (NLS) are not known. Such domains were suggested but are still under debate (Wang *et al.*, 2015). The DBD of WC-1, a region that was suggested as NLS previously, was found to assist in DNA binding of WC-1 and to mediate interactions with FFC.

PAS proteins domains mediate protein-protein interaction and are conserved among core clock elements of other species (King *et al.*, 1997; Linden and Macino, 1997; Reddy *et al.*, 1984). The PAS domains of WC-1 and WC-2 interact to form the WCC and are likely involved in the interaction with FRQ. The interaction of WC-1 with WC-2 is essential for the stability of WC-1 and thus for the steady-state level of WC-1 and the proper function of WCC (Ballario *et al.*, 1998; Cheng *et al.*, 2002). The tight relationship of WC-1 and WC-2 is illustrated by the fact that knocking out either WC-1 or WC-2 fully abolishes the circadian clock of *N. crassa*.

In response to light, the LOV domain of WC-1 can dimerize with another LOV domain and form the light-induced WCC (L-WCC) (Froehlich *et al.*, 2002; He *et al.*, 2002). The light-dependent function of WCC will be outlined more detailed in the following chapter 1.7.

The ZnF of both WC-1 and WC-2 allows binding of WCC to target genes. The unique feature of the *N. crassa* WCC is to bear two different activities that are reflected in two different subsets of target genes (Cheng *et al.*, 2003; Collett *et al.*, 2002; He *et al.*, 2002):

The circadian activity of WCC. WCC protomers control the expression of clock-controlled genes by binding to a conserved DNA-binding motif, the clock box (c-box). For example, the clock-controlled gene *frq* is activated by binding of a WCC protomer to the *frq* clock box (see chapter 1.4; Froehlich *et al.*, 2003). The circadian activity, especially the expression of *frq*, of WCC drives the circadian clock of *N. crassa* and is independent of the WC-1 LOV domain (see Figure 1.6).

The light-dependent activity of WCC. The homodimer L-WCC consists of two WC-1 molecules but the number of WC-2 molecules in L-WCC is still under debate (Malzahn

et al., 2010; Wang *et al.*, 2015). The L-WCC controls the expression of light-inducible genes, e.g. *frq*. Light-dependent transcription of *frq* is activated by binding of a WCC protomer to the *frq* PLRE and represents the synchronization of the *N. crassa* circadian clock with the environment. The name White Collar is derived from the white color of WC-1 or WC-2 mutants. Some of the light-inducible target genes of WCC are the *albino* (*al*) genes that code for enzymes of the carotenoid pigment synthesis pathway. If the blue light reception of WC-1 is impaired either by knock out, mutation or instability in the absence of WC-2 or if DNA binding of L-WCC is impaired, the expression of albino genes and the production of orange carotenoids are abolished (see Figure 1.6; (Chen *et al.*, 2009; Harding and Turner, 1981).

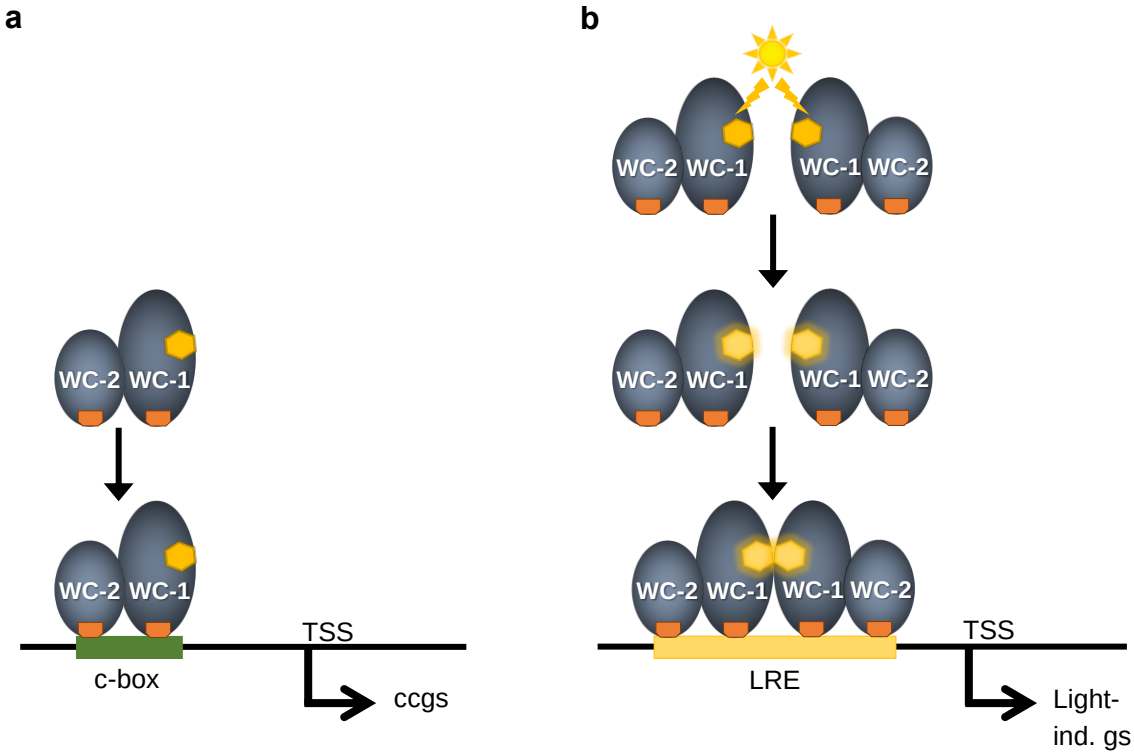

Figure 1.6: The circadian vs. the light-induced activity of WCC.
1.6a: A WCC protomer consisting of one molecule WC-1 and one molecule WC-2 binds to the c-box in the promoter region of clock-controlled genes (*ccgs*) and actives transcription (ZnF DNA binding domains shown in orange). **1.6b**: When the LOV domain (yellow hexagon) of WC-1 receives blue light, molecular rearrangements allow the dimerization of two LOV domains and thus the formation of light-induced WCC (L-WCC). Here, L-WCC is shown as dimer of two WCC protomers (see text for number of molecules in L-WCC). Only L-WCC, not two single WCC protomers can activate the transcription of light-inducible genes. Most likely, the sum of all interactions including the LOV-LOV interaction is required to stabilize binding to DNA and to allow recruitment of the transcriptional machinery. (Figure 1.6 was designed based on the references mentioned in chapter 1.5)

The molecular base of these two different activities of WCC are different functions of the ZnF domains of WC-1 and WC-2. DNA-binding of the light-induced WCC requires mainly the ZnF of WC-2, whereas DNA-binding for circadian functions (= "driving the inner rhythm") requires both the ZnF of WC-2 and WC-1 (Cheng *et al.*, 2003; Wang *et al.*, 2015).

1.6. The circadian phosphorylation of WCC

Both WC-1 and WC-2 are phosphorylated in response to light (Schwerdtfeger and Linden, 2000; Talora *et al.*, 1999) as well as over the course of a circadian day (circadian phosphorylation) (Schafmeier *et al.*, 2005). In an initial study, the first 5 phosphorylation sites of WC-1 were mapped but no phosphorylation sites of WC-2 were identified (He *et al.*, 2005). These 5 phosphorylation sites were found to be involved in the circadian phosphorylation only. As an important key to the mechanism of the circadian clock, FRQ was found to mediate the circadian phosphorylation of WCC by CK1 and CK2 to inactivate the transcription factor (He *et al.*, 2006; Schafmeier *et al.*, 2005). As outlined in chapter 1.3, the inactivation of WCC by phosphorylation is both a negative and a positive feedback of FRQ on WCC (Schafmeier *et al.*, 2008). The kinases PKC, PKA, GSK3, CK1 and CK2 were shown to phosphorylate and inactivate WCC, the phosphatases PP4 and PP2A were found to antagonize the phosphorylation WCC (Cha *et al.*, 2008; Franchi *et al.*, 2005; He *et al.*, 2006; Huang *et al.*, 2007; Schafmeier *et al.*, 2008; Tataroglu *et al.*, 2012). At the beginning of the experimental work for this thesis, in total nine phosphorylation sites of WC-1 and one phosphorylation site of WC-2 were known (He *et al.*, 2005; Sancar *et al.*, 2009). After finishing experimental work for this thesis, 80 phosphorylation sites of WC-1 and 15 phosphorylation site of WC-2 were published by Wang *et al.*, 2019. Refer to chapter 4.1 for a detailed comparison and discussion of this study in the context of the results by Wang *et al.*, 2019. Taken together, the circadian phosphorylation of WCC is well understood. But only little is known about the light-induced phosphorylation that is described in the following chapter.

1.7. The light-induced phosphorylation of WCC

In contrast to the circadian phosphorylation, the light-induced phosphorylation of WCC occurs on a much shorter time scale. In response to light, WCC binds to target genes and increasing phosphorylation of both WC-1 and WC-2 is observed within a few minutes reaching a maximum hyperphosphorylation after approximately 30 min. Interestingly, the light-induced phosphorylation of WC-1 is transient whereas the light-induced phosphorylation of WC-2 is persistent. After about 120 min, WC-1 is hypo-phosphorylated again but does not reach the low level of phosphorylation as in the dark before the light induction (see Figure 1.7; Schwerdtfeger and Linden, 2000; Talora *et al.*, 1999). The time range of the light-induced phosphorylation roughly correlates with the light-induced activity of WCC and phosphorylation was shown to inhibit binding of WCC to target genes (He and Liu, 2005). In accordance with the inhibitory function, the light-induced phosphorylation occurs when WCC is localized in the nucleus and only functional WC-1 and WC-2 is phosphorylated (Schwerdtfeger and Linden, 2000). Furthermore, light-induced, hyperphosphorylated WC-1 is degraded within 120 min after light-induction (Talora *et al.*, 1999). But since the *wc-1* gene itself is a light-inducible gene under control of L-WCC, the degradation of hyperphosphorylated WCC is balanced with newly synthesized, hypophosphorylated WC-1 (Ballario *et al.*, 1996; Kaldi *et al.*, 2006).

The study of the circadian phosphorylation of WCC revealed hints that FRQ-dependent CK-1a and CK2 activity is also involved in the light-induced phosphorylation of WCC (He *et al.*, 2006).

The structural basis for light reception in *N. crassa* is the LOV (light-oxygen-voltage) domain of WC-1 (Ballario *et al.*, 1998; He *et al.*, 2002). LOV domains are a subgroup of PAS domains combining the receptor function for environmental cues like light, oxygen and voltage with a protein-protein interaction domain (Froehlich *et al.*, 2002). In WC-1, blue light is sensed by the formation of a covalent photoadduct between a cysteinyl residue and stoichiometrically bound FAD (flavin cofactor) (Froehlich *et al.*, 2002; Salomon *et al.*, 2000; Swartz *et al.*, 2001; Zoltowski *et al.*, 2007; Zoltowski *et al.*, 2009). The formation of the photoadduct causes a conformational movement of a helix that opens up an interface for the dimerization of two light-activated LOV domains (Corchnoy *et al.*, 2003; Harper *et al.*, 2003). L-WCC is formed by the dimerization of two WC-1 LOV domains and only homodimer L-WCC, not monomeric WCC can bind stably enough to the promoter sequences of light-inducible genes to initiate transcription (Malzahn *et al.*, 2010; Wang *et al.*, 2015). The structural and mechanistic details of L-WCC are the key to the complex regulation of the light-induced activity of WCC.

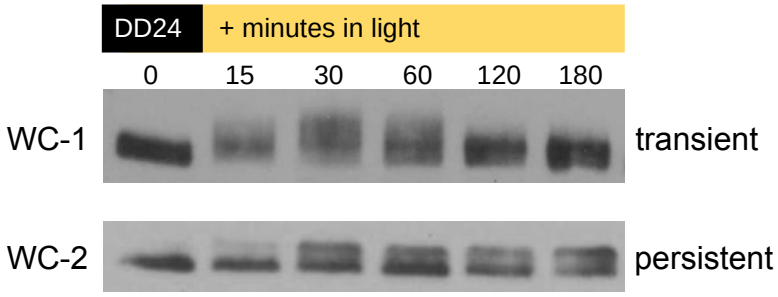

Figure 1.7: Western Blot of a light-induction experiment in a *N. crassa wild type* strain.
The first sample is taken in darkness after growing the culture for 24 h in dark (**DD24**). The culture is shifted to light and samples are taken at the time points indicated (**minutes in light**). Both WC-1 and WC-2 are hypophosphorylated after growth for 24 h in darkness. In response to light, WC-1 is phosphorylated transiently and the hyperphosphorylation appears as a broad smear in the Western Blot. The phosphorylation of WC-1 reaches a maximum after approx. 30 min of light induction and decreases to a minimum after 120 min of light-induction. However, the hypophosphorylation of WC-1 after 120 min of light induction is higher than at DD24. In contrast to WC-1, the light induced phosphorylation of WC-2 is persistent and appears as distinct band. But the timeframe of the phosphorylation of WC-2 equals WC-1, the maximum hyperphosphorylation of WC-2 is reached as well after 30 min of light induction. (Western Blot by Linda Ebelt, showing *N. crassa wt* strain. Experiment performed according to Schwerdtfeger and Linden, 2000; Talora *et al.*, 1999)

1.8. Regulation of the light-induced activity of WCC

Regulation of the light-induced transcription is ensured by several mechanisms. As outlined above, light-induced phosphorylation is most likely a negative regulator of L-WCC (He and Liu, 2005). Another possible mechanism, the decay of the FAD-Cysteine photoadduct, can be excluded since the photoadduct of WC-1 is extremely stable ($t_{½} \approx 4$ hr) (Malzahn *et al.*, 2010).

An important regulator of the light-induced transcription by WCC is the small protein VVD. L-WCC drives the expression of *vvd* by binding to the LRE in the *vvd* promoter.

In response to light, the expression of *vvd* increases dramatically. VVD is very short (21 kDa) and consists of a LOV domain very similar to the WC-1 LOV domain and an N-terminal cap (Heintzen *et al.*, 2001; Zoltowski *et al.*, 2007). Expressed and translated quickly upon illumination, blue light causes the same conformational change in the VVD LOV domain as in the WC-1 LOV domain yielding light-activated L-VVD (Schwerdtfeger and Linden, 2003; Zoltowski *et al.*, 2007). Located in the nucleus, L-VVD dimerizes with the light-activated WC-1 LOV domain and disrupts L-WCC homodimers (see Figure 1.8).

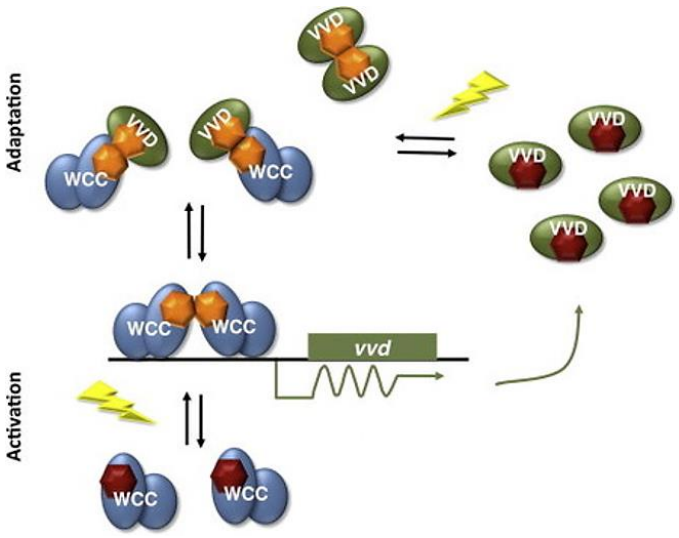

Figure 1.8: Mechanism of photoadaptation in *N. crassa*.
Blue light induces the dimerization of two LOV domains, in both WC-1 and in VVD. The dimerization of two WC-1 LOV domains forms the L-WCC that activates the rapid expression of VVD. Via its LOV domain, VVD forms homodimers with itself or heterodimers with light-induced WC-1. The formation of heterodimers disrupts L-WCC and thereby inactivates it. The amount of VVD expression depends on the amount of light-activated WCC which in turn depends on the light intensity. Thus, the light-induced VVD level is adapted for the light intensity and balances the amount of active L-WCC. (Figure modified acc. to Schafmeier and Diernfellner, 2011)

The competition of L-VVD/WCC dimerization with L-WCC homodimerization regulates the light-induced activity of WCC. The *vvd* promoter can respond to a huge range of light intensities since it is saturated at very high light intensities. Due to that feature of the *vvd* promoter, the amount of L-VVD correlates with the light intensity and subsequently the amount of L-WCC. Low levels of light activate low levels of WCC and only low levels of VVD are expressed (Chen *et al.*, 2010; Malzahn *et al.*, 2010). The correlation of L-VVD and L-WCC protein level is possible since the photoadduct of VVD is similar stable as the photoadduct of WCC (VVD: $t_{½} \approx 5$ hr) and re-activation of either VVD or WCC due to spontaneous photoadduct decay is excluded over several hours (Zoltowski *et al.*, 2009). For both VVD and WCC, the stability of the photoadduct and the stability of the WCC/WCC or WCC/VVD dimers should not be mistaken. The photoadducts of both WCC and VVD are very stable and allow dimerization of the respective LOV domains as long as the photoadduct lasts. The WCC/WCC or WCC/VVD dimers are not stable

and allow rapid exchange of the interaction partner, the basis for the competition of L-VVD with the L-WCC homodimerization (Dasgupta *et al.*, 2015; Zoltowski *et al.*, 2009). The negative feedback loop formed by L-WCC and VVD is named photoadaptation. On prolonged light exposure, the light response is attenuated depending on the previous intensity of light response. Following a light response, the system remains sensitive to escalating changes in light intensity. After dusk, an appropriate small pool of VVD remains that inactivates L-WCC caused by bright moon light or unusual light sources in the night to maintain the phase of the endogenous circadian clock. Taken together, the small protein VVD is essential for the photoadaptation in *N. crassa*, a process required for the correct assessment and deciphering of changes in light intensities (Chen *et al.*, 2010; Malzahn *et al.*, 2010).

Beside phosphorylation and VVD, the activity of the transcription factor WCC is regulated as well by the more general regulation of the chromatin structure on WCC target genes. Due to the high density of the eukaryotic nucleus, accessibility of genes interferes with dense packing of the DNA. Thus, chromatin structure and nucleosomes are a critical target of transcriptional regulation. The accessibility of genomic DNA for the RNA polymerase II is regulated by two major subclasses of chromatin-modifying enzymes, the ATP remodeling complexes and the HAT or HDAC complexes (reviewed in Narlikar *et al.*, 2002; reviewed in Flaus and Owen-Hughes, 2011). Studies in the past years have suggest circadian clock-specific roles for the ATP-dependent chromatin-remodeling enzymes CLOCKSWITCH (CSW-1) and SWI/SNF (Belden, Loros *et al.*, 2007; Wang *et al.*, 2014). Another study employed the light-induced activity of WCC as tool to study the refractoriness of promoters and suggested that refractory promoters carry a physical memory of their recent transcription history (Cesbron *et al.*, 2015).

1.9. Phosphorylation as general regulator of gene transcription

To unravel the mechanism of the phosphorylation of the transcription factor WCC, it is crucial to understand the details of the transcription factor activity and transcription initiation since phosphorylation is an important regulator of these processes. WCC belongs to the large group of gene-specific transcription factors that activate or repress transcription by affecting RNA Polymerase II (RNAP II) indirectly. Gene-specific transcription factors bind to factors that regulate RNAP II directly or indirectly like the Mediator complex or chromatin remodeling complexes (reviewed in Poss *et al.*, 2013).

The Mediator complex is a transcriptional coactivator that is globally required for initiation of gene expression. It is a large multi-unit protein complex that stabilizes the pre-initiation complex (PIC), facilitates transcription initiation and is involved in the regulation of elongation. The mediator complex is characterized by transience, by variability of the subunit composition and by a high degree of structural flexibility depending on the interaction partner. It is the main binding interface for gene-specific transcription factors that change the structure of the Mediator complex upon binding (see Figure 1.9). The “active” structural state of the Mediator complex facilitates transcription

initiation by stabilizing RNAP II orientation on the DNA within the PIC (reviewed in Poss *et al.*, 2013; El Khattabi *et al.*, 2019).

The PIC consists of RNAP II and the general transcription factors TFIIA, TFIIB, TFIID, TFIIE, TFIIF, and TFIIH. The assembly of the PIC at transcription start site (TSS) of the promoter is a well-orchestrated process and only a correctly assembled PIC can release RNAP II to elongation (see Figure 1.9; Schilbach *et al.*, 2017; reviewed in Harper and Taatjes, 2018).

Phosphorylation is an important regulatory tool to control different stages of gene transcription. The C-terminal domain (CTD) of RNAP II contains tandem hepta-peptide repeats of Y_1-S_2-P_3-T_4-S_5-P_6-S_7 that represent a platform for the integration of regulatory signals. Numerous factors from all stages of transcription and co-transcriptional processes apply post-translational modifications to RNAP II-CTD (reviewed in Shandilya and Roberts, 2012).

The Serine 5 (S5) residue of the RNAPII-CTD repeats is phosphorylated during PIC assembly by CDK7, a subunit of the general transcription factor TFIIH. The S5 phosphorylation is recognized by the capping enzyme and is the signal for the attachment of the methylguanosine cap to the 5′ end of the early, ~25 nucleotide, nascent mRNA. Since 5′ capping is the signal for productive transcription initiation, RNAPII-CTD S5 phosphorylation is a crucial signal for transcription initiation. Beside RNAPII-CTD S5, CDK7 subunit of TFIIH phosphorylates other targets as well. CDK7 also phosphorylates the S7 residue of the RNAPII-CTD repeats that plays a role in termination, 3′ processing and RNAPII-pausing. Furthermore, CDK7 is involved in the phosphorylation of TFIIB that is a trigger for productive initiation of transcription of several genes. Interestingly, some studies found CDK7 to be involved in the phosphorylation of gene-specific transcription factors (reviewed in Inamoto *et al.*, 1997; Ko *et al.*, 1997; Shandilya and Roberts, 2012). An important function of CDK7 is the phosphorylation and activation of CDK9, another major RNAPII-CTD kinase (reviewed in Rimel and Taatjes, 2018).

CDK9 is a subunit of the positive transcription elongation factor b (P-TEFb) and phosphorylates the Serine 2 (S2) residue of the RNAPII-CTD repeats. P-TEFb is a crucial factor for the initiation of productive elongation. S2 phosphorylation increases during RNAPII progression towards the 3′end of the gene and is accompanied by gradual dephosphorylation of S5 residues. This phospho-code in the RNAPII-CTD provides a platform for the docking of transcription-associated proteins and orchestrates the timing of their activity during the different stages of transcription. Additional to S2 phosphorylation, P-TEFb has a positive effect on elongation by mediating the inhibition of the negative elongation factors DSIF (DRB sensitivity-inducing factor) and NELF (negative elongation factor). These two proteins are also targets of CDK9 phosphorylation (reviewed in Bowman and Kelly, 2014; Shandilya and Roberts, 2012).

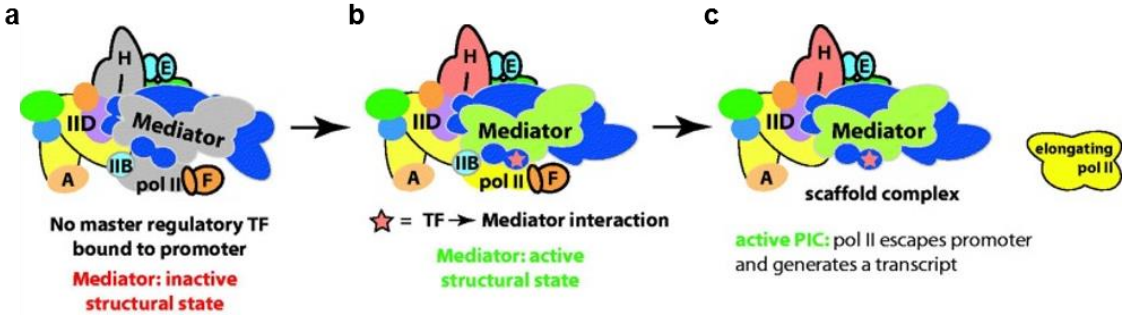

Figure 1.9: A model of transcription initiation by binding of a specific transcription factor (TF) to the Mediator complex.
1.9a: The first panel shows the model of a fully assembled but paused PIC and Mediator complex, a specific TF is absent (RNAPII = pol II in grey; general TFs TFIIA, B, D, E, F and H are indicated as letters and in various colors; Mediator complex in grey). **1.9b**: Binding of a specific TF initiates the active conformation of the Mediator complex (specific TF indicated by a star; RNAPII = pol II color turns from grey to yellow; Mediator complex color turns from grey to green). **1.9c**: The active conformation of the Mediator complex allows the escape of RNAPII (pol II) from the promoter region and to start productive elongation. (Note: DNA is not shown in this figure to facilitate the presentation; Figure modified acc. to Poss *et al.*, 2013)

The third regulatory kinase of the transcriptional machinery is CDK8 (and its paralog CDK19 in vertebrates), a subunit of the kinase module of the Mediator complex. The function and roles of CDK8 are not fully understood to date but intense research has shown that CDK8 is not required generally for expression, at least in some organisms. Numerous functions and roles of CDK8 in transcription and far beyond in other cellular processes were identified. The effects of CDK8 are often pleiotropic, cell type-, context- and organism-specific. Regarding transcription, CDK8 (and CDK19) was found to control Mediator structure and function by phosphorylation, to phosphorylate some general transcription factors, elongation factors, chromatin remodelers and modifiers and, interestingly, to phosphorylate gene-specific transcription factors (reviewed in Dannappel *et al.*, 2019; Fant and Taatjes, 2019; Poss *et al.*, 2013). Based on a study in *Saccharomyces cerevisiae*, the black widow model of transcription activation was postulated. Srb10, the homolog of CDK8 in *Saccharomyces cerevisiae*, was found to phosphorylate the gene-specific transcription factor GCN4. This phosphorylation, together with the phosphorylation by kinase Pho85, targets the transcription factor for ubiquitin-mediated proteolysis. This study showed for the first time that the transcriptional machinery controls the abundance of an active gene-specific transcription factor and added this new mechanism, the black widow model, to the known mechanisms of controlled termination of transcriptional activity (Chi *et al.*, 2001; reviewed in Tansey, 2001). The name "black widow model" was derived from spiders that kill the male mating partner after productive activity.

1.10. Aim of this thesis

Phosphorylation is the main post-translational modification involved in the regulation of the *N. crassa* circadian clock (reviewed in Mehra *et al.*, 2009). The phosphorylation of FRQ and the circadian phosphorylation of WCC are well understood but the mechanism of the light-induced phosphorylation of WCC is still unresolved.

The aim of this PhD project is to unravel the mechanism of the light-induced phosphorylation of WCC. Basically, phosphorylation of a protein is the addition of negative charges to the protein to induce either electrostatic repulsion from other negative charges or electrostatic attraction to positive charges. Phosphorylation of a transcription factor can modify its conformation, can modify its interaction with other proteins or can induce electrostatic repulsion from the negatively charged DNA. Modification of the interaction with other proteins can result in degradation or stabilization of the transcription factor and in its intracellular translocation (reviewed in Filtz *et al.*, 2014).

Applying these general thoughts to WCC, the main research questions are:

What triggers the light-induced phosphorylation of WCC: the light-induced conformational change in the WC-1 LOV domain; the light-induced dimerization of two WCC-protomers; the binding to light-inducible genes?

What are the phosphorylation sites and what do they tell about the mechanism?

Which kinases are involved?

What are the consequences and the function of the light induced phosphorylation of WCC?

Why is WC-1 transiently and WC-2 persistently phosphorylated in response to light?

How does the light-induced phosphorylation of WCC differ from the circadian phosphorylation?

2. Material and Methods

2.1. Material

2.1.1. Bacterial strains

Table 2.1: Chemically competent *Escherichia coli* strain used for cloning and amplification of plasmids.

Strain	Genotype	Company
Escherichia coli DH5α	*F*$^-$ *ϕ*80*lac*ZΔM15 Δ(*lac*ZYA-*arg*F) U169 *deo*R *rec*A1 *end*A1 *hsd*R17(r_k^-, m_k^+) *pho*A *sup*E44 *thi-1 gyr*A967 *rel*A1 λ$^-$	Stratagene (California, USA; part of Agilent, California, USA)

2.1.2. *N. crassa* strains

Table 2.2: List of *N. crassa* strains used in this study.

Strain	Genotype	Relevant Phenotype	Reference
wt, *bd*	ras-1^{bd}	Wild type, can be grown in race tubes	FGSC #1858
wt	ras-1^{wt}	Wild type, cannot be grown in race tubes	FGSC #2489
Δ*mdk-1* (het)	ras-1^{wt}, mdk-1::HygB^r heterokaryon	Knockout of *mitotic division kinase-1*, NCU07580.2	FGSC #14539
Δ*stpk47*	ras-1^{wt}, stpk47::HygB^r	Knockout of *serine / threonine protein kinase-47*, NCU06685.2	FGSC #17961
Δ*mapk-1*	ras-1^{wt}, mapk-1::HygB^r	Knockout of *mitogen-activated protein kinase-1*, NCU09842.2	FGSC #11320
Δ*mapk-2* (het)	ras-1^{wt}, mapk-2::HygB^r heterokaryon	Knockout of *mitogen-activated protein kinase-2*, NCU02393.2	FGSC #11482
Δ*mapk-2* (ssi)	ras-1^{wt}, mapk-2::HygB^r single spore isolate	Knockout of *mitogen-activated protein kinase-2*, NCU02393.2	FGSC #21728
Δ*wc-2, bd, qa-2 tap- wc-2*	ras-1^{bd}, wc2::HygB^r, his3::pqa2-tap-wc2-twc2	*wc-2* knockout with exogenous expression of TAP-tagged *wc-2* (tagged at the N-terminus) under control of *qa*-inducible promoter	(Sancar *et al.*, 2009)
Δ*frq* (*frq^{10}*), *bd*	ras-1^{bd}, frq^{10}	*frq* knockout "*frq10*" from FGSC	FGSC #7490
Δ*frq, bd, his$^-$*	ras-1^{bd}, frq:: HygB^r, Δhis3	*frq* knockout generated in the Brunner laboratory, histidine-auxotroph	Ibrahim Cemel
Δ*FCD1+2, bd*	ras-1^{bd}, frq^{10}, his3::pfrq-frq FCD1+2-tfrq	*frq* knockout with exogenous expression of *frq* lacking the FCD1 and the FCD2 domains	(Querfurth *et al.*, 2011)
Δ*wc-2, bd, his$^-$*	ras-1^{bd}, wc2::HygB^r, Δhis3	*wc-2* knockout, histidine-auxotroph	Andrea Molt
Δ*wc-2*, Δ*frq, bd, his$^-$*	ras-1^{bd}, wc2::HygB^r, frq:: HygB^r, Δhis3	*wc-2* knockout, frq knockout, histidine-auxotroph, used for crossing of *wc-2* mutant strains listed below	This study
wc-2 rtr. wild type, bd	ras-1^{bd}, wc2::HygB^r, his3::pwc2-wt wc2-twc2	*wc-2* knockout with exogenous expression of *wt wc-2*	This study
wc-2 allA, bd	ras-1^{bd}, wc2::HygB^r, his3::pwc2-allA wc2-twc2	*wc-2* knockout with exogenous expression of *wc-2* S80A, S82A, T86A, S118A, S128A, S129A, T136A, T138A, T139A, T140A,	This study

		T141A, S142A, T287A, S331A, S336A, T339A, S341A, T344A, S390A, S394A, S433A, T435A, T523A	
wc-2 allD, bd	ras-1^{bd}, wc2::HygB^{r}, his3::pwc2-allD wc2-twc2	*wc-2* knockout with exogenous expression of *wc-2* S80D, S82D, T86D, S118D, S128D, S129D, T136D, T138D, T139D, T140D, T141D, S142D, T287D, S331D, S336D, T339D, S341D, T344D, S390D, S394D, S433D, T435D, T523D	This study
wc-2 6AP, bd	ras-1^{bd}, wc2::HygB^{r}, his3::pwc2-6AP wc2-twc2	*wc-2* knockout with exogenous expression of *wc-2* T86A, S118A, T136A, T339A, S433A, T523A	This study
wc-2 6DP, bd	ras-1^{bd}, wc2::HygB^{r}, his3::pwc2-6DP wc2-twc2	*wc-2* knockout with exogenous expression of *wc-2* T86D, S118D, T136D, T339D, S433D, T523D	This study
wc-2 3DP N-terminal, bd	ras-1^{bd}, wc2::HygB^{r}, his3::pwc2-3DP N-terminal wc2-twc2	*wc-2* knockout with exogenous expression of *wc-2* T86D, S118D, T136D	This study
wc-2 3DP C-terminal, bd	ras-1^{bd}, wc2::HygB^{r}, his3::pwc2-3DP C-terminal wc2-twc2	*wc-2* knockout with exogenous expression of *wc-2* T339D, S433D, T523D	This study
wc-2 rtr. wild type P_{tcu-1} *frq, bd*	ras-1^{bd}, wc2::HygB^{r}, his3::pwc2-wt wc2-twc2, frq::ptcu1-wt frq-tfrq	*wc-2* knockout with exogenous expression of *wt wc-2* and expression of *frq* under control of a copper-tuneable promoter	This study
wc-2 RK/DD, bd	ras-1^{bd}, wc2::HygB^{r}, his3::pwc2-wc2 RK/DD-twc2	*wc-2* knockout with exogenous expression of *wc*-2 R480D, K481D	This study
wc-2 RK/DD P_{tcu-1} *frq, bd*	ras-1^{bd}, wc2::HygB^{r}, his3::pwc2-wc2 RK/DD -twc2, frq::ptcu1-wt frq-tfrq	*wc-2* knockout with exogenous expression of *wc-2* R480D, K481D and expression of *frq* under control of a copper-tuneable promoter	This study
wc-2 RK/DD 6DP P_{tcu-1} *frq, bd*	ras-1^{bd}, wc2::HygB^{r}, his3::pwc2-6DP wc2 RK/DD-twc2, frq::ptcu1-wt frq-tfrq	*wc-2* knockout with exogenous expression of *wc-2* T86D, S118D, T136D, T339D, S433D, R480D, K481D, T523D and expression of *frq* under control of a copper-tuneable promoter	This study

2.1.3. Plasmids and P_{tcu-1} construct

In this study, various mutants of *wc-2* were generated based on the plasmid pFH62 (generated by Felix Heise, Laboratory of Prof. Dr. Michael Brunner). The plasmid carries parts of the *his3* gene sequence to restore the *his3* gene function when integrated into the non-functional *his3* gene locus. A 3372 bp fragment of the wc-2 gene (999 bp wc-2 5´UTR, 1836 bp wc-2 ORF, 537 bp 3´UTR) was inserted into pFH62 by HindIII and SpeI generating pFH62-*wc-2 rtr. wild type*.

To generate phosphorylation site mutants of *wc-2*, appropriate fragments of *wc-2* carrying the respective mutations were synthesized by GENEWIZ Germany GmbH, Leipzig, Germany and inserted into pFH62-*wc-2 rtr. wild type*. The DNA fragments *wc-2 6AP*,

wc-2 6DP, wc-2 3DP N-terminal, wc-2 3DP C-terminal were inserted into pFH62-*wc-2 rtr. wild type* by AflII and NotI. The DNA fragments *wc-2 allA, wc-2 allD* replaced the respective wild-type sequence in pFH62-*wc-2 rtr. wild type* by PCR-based cloning. For a fast clone check prior sequencing, the restriction site for MluI was introduced as silent mutation in the ORF of *wc-2 allA* and the restriction site for KasI was introduced as silent mutation in the ORF of *wc-2 allD.*

The plasmids pFH62- *wc-2 RK/DD* and pFH62- *wc-2 RK/DD 6DP* were generated by site-directed mutagenesis of the plasmids pFH62-*wc-2 rtr. wild type* and pFH62-*wc-2 6DP*, respectively.

Prior transformation, the pFH62-based plasmids were linearized with the restriction enzyme SspI.

Table 2.3: List of plasmids used in this study.

Plasmid	Source
pFH62	Felix Heise
pFH62-*wc-2 rtr. wild type*	This study
pFH62-*wc-2 6AP*	This study
pFH62-*wc-2 6DP*	This study
pFH62-*wc-2 3DP N-terminal*	This study
pFH62-*wc-2 3DP C-terminal*	This study
pFH62-*wc-2 allA*	This study
pFH62-*wc-2 allD*	This study
pFH62- *wc-2 RK/DD*	This study
pFH62- *wc-2 RK/DD 6DP*	This study

The disruption of the *frq* promoter by insertion of P_{tcu-1} promoter was performed by transformation of *N. crassa* with overlapping PCR fragments acc. to the method described by Lamb *et al.*, 2013. With the primers used, 456 bp upstream from the *frq* start codon ATG were deleted to disrupt the *frq* promoter.

2.1.4. Primer

Table 2.4: List of primers used in this study.

The primers for PCR, for the assembly of P_{tcu-1} *frq*, for site-directed mutagenesis and for sequencing are assigned to a LE-number (LE = Linda Ebelt). Primers and probes for qPCR are not numbered. The qPCR probes are tagged with 6-FAM (5`) and TAMRA (3`). F = forward, R = reverse.

Primer for PCR

No.		F/R	Primer	Sequence (5'→ 3')
LE	75	F	wc-2 F-500 AscI	TATA GGCGCGCC ACTTCACCTTTACTCTCTGC
LE	76	R	wc-2 R+500 NotI	AATAATAA GCGGCCGC GTAACAAACTCCTCTCCATACC
LE	99	F	wc-2 5UTR HindIII	GGG AAGCTT CAATACGTATCCATGAACCTCG
LE	100	R	wc-2 ORF SpeI R	TTTTTT ACTAGT CTATCCCATATGATCGCCCATG
LE	101	F	wc-2 C-PCR F	GAATACGTGTGCACCGACTGC
LE	102	R	TrpC R	TGCGAACCCAGGGCTGGTG
LE	123	F	pUC57wc2 N F	AACGACGGCCAGTGAATTCGAGC
LE	124	R	pUC57wc2 N R	TGACCATGATTACGCCAAGCTTCC
LE	184	F	P1 wc2-PCRclon	GACCCACAGGACATGATGTCG
LE	185	R	P2 wc2-PCRclon	CCCAGGAAACACTGAAGTATCC

LE	186	R	P3 wc2-PCRclon	TTGTGACCGCCTATACCTCC
LE	187	F	P4 wc2-PCRclon	GAACGCCAACAACAACAATAACG

Primer for PCR (P_{tcu-1} *frq*)

No.		F/R	Primer	Sequence (5'→ 3')
LE	179	F	P1B frq F	CAAGTCCTCAAGTCAAGCACC
LE	180	R	P2B frq R	tttaggtcga ATCAAGCAGCGACAATCTTGG
LE	181	F	P3B frq F	GCTGCTTGAT tcgacctaaatctcggtgacg
LE	48	R	bar P4 R	atcgtcaaccactacatcgaga
LE	49	F	bar P5 F	ggagacgtacacggtcgact
LE	166	R	P6 frq R	TATCCGCCAT GGTTGGGGATGTGTGTGC
LE	167	F	P7 frq F	ATCCCCAACC ATGGCGGATAGTGGGGA
LE	168	R	P8 frq R	CTTCAGTTCCTCCTTAAGCCG

Primer for site-directed mutagenesis

No.		F/R	Primer	Sequence (5'→ 3')
LE	190	F	w-2 RK-DD ApaI F	CTCGATTCCCCCGAATGGgacgAtGGgCCcAGTGGACCCAAG ACAC
LE	191	R	w-2 RK-DD ApaI R	GTGTCTTGGGTCCACTgGGcCCaTcgtcCCATTCGGGGGAAT CGAG
LE	192	F	2RK/DD ApaI F	GGACGATGGGCCCAGTGGACCCAAGACACTATGCAATGCCTG
LE	193	R	2RK/DD ApaI R	CTGGGCCCATCGTCCCATTCGGGGGAATCGAGCGTACC
LE	194	F	w-2 RK-DDs F	CGATTCCCCCGAATGGgacgAtGGCCCTAGTGGACCCAAG
LE	195	R	w-2 RK-DDs R	CTTGGGTCCACTAGGGCCaTcgtcCCATTCGGGGGAATCG
LE	196	F	w-2 RK-DDl F	GCTCGATTCCCCCGAATGGgacgAtGGCCCTAGTGGACCCAA GAC
LE	197	R	w-2 RK-DDl R	GTCTTGGGTCCACTAGGGCCaTcgtcCCATTCGGGGGAATCG AGC

Primer for sequencing

(When the requirements for sequencing were met, PCR primers were used for sequencing as well)

No.		F/R	Primer	Sequence (5'→ 3')
LE	36	R	TAP WC2 PCR R	CAACATCGAGACTCATCGACATTCC
LE	37	R	TAP WC2 SEQ R	TCGGAAGTCATCTGCAGC
LE	38	R	TAP WC2 SEQ2 R	GAGACTCATCGACATTCC
LE	95	F	wc-2 NseqF	GTTAATACTTCAGTTCCCACC
LE	96	R	wc-2 NseqR	GGTAGAACAGTCGCAATTGG
LE	97	F	wc-2 CseqF	CCTGACCGAATTCACCAAGC
LE	98	R	wc-2 CseqR	AAGCTGCACATGTCAAGACC
LE	103	R	wc-2 UTR Seq R	CGTAGAGGTGGTAGACAGG
LE	134	F	pFH64upHis F	GCAGATTGTACTGAGAGTGC
LE	135	R	pFH64downHis R	GGAAGTATGAGTCACAGCACC
LE	138	F	LE75Seq F	ACTTCACCTTTACTCTCTGC
LE	139	R	LE76Seq R	GTAACAAACTCCTCTCCATACC
LE	140	F	LE99Seq F	CAATACGTATCCATGAACCTCG
LE	141	F	pFH64inHis1 F	AGGACTGGAGATGCTAAGG
LE	142	F	pFH64inHis2 F	AGAGCATCACCAAGGTCG
LE	143	R	wc2-3UTR700 R	GCATTGCCATTAAGAGTCC
LE	156	F	wc2 ORF start F	ATGTCTCACGGACAGCCTCC
LE	157	R	wc2 ORF end R	CTATCCCATATGATCGCCCATG
LE	158	F	wc2 Seq 1 F	CTGGATCCAGCATGTATGG
LE	159	F	wc2 Seq 2 F	TGACGTTATGATGCCACCACC

Primer and probes for qPCR

			Primer/Probe	Sequence (5'→ 3')
-	-	F	*vvd* F	ACGTCATGCGCTCTGATTCTG
-	-	R	*vvd* R	AAAAGCTTCCGAGGCGTACA
-	-	-	*vvd* probe	6-FAM-CGACCTGAAGCAAAAAGACACGCCA-TAMRA
-	-	F	*al-2* F	ACCTGGCCAATTCGCTCTTT
-	-	R	*al-2* R	GACAGAAGGAGTACAGCAGGATCA
-	-	-	*al-2* probe	6-FAM-CTGGTCGACTCCGCATT-TAMRA
-	-	F	*frq total* F	TTGTAATGAAAGGTGTCCGAAGGT
-	-	R	*frq total* R	GGAGGAAGAAGCGGAAAACG
-	-	-	*frq total* probe	6-FAM-ACCTCCCAATCTCCGAACTCGCCTG-TAMRA
-	-	F	*actin* F	GATGACACAGATCGTTTTCGAGACT
-	-	R	*actin* R	CGGAGGCGTAGAGAGAAAGGA
-	-	-	*actin* probe	6-FAM-CCGCCTTCTACGTCTCCATCCA-TAMRA
-	-	F	*vvd LRE* F	GTCCCTCGATGGTTTAGCAG
-	-	R	*vvd LRE* R	TGGATGGCAGTGTAGAATGG
-	-	-	*vvd LRE* probe	6-FAM-CTGCGATCGGTCAGCATCGC-TAMRA
-	-	F	*frq LRE* F	GCAGAGGACCCTGAACTTTTC
-	-	R	*frq LRE* R	TCTCTTGCTCACTTTCCCACAG
-	-	-	*frq LRE* probe	6-FAM-CCGCTCGATCCCCTGGAACCTG-TAMRA
-	-	-	sense frq cDNA synthesis primer	TCACGAGGATGAGACGTCC

2.1.5. Antibodies

Table 2.5: Primary and secondary antibodies used in this study.

Primary antibody

Antibody	Epitope / Features	Origin	Reference	Dilution
α-WC1	Anti-WC1 c-term, T2, d100, glycine, 28.04.2014	rabbit, polyclonal	Pineda Antikörper-Service, Berlin, Germany	1:1000
α-WC1	Anti-WC1 c-term, T3, d100, glycine., 29.04.2014	rabbit, polyclonal	Pineda Antikörper-Service, Berlin, Germany	1:1000
α-WC2	Anti-WC2-GST, Citrate 29.06.12	rabbit, polyclonal	Pineda Antikörper-Service, Berlin, Germany	1:500
α-WC2	Anti-WC2-GST, T1, glycine, 230 d, 30.03.2015	rabbit, polyclonal	Pineda Antikörper-Service, Berlin, Germany	Used for WC-2 IP
α-WC2	Anti-WC2-GST, glycine, 03.11.2016	rabbit, polyclonal	Pineda Antikörper-Service, Berlin, Germany	1:200
α-WC2	Anti-WC2-GST, T2, d123, glycine, 08.03.2017	rabbit, polyclonal	Pineda Antikörper-Service, Berlin, Germany	1:500
α-FRQ	Anti-FRQ, aa 65-100, N-terminal domain of FRQ	mouse, monoclonal	Generated by cell culture in the Brunner laboratory	1:20

Secondary antibody

Antibody	Epitope / Features	Origin	Reference	Dilution
α-rabbit	Anti-rabbit IgG, HRP-coupled	goat, polyclonal	Cat.-No. 1721019, Bio-Rad Laboratories, Inc., Hercules, USA	1:10000
α-mouse	Anti-mouse IgG, HRP-coupled	goat, polyclonal	Cat.-No. 1706516, Bio-Rad Laboratories, Inc., Hercules, USA	1:10000

2.1.6. Solutions, buffer, culture media

2.1.6.1. Solutions

Table 2.6: Solutions used in this study.

50x Vogel´s salt solution (Vogel, 1956)	123,5 g $Na_3Citrat$ x 2 H_2O; 250 g KH_2PO_4; 100 g NH_4NO_3; 10 g $MgSO_4$ x 7 H_2O; 5 g $CaCl_2$ x 2 H_2O; 5 mL Micronutrients; Biotin 0,5 mg/mL 500 µL; complete with H_2O (desalted) to 1000 mL, add 2 mL Chloroform
50x Vogel´s salt solution w/o nitrogen (NH_4NO_3)	123,5 g $Na_3Citrat$ x 2 H_2O; 250 g KH_2PO_4; 10 g $MgSO_4$ x 7 H_2O; 5 g $CaCl_2$ x 2 H_2O; 5 mL Micronutrients; Biotin 0,5 mg/mL 500 µL; complete with H_2O (desalted) to 1000 mL, add 2 mL Chloroform
Micronutrients	5 g Citric acid; 5 g $ZnSO_4$ x 7 H_2O; 1 g $(NH_4)_2Fe(SO_4)_2$ x 6 H_2O; 0,25 g $CuSO_4$ x 5 H_2O; 0,05 g $MnSO_4$ x H_2O; 0,05 g H_3BO_3 (water-free); 0,05 g Na_2MoO_4 x 2 H_2O; complete with H_2O (desalted) to 100 mL, add 1 mL Chloroform
2x Westergaard´s solution (Westergaard and Mitchell, 1947)	0,2 % (w/v) KNO_3; 0,2 % (w/v) KH_2PO_4; 0,1 % (w/v) $MgSO_4$ x 7 H_2O; 0,02 % (w/v) NaCl; 0,02 % (w/v) $CaCl_2$; 0,02 % (v/v) micronutrients, pH 6,5 (KOH), autoclave
10x FIGS (Brockman and Serres, 1963)	2,5 g D(-)Fructose,;2,5 g D(+)Glucose; 100 g L(-)Sorbose, add 500 mL H_2O (desalted), autoclave
Quinic acid	30% (w/v) in H_2O, pH 5,5-6
Glycine	1.25 M in H_2O
Biotin	0,5 mg/mL in 50% (v/v) EtOH
Hygromycin	100 mg/mL in H_2O
Thiolutin	2,5 mg/mL in DMSO
PMSF (Phenylmethylsulfonylfluorid)	34 mg/mL in Isopropanol
Leupeptin	1 mg/mL in H_2O
Pepstatin A	1 mg/mL in MeOH
SDS	10% (w/v) in H_2O
p-Coumaric acid	0,015 g/mL in DMSO
Luminol	0,044 g/mL in DMSO
APS (Ammoniumpersulfat)	10% (w/v) in H_2O
Developer solution	0,1 M Tris/HCl pH 8,8, 220 µg/ml luminol, 37,5 µg/ml p-coumaric acid, 0,09‰ H_2O_2
Ponceau-S staining solution	0,2 % Ponceau-S in 3 % TCA.
Coomassie fixing solution	2 % acetic acid, 40 % methanol, ultrapure water
Coomassie staining solution	20 % methanol, 1 x Roti®-Blue (5 x Roti®-Blue, Art.-No. A152.1, Carl Roth GmbH + Co. KG, Karlsruhe, Germany), ultrapure water
Ampicillin	100 mg/mL, use 1:1000

2.1.6.2. Buffers

Table 2.7: Buffers used in this study.

TAP buffer	50 mM Tris; 150 mM NaCl; 1.5 mM $MgCl_2$ * 6 H_2O; 0,1 % (v/v) NP-40 99 % (Nonidet P 40); pH 7,5; filter sterile completed right before usage with: 1:2000 DTT; 1:200 PMSF, 1:1000 Leupeptin, 1:1000 Pepstatin A, PhosSTOP™ (Roche, Merck KGaA, Darmstadt, Germany 1x/15 mL)
B-PEX buffer	50 mM HEPES (pH 7,4); 137 mM NaCl; 5 mM EDTA; 10 % (v/v) glycerol; filter sterile completed right before usage with:

	1:200 PMSF, 1:200 Leupeptin, 1:200 Pepstatin A, PhosSTOP™ (Roche, Merck KGaA, Darmstadt, Germany 1x/10 mL)
Denat. PEX buffer	50 mM HEPES pH 7,5; 500 mM NaCl; 5 mM Glycine; 8 M Urea
4x LDS buffer	NuPAGE™ LDS Sample Buffer, Novex™ by life technologies completed right before usage with: 1:20 DTT
4x Laemmli buffer	277,8 mM Tris-HCl pH 6,8; 44,4 % (v/v) glycerol; 4,4% SDS; 0,02 % bromophenol blue completed right before usage with: 1:10 β-Mercaptoethanol
PBS buffer	137 mM NaCl; 2,7 mM KCl; 4,3 mM Na_2HPO_4 x 7 H_2O; 1,4 mM KH_2PO_4 completed right before usage with: 1:200 PMSF, 1:200 Leupeptin, 1:200 Pepstatin A, PhosSTOP™ (Roche, Merck KGaA, Darmstadt, Germany 1x/10 mL)
SDS-PAGE buffer	50 mM Tris-HCl pH 8,3; 384 mM glycin; 0,1 % SDS
Western Blot transfer buffer	20 mM Tris; 150 mM glycine; 20 % (v/v) Methanol; 0,08 % (w/v) SDS
Tris-Buffered Saline (TBS)	10 mM Tris-HCl pH 7,4; 150 mM NaCl
2xCTAB buffer	100 mM Tris-HCl; pH 7,5-8; 2% (w/v) CTAB (Hexadecyltrimethylammonium); 1,4 M NaCl; 20 mM EDTA; pH 7,5-8; 1% sodium bisulfite, heat up to 60°C
TAE buffer	40 mM Tris; 0,11 % (w/v) acetic acid; 2,2 mM EDTA

2.1.6.3. Culture media

Table 2.8: Media used in this study for the cultivation of *N. crassa* and *E. coli*.

Culture media for *N. crassa*	
Liquid N-medium standard growth medium	2 % (w/v) glucose; 0,5 % (w/v) arginine; 1x Vogel´s salt solution
Solid N-medium standard growth medium	2 % (w/v) glucose; 0,5 % (w/v) arginine; 1x Vogel´s salt solution; 0,5 mg/mL biotin; 2 % (w/v) agar If required: 0,5 mg/mL histidine: autoclave If required: 200 µg/mL Hygromycin
Solid medium with Glufosinate (Proline is the only source of nitrogen to increase the uptake of Glufosinate)	1,5 % (w/v) sucrose; 0,5 % (w/v) L-Proline; 1x Vogel´s salt solution w/o NH_4NO_3; 1 % (w/v) agar If required: 0,5 mg/mL histidine autoclave 250 µg/mL Glufosinate
Racetube medium (based on Sargent and Kaltenborn, 1972)	0,2 % (w/v) glucose; 0,17 % (w/v) arginine; 1x Vogel´s salt solution; 0,5 mg/mL biotin; 2,2 % (w/v) agar
Bottom agar w/ and w/o Histidine with Hygromycine with Glufosinate	0,36 % (w/v) arginine; 1x Vogel´s salt solution; 1,5 % (w/v) agar If required: 0,5 mg/mL histidine autoclave 1x FIGS solution If required: 200 µg/mL Hygromycin If required: 250 µg/mL Glufosinate
Top agar	18,2 % (w/v) sorbitol; 1x Vogel´s salt solution; 2,8 % (w/v) agar autoclave 1x FIGS solution
2x Westergaard´s solution (Westergaard and Mitchell, 1947)	0,2 % (w/v) KNO_3; 0,2 % (w/v) KH_2PO_4; 0,1 % (w/v) $MgSO_4$ x 7 H_2O; 0,02 % (w/v) NaCl; 0,02 % (w/v) $CaCl_2$; 0,02 % (v/v) micronutrients, pH 6,5 (KOH), autoclave

Westergaard´s agar (Westergaard and Mitchell, 1947)	1x Westergaard's solution; 0,2 % (w/v) sucrose; 0,5 mg/mL biotin; 2 % (w/v) agar If required: 0,3 mg/mL histidine Autoclave

Culture media for *E. coli*

LB liquid medium	2,5 % (w/v) LB powder Autoclave 100 µg/mL Ampicillin
LB agar	2,5 % LB powder; 1,5 % (w/v) agar Autoclave 100 µg/mL Ampicillin
SOC medium	2 % (w/v) tryptone; 0,5 % (w/v) yeast extract; 10 mM NaCl; 2,5 mM KCl; 10 mM $MgCl_2$; 10 mM $MgSO_4$; 20 mM glucose

2.2. Methods

2.2.1. Neurospora methods

2.2.1.1. Cultivation of *N. crassa* to isolate conidia

Solid N-medium in either a 500 mL Erlenmeyer flask or in a glass tube was inoculated with *N. crassa* conidia suspension and incubated in constant darkness at 30°C for 1-2 days (incubator, BINDER GmbH, Tuttlingen, Germany). After that, the culture was incubated for 4-6 days at room temperature exposed to daylight. The conidia were washed off the mycelia with 4°C cold 1 M sterile sorbitol solution. For a 500 mL Erlenmeyer flask, 50 mL 1 M sterile sorbitol solution were used, for a glass tube, 2 mL 1 M sterile sorbitol solution were used. For the use of the conidia as stock for further inoculation, the conidia suspension from the glass tube was stored at -20°C for up to one year.

For use of the conidia for transformation, the conidia suspension from the 500 mL Erlenmeyer flask was filtered through sterile gauze. The conidia were pelleted at 2000 rpm, 4°C for 5 min (Multifuge 1 L-R, Heraeus™, Thermo Fisher Scientific Inc., Waltham, USA). The supernatant was discarded and the conidia pellet was resuspended in 50 mL 4°C cold 1 M sorbitol solution. The conidia were pelleted a second time at 1600 rpm, 4°C for 5 min. The supernatant was discarded and the conidia pellet was resuspended in 50 mL 4°C cold 1 M sorbitol solution. The conidia were pelleted a third time at 1200 rpm, 4°C for 5 min. The supernatant was removed and discarded without disturbing the fragile conidia pellet. The conidia pellet was resuspended in the remaining supernatant to yield a viscous conidia suspension. If too dense, 50-100 µL 4°C cold 1 M sorbitol solution were added. The conidia suspension was kept on ice until rapid progression of the transformation procedure.

2.2.1.2. Cultivation of *N. crassa* in liquid culture

To acquire cell material for Protein-, DNA- and RNA-analysis, *N. crassa* was cultured in liquid N-medium.

To harvest the whole culture at once, N-medium in an Erlenmeyer flask (e.g. 150 mL N-medium in a 500 mL Erlenmeyer flask) was inoculated with conidia suspension described under 2.2.1.1. The culture was incubated at 25°C and 100 rpm for 2,5 days in a Multitron incubator (Infors AG, Bottmingen, Switzerland) under light conditions as indicated in the respective experiment. Harvest of the mycelia was performed by filtration of the mycelia through filter paper in a Buechner funnel and subsequent drying on paper towel. The harvest was performed quickly to avoid degradation of cellular components and the dried mycelia were frozen immediately in liquid nitrogen and stored at -80°C.
To harvest samples from the same culture at different time points of light induction, 20 mL N-medium in a petri dish (diameter: 8,5 cm) were inoculated with conidia suspension described under 2.2.1.1. This preculture was sealed with parafilm, incubated at 30°C without shaking (incubator, BINDER GmbH, Tuttlingen, Germany) for 2 days to grow a mat of mycelia. From the mat of mycelia, mycelia discs cut out with a sterile pipette tip were transferred to fresh N-medium in an Erlenmeyer flask (e.g. 150 mL N-medium in a 500 mL Erlenmeyer flask). This culture was incubated at 25°C and 100 rpm for 8 hrs in a Multitron incubator (Infors AG, Bottmingen, Switzerland) in constant light. The incubation was continued for 24 h in constant darkness (DD) and at time point DD24, light was switched on for 2 h (light induction). Samples were harvested at different time points by drying the mycelia patches manually on paper towel. As described above, harvest was performed quickly and the dried mycelia were frozen immediately in liquid nitrogen and stored at -80°C.

2.2.1.3. Cultivation of *N. crassa* in liquid culture for TAP

To perform a light induction of 15 min and to harvest a reference sample (0 min light induction), 1,2 L liquid N-medium in a 3L flasks (4 flasks per sample) was inoculated with an appropriate amount of conidia. The culture was grown at 25 °C and 100 rpm in constant light for 2 days and transferred in constant darkness for 24 h (Multitron incubator, Infors AG, Bottmingen, Switzerland). After 12 h in dark, 0.3 % quinic acid (30% stock) was added to induce the expression of TAP-WC-2 for 12 h. Prior to harvest, 0.3 % formaldehyde were added to the culture and incubated for 10 min. The cross-linking was stopped by addition of 125 mM Glycine and incubation for 5 min. For the light induction sample, the cross-linking and Glycine-incubation were performed after 15 min light induction. Each 1,2 L culture was harvested by filtration using a filter paper of 240 mm diameter. The mycelia patch was dried quickly on paper towel, frozen immediately in liquid nitrogen and stored at -80°C.

2.2.1.4. Thiolutin assay

The *N. crassa* culture was performed with mycelia discs as describe in 2.2.1.2. After 22 h in DD, 30 mL fresh N-medium with 12 µg/mL thiolutin were prepared in 100 mL Erlenmeyer flasks. After 22,5 h in DD, the mycelia patches from the initial culture were transferred under red light (no impact on the *N. crassa* circadian clock) to the fresh N-medium containing thiolutin. The *N. crassa* culture was incubated with 12 µg/mL

thiolutin in DD for 90 min. At DD24, the light induction was started. For each time point to sample, a separate 100 mL Erlenmeyer flasks with 30 mL fresh N-medium and 12 µg/mL thiolutin was prepared to ensure comparable light induction conditions for each time point to harvest.

2.2.1.5. Race tube assay

The racetube assay (Baker *et al.*, 2012; Ryan *et al.*, 1943; Sargent and Kaltenborn, 1972) was performed to measure the rhythm of conidiation as output of the circadian clock. Liquid racetube medium was injected into a racetube (hollow glass tube, both ends bent upwards). When the racetube medium was solidified, one end of the layer of medium was inoculated with 10-20 µL conidia suspension of *N. crassa bd* strains. Both ends of the racetube were closed with cotton plugs. The racetubes were incubated at 25°C in constant light (LL) for approx. 1 day. When growth was visible, the racetubes were transferred to constant darkness (DD), 25°C (Multitron incubator, Infors AG, Bottmingen, Switzerland) and the growth front was marked on each racetube once per day for 7-9 days under red light (no impact on the *N. crassa* circadian clock). When the growth front reached the end of the racetubes, the racetubes were scanned and the banding of conidiation was analyzed with Chrono II software (Roenneberg, LMU Munich). This software recognizes the pattern of conidiation and the marks. The marks are assigned manually with the respective time of marking and with this time frame, the software calculates the rhythm of the respective *N. crassa bd* strain in the racetube.

2.2.1.6. Transformation of *N. crassa*

DNA was transformed into *N. crassa* by electroporation of conidia. First, bottom agar with the respective selective agent was prepared. 10 mL aliquots of liquid top agar were prepared and kept at 60°C to reach this temperature. The volume of 250 ng – 1000 ng of a linearized plasmid or a fragment of DNA was reduced to 10 µL or below, if required, by evaporation in a SpeedVac (Sc 110, Savant) and kept on ice. For transformation of the $P_{tcu\text{-}1}$-*frq* DNA fragment acc. to Lamb *et al.*, 2013, 150 ng and 300 ng were used. The conidia suspension was prepared as described (see 2.2.1.1). The DNA solution was added to 55 µL of conidia suspension and gently mixed. The DNA/conidia mix was incubated for 5 min on ice. After that, the suspension was transferred to a 0,2 cm electroporation cuvette. An electric pulse of 600 Ω, 1,5 kV/cm, 25µF was applied to the DNA/conidia mix and immediately after pulsing, the conidia were resuspended in 1 mL ice-cooled 1 M sorbitol. The 10 mL aliquots of 60°C warm top agar was allowed cool down at room temperature for approx. 3-5 min, the conidia were diluted in the liquid 10 mL top agar and spread on bottom agar. When the top agar was solidified, the plates were incubated at 30°C for 3 days (incubator, BINDER GmbH, Tuttlingen, Germany). Colonies of *N. crassa* transformants were excised and grown on solid N-medium for further testing.

2.2.1.7. Crossing *N. crassa* strains

Transformants of *N. crassa* were generated in this study by electroporation of conidia that contain more than one nucleus. Thus, very likely not all nuclei of one conidium receive

the transformed DNA. As a consequence, the expression level of a manipulated gene might differ among *N. crassa* strains. To eliminate that difference, *N. crassa* were crossed to obtain homokaryon strains. However, especially the *wc-2* transformants into the *his-locus* yielded heterokaryon strains of WC-2 expression at same level as the wild type, so that initial experiments could be performed with these strains already. In parallel, crossing was performed.

To cross two *N. crassa* strains, solid Westergaard´s medium (Westergaard and Mitchell, 1947) in a petri dish was inoculated with conidia suspension (see 2.2.1.1) in three different approaches to obtain sufficient ascospore formation. First, strain one was allowed to cover the surface of the solid medium with mycelia and then, the second strain was applied on top by tiny drops of conidia suspension. Second, the same approach was performed by inoculating the second strain first. Third, both strains were inoculated at the same time on two opposite sides of the petri dish and ascospore formation was expected in the area, where the growth fronts met. The petri dishes were sealed with parafilm to prevent conidia formation at incubated with the solid medium down at rt in light-dark-cycles for several weeks until ascospore formation. The black ascospores accumulated in the lid of the petri dish, were washed off with 1-2 mL sterile, purified water and stored in sterile, purified water at 4°C.

The ascospore concentration was determined by counting the ascospores in a 10 µL water drop under the binocular microscope. 1000 ascospores in an appropriate volume of sterile, purified water were activated at 60°C for 30 min. To obtain optimal growth density, 100, 250 and 500 ascospores were plated on bottom agar (in petri dish) that contained selective markers of histidine, if required. The petri dishes were incubated at 30°C (incubator, BINDER GmbH, Tuttlingen, Germany) in a closed, but aerated plastic box together with an open petri dish filled with sterile, purified water to create a humid atmosphere for optimal germination of the ascospores. After one or two days, clones were excised with a sterile scalpel in an early state of germination under the binocular microscope. The germinating ascospore was still visible among the growing mycelia to ensure that only clones from a single ascospore were selected and to prevent fusion of different clones. The clones were transferred to solid N-medium to generate conidia for further testing (see 2.2.1.1).

2.2.2. Protein Methods

2.2.2.1. Denaturing total protein extracts from *N. crassa*

For the analysis of protein phosphorylation by SDS-PAGE and Western Blot, denaturing total protein extracts from *N. crassa* were made. The denat. PEX buffer was prepared right before usage and used at 65°C (heated on a magnetic stirrer, Heidolph Instruments GmbH & CO. KG Schwabach, Germany). 800 µL of the hot denat. PEX buffer was added to 500 µL frozen *N. crassa* mycelia powder, mixed immediately with a spatula and transferred to a 65°C hot ThermoMixer (Eppendorf AG, Hamburg, Germany). The well-dissolved suspension was incubated at 65°C and 950 rpm for 5 min. The suspension was

centrifuged at rt and rmp max (Centrifuge 5415 D, Eppendorf AG, Hamburg, Germany) for 15 min and the supernatant was transferred to a fresh tube at rt. The concentration of the protein extract was measured with the NanoDrop ND-1000 UV-Vis Spectrophotometer (NanoDrop Technologies LLC by Thermo Fisher Scientific Inc., Waltham, USA). A sample from the total protein extract was taken, 4x Laemmli buffer was added and the sample was incubated at 95°C for 5 min (ThermoMixer, Eppendorf AG, Hamburg, Germany). The sample in Laemmli buffer was diluted 1:3 with 1x Laemmli buffer to reduce the Urea concentration for better running conditions in the SDS-PAGE. 300 µg total protein were loaded in SDS-PAGE. The remaining total protein extract was stored at -80°C.

2.2.2.2. Native total protein extracts from *N. crassa*

For native total protein extracts from *N. crassa*, 700 µl complete, 4°C cold B-PEX buffer were added to 500 µL frozen *N. crassa* mycelia powder and mixed immediately by vortexing. The suspension was incubated on ice for 20 min, vortexed every 5 min and then centrifuged at 20000g and 4°C for 20 min (Centrifuge 5417 R, Eppendorf AG, Hamburg, Germany). The supernatant was transferred to a fresh tube and kept on ice. The concentration of the protein extract was measured with the NanoDrop ND-1000 UV-Vis Spectrophotometer (NanoDrop Technologies LLC by Thermo Fisher Scientific Inc., Waltham, USA). A sample from the total protein extract was taken, 4x Laemmli buffer was added and the sample was incubated at 95°C for 5 min (ThermoMixer, Eppendorf AG, Hamburg, Germany). 400 µg total protein were loaded in SDS-PAGE. The remaining total protein extract was stored at -80°C.

2.2.2.3. Tandem affinity purification

With tandem affinity purification, tagged WC-2 was purified from *N. crassa* total protein extracts in a two-step (tandem) purification acc. to Sancar *et al.*, 2009.

Total protein extraction

The frozen cell material was grinded to powder with a mixer mill in 30 s intervals at a frequency of 30 s-1 (RETSCH GmbH, Haan, Deutschland. For protein extraction, the sterile filtered, 4°C cool TAP buffer was completed with DTT, PMSF, Leupeptin, Pepstatin A and PhosSTOP™ (Roche, Merck KGaA, Darmstadt, Germany 1x/10 mL)) right before usage and kept on ice. Per sample, 150 mL cell powder were quickly resuspended (magnetic stirrer, Heidolph Instruments GmbH & CO. KG Schwabach, Germany) on ice in maximum 250 mL complete TAP buffer until a smooth, liquid suspension was obtained. For pre-clearing, the cell suspension was centrifuged in 500 mL centrifuge tubes for 30 min at 10 000g and 4°C (JA 10 rotor, Avanti J-25 centrifuge, Beckman Coulter Inc., Brea, USA). The supernatant was transferred on ice to 60 mL ultracentrifuge tubes. Ultracentrifugation was performed at 38 krpm, 1 h (T647.5 rotor, Sorvall™ WX Ultracentrifuge, Thermo Scientific™ by Thermo Fisher Scientific Inc., Waltham, USA). The clear supernatant was transferred on ice by a syringes and needles. The supernatants from several ultracentrifuge tubes belonging to the same sample were

pooled. In case that the supernatant was too cloudy due to insufficient lipid separation, the supernatant was transferred to a new ultracentrifuge tube on ice and ultracentrifugation was performed again. The concentration of the protein extract was measured with the NanoDrop ND-1000 UV-Vis Spectrophotometer (NanoDrop Technologies LLC by Thermo Fisher Scientific Inc., Waltham, USA). A sample from the protein extract was taken, 4x Laemmli buffer was added and the sample was incubated at 95°C for 10 min (ThermoMixer, Eppendorf AG, Hamburg, Germany).

First purification: Protein A/IgG

In the first purification step, the Protein A tag was precipitated with IgG beads. All steps were performed at 4°C. Per sample, 600 µL IgG beads in a 2 mL tube were washed with 5 x 2 mL complete TAP buffer (w/o Phos-Stop), (sedimentation at 1000 rpm, 4°C, 1 min, Centrifuge 5417 R, Eppendorf AG, Hamburg, Germany). The washed 600 µL IgG beads were resuspended in complete TAP buffer (w/o Phos-Stop) and split equally on several 50 mL tubes depending on the volume of the protein extract of each sample. The protein extract was added to the IgG beads and was incubated overnight at 4°C on a roller mixer. The IgG beads were sedimented at 2000 rpm and 4°C for 4 min (Multifuge 1 L-R, Heraeus™, Thermo Fisher Scientific Inc., Waltham, USA) and from the supernatant, the sample IgG flow through was taken, 4x Laemmli buffer was added and the sample was incubated at 95°C for 10 min (ThermoMixer, Eppendorf AG, Hamburg, Germany). The IgG beads were washed three times in 25 mL complete TAP buffer (w/o Phos-Stop) by incubation on the roller mixer at 4°C for 5 min and subsequent centrifugation at 2000 rpm and 4°C for 4 min.

TEV cleavage

TEV cleavage was performed to remove the precipitated protein from the IgG beads. The IgG beads pellet in the 50 mL tube was resuspended in 1 mL TEV buffer (complete TAP buffer w/o Phos-Stop and 1 mM DTT), transferred to a 2 mL tube and pelleted at 1000 rpm, 4°C for 1 min (Centrifuge 5417 R, Eppendorf AG, Hamburg, Germany). Resuspension and pelleting were repeated until all beads were captured. As first TEV elution step, 600 µl IgG beads were incubated with 600 µl TEV buffer and 120 u TEV-protease at 16°C for 2 h on a turning wheel. The IgG beads were pelleted (1000 rpm, 4°C for 1 min) and the supernatant was stored at 4°C. The IgG beads were resuspended in 600 µl TEV buffer and incubated with 120 u TEV-protease at 16°C o/n on a turning wheel. After this second TEV elution step, the IgG beads were pelleted (1000 rpm, 4°C for 1 min). The supernatants of the first and the second elution were pooled and stored at 4°C. For the final capture, the IgG beads were resuspended in 600 µl TEV buffer w/o TEV-protease and incubated at 4°C for 1 h on a turning wheel. The IgG beads were pelleted (1000 rpm, 4°C for 1 min) and the supernatant was pooled with the supernatants from the first and second elution. A sample from the TEV elution was taken, 4x LDS buffer completed with DTT was added and the sample was incubated at 72°C for 10 min (ThermoMixer, Eppendorf AG, Hamburg, Germany). The IgG beads were resuspended

in an equal volume of 2x Laemmli buffer and incubated at 95°C for 10 min (ThermoMixer, Eppendorf AG, Hamburg, Germany).

Second purification: CaM/CaM beads

For the CaM purification step, $CaCl_2$ (4°C) was added to the TEV elution to set a final concentration of 2 mM $CaCl_2$. Per sample, 360 µL CaM beads in a 2 mL tube were washed with 3 x 2 mL complete, 4°C cold CaM binding buffer (sedimentation at 1000 rpm, 4°C, 1 min, Centrifuge 5417 R, Eppendorf AG, Hamburg, Germany). The washed CaM beads were resuspended in the TEV elution and incubated at 4°C for 2,5 h on a turning wheel. The CaM beads were pelleted (1000 rpm, 4°C for 1 min). A sample of the supernatant (CaM flow through) was taken, 4x Laemmli buffer was added and the sample was incubated at 95°C for 10 min (ThermoMixer, Eppendorf AG, Hamburg, Germany). The CaM bead pellet was washed with 6 x 2 mL complete CaM binding buffer (sedimentation at 1000 rpm, 4°C, 1 min).

Elution from CaM beads

The washed CaM bead pellet was incubated 3x with 400 µl CaM elution buffer at room temperature for 10 min on a turning wheel, sedimentation was performed at 1000 rpm, 4°C for 1 min (Centrifuge 5417 R, Eppendorf AG, Hamburg, Germany). The three supernatants collected during elution were kept at 4°C and pooled. A sample from the CaM elution was taken, 4x LDS buffer completed with DTT was added and the sample was incubated at 72°C for 10 min (ThermoMixer, Eppendorf AG, Hamburg, Germany). The CaM beads were resuspended in an equal volume of 2x Laemmli buffer and incubated at 95°C for 10 min (ThermoMixer, Eppendorf AG, Hamburg, Germany).

TCA-DOC precipitation

TCA-DOC precipitation was performed to concentrated the proteins in the CaM elution for further analysis by SDS-PAGE and mass spectrometry. CaM elution was stirred vigorously after addition of 0.015 % DOC and incubated at room temperature for 10 min. 5 % TCA were added and the solution was incubated for 30 min on ice. The precipitated proteins were pelleted at 4°C and rmp max. for 30 min (Centrifuge 5417 R, Eppendorf AG, Hamburg, Germany). 200 µL -20°C cold acetone were added to the pellet and the solution was incubated o/n at 4°C. Next, the solution was pelleted at 4°C and rmp max. for 90 min. The supernatant was removed thoroughly and the pellet was air-dried at room temperature for 30 min. The pellet was dissolved in 20 µL 2x LDS sample buffer and incubated at 72°C for 10 min (ThermoMixer, Eppendorf AG, Hamburg, Germany).

2.2.2.4. WC-2 Immunoprecipitation

For a αWC-2 immunoprecipitation (IP) with 100 mg total protein, 8x 500 µL grinded *N. crassa* mycelia powder was aliquoted in 2 mL tubes and kept frozen at -80°C.

For total protein extraction, 4°C cold B-PEX buffer was completed with PMSF, Leupeptin, Pepstatin A and PhosSTOP™ (Roche, Merck KGaA, Darmstadt, Germany 1x/10 mL). 600 µL ice-cold complete B-PEX buffer were added to 500 µL frozen *N. crassa* mycelia powder. The sample was vortexed immediately, incubated for 20 min on ice and vortexed every 5 min. The suspension was centrifuged at 20 000g and 4°C for

20 min (Centrifuge 5417 R, Eppendorf AG, Hamburg, Germany). The supernatants of eight 2 mL tubes belonging one sample were pooled and kept on ice. The concentration of the protein extract was measured with the NanoDrop ND-1000 UV-Vis Spectrophotometer (NanoDrop Technologies LLC by Thermo Fisher Scientific Inc., Waltham, USA). A sample from the total protein extract was taken, 4x Laemmli buffer was added and the sample was incubated at 95°C for 5 min (ThermoMixer, Eppendorf AG, Hamburg, Germany).

For immunoprecipitation, 100 mg total protein were gently mixed with 5 µg of the polyclonal αWC-2 antibody "T1, glycine, 230 d, 30.03.2015" (30 µg/mL, generated for the Brunner lab) and incubated o/n at 4°C unmoved to allow binding of αWC-2 antibody to WC-2. Various samples were adjusted to the same volume and subsequently the same concentration of total protein and antibody by adding complete B-PEX buffer.

50 µL Protein A Sepharose beads were washed 2x with 1,5 mL complete, 4°C cold PBS buffer (completed with PMSF, Leupeptin, Pepstatin A and PhosSTOP™ (Roche, Merck KGaA, Darmstadt, Germany 1x/10 mL)) and sedimented at 100 g and room temperature for 2 min (Centrifuge 5415 D, Eppendorf AG, Hamburg, Germany). The washed beads were added to the protein-antibody mix and the solution was incubated at 4°C on a rotation wheel for 1,5 h to allow binding of the antibody-protein complexes to the beads. Ice-cold, fresh, complete PBS buffer was prepared right before bead wash. The beads were sedimented at 100 g and 4°C for 2 min (Centrifuge 5417 R, Eppendorf AG, Hamburg, Germany). A sample of the supernatant was taken, 4x Laemmli buffer was added and the sample was incubated at 95°C for 5 min (ThermoMixer, Eppendorf AG, Hamburg, Germany). The beads were washed three times with 1 mL ice-cold, complete PBS buffer. After that, the beads were washed two more times and incubated in 1 mL ice-cold, complete PBS buffer at 4°C on a rotation wheel for 5 min before sedimentation.

For elution of the precipitated protein, the beads were resuspended in 100 µL 2x LDS sample buffer and incubated at 72°C and shaking at 900 rpm for 10 min (ThermoMixer, Eppendorf AG, Hamburg, Germany). After sedimentation at 100 g and rt for 2 min, the supernatant was transferred to a fresh tube and kept at rt. The beads were resuspended again in 50 µL 2x LDS sample buffer and incubated at 72°C and shaking at 900 rpm for 5 min (ThermoMixer, Eppendorf AG, Hamburg, Germany). After sedimentation, the supernatant was combined with the previous one. The sample in LDS buffer was either stored at - 20°C or loaded on an SDS gel.

As control for the specificity of the precipitation, a no antibody control was included. For identification of the antibody bands in the SDS-gel, the total protein extract from a wc-2 knock out strain was included as control.

2.2.2.5. Dephosphorylation of proteins

Dephosphorylation of proteins was performed with λ-phosphatase (New England Biolabs Inc., Ipswich, USA). 200 µg total protein (see 2.2.2.2) were incubated with 1x NEBuffer Pack for Protein Metallo-Phosphatases (PMP, 10x stock, New England Biolabs Inc., Ipswich, USA) and 1 mM $MnCl_2$ (10 mM stock, New England Biolabs Inc., Ipswich,

USA) in a final volume of 30 µL at 30°C for 1 h (ThermoMixer, Eppendorf AG, Hamburg, Germany). 10 µL 4x Laemmli buffer were added and the sample was incubated at 95°C for 5 min (ThermoMixer, Eppendorf AG, Hamburg, Germany) to stop the reaction and denaturate the proteins for further analysis by SDS-PAGE.

2.2.2.6. SDS-PAGE, hand-made gels

SDS-PAGE was performed based on Laemmli, 1970. The gel equipment was built by the Heidelberg university workshop. The stacking gel (2 cm x 15 cm x 0.8 mm, 5 % acrylamide, 0.5 % bisacrylamide, 60 mM TRIS/HCl pH 6.8, 0.1 % SDS, 0.05 % APS, 0.1 % TEMED) was prepared on top of the separating gel (8 cm x 15 cm x 0.8 mm, 12 % acrylamide, 0.2 % bisacrylamide, 375 mM TRIS/HCl pH 8.8, 0.1 % SDS, 0.05 % APS, 0.05 % TEMED). Gels were run in SDS-PAGE buffer at 5-8 mA, 200 V, 100 W for approx. 15 h. High current and long running time was used for high resolution of the phosphorylation of WC-1 and WC-2.

2.2.2.7. SDS-PAGE, pre-cast gels

For further analysis of proteins by mass spectrometry, the precast NuPAGE™ 4-12% Bis-Tris gels (8 cm x 8 cm x 0,1 cm, 10 wells, Novex™ by life technologies) were used in the Mini Gel Tank XCell SureLock™ Mini (Novex™ by life technologies). The gels were run in 1x NuPAGE™ MOPS SDS Running Buffer (20X stock, Novex™ by life technologies) at 100 V, 200 mA for 6-7 min and then at 160 V, 200 mA for 1 h.

2.2.2.8. Western Blot

Following SDS-PAGE, proteins were transferred onto nitrocellulose membranes (Amersham Protran 0.45 µm, GE Healthcare, Cat.-No. 10600016) by semi-dry electro blotting at 250 mA (one hand-made gel per blotting chamber) or 400 mA (two hand-made gels per blotting chamber) for 2 h 22 min in transfer buffer. After blotting, the membranes were stained with Ponceau-S staining solution and rinsed with purified water to remove unbound stain. The blotting efficiency and equal loading were checked and the membranes were destained in TBS buffer for 15 min (gently shaking on a rocking shaker). The membranes were blocked 5 % (w/v) milk powder in TBS (5 % milk/TBS) buffer for 30-45 min at rt (gently shaking on a rocking shaker). Depending on the requirements of the primary antibody, the membranes were either probed with the primary antibody in o/n at 4°C and with the secondary antibody for 2 h at rt or with the primary antibody for 2 h at rt and with the secondary antibody o/n at 4°C (always gently shaking on a rocking shaker). All antibodies were diluted in 5 % milk/TBS. Between primary and secondary antibody, the membranes were washed 3x 10 min with TBS buffer at rt (gently shaking on a rocking shaker). After probing with the secondary antibody, the membranes were washed 3x 10 min with TBS buffer at rt (gently shaking on a rocking shaker) and developer solution was added. After very short incubation at rt, chemiluminescent signal were recorded on x-ray films (Fujifilm SuperRX-N, Cat.-No. 47410 19284).

2.2.2.9. Coomassie staining of protein gels

Proteins separated in a precast NuPAGE™ 4-12% Bis-Tris gels (Novex™ by life technologies) were stained with Colloidal Coomassie Brilliant Blue dye. The gel was quickly rinsed in ultrapure water and then incubated in the Coomassie fixing solution for 1 h at rt (gently shaking). After fixing, the gel was incubated in Coomassie staining solution for 2 h at rt (gently shaking). The Coomassie staining solution was exchanged by fresh one and the gel was incubated o/n at 4°C (gently shaking). The next day, the gel was destained in 25 % methanol (ultrapure water) for approx. 30 min at rt until the background was sufficiently removed but the protein bands were clearly visible. The Coomassie-stained gel was stored in ultrapure water at 4°C.

2.2.2.10. Silver staining of protein gels

Silver staining of proteins separated in a precast NuPAGE™ 4-12% Bis-Tris gels (Novex™ by life technologies) was performed with the SilverQuest™ silver stain Kit (SilverQuest™ by life technologies) according to the manufacturer´s protocol. The silver-stained gel was stored in ultrapure water at 4°C.

2.2.2.11. Mass spectrometry

The identification of purified proteins and the analysis of phosphorylation sites of WC-1 and WC-2 by mass spectrometry were performed by the mass spectrometry facility of the Biochemistry Center Heidelberg (BZH, Johannes Lechner) and by the ZMBH Core facility for mass spectrometry and proteomics (ZMBH, Thomas Ruppert). All methods and protocol presented in this section were provided by these two facilities (as indicated).

In-gel digestion of proteins

Coomassie-stained proteins were cut out from gels, the gel slices were washed with 150 µL of water (10 min at rt) and shrunk by incubation with 175 µL acetonitrile (15 min at rt). Acetonitrile was removed, and gel slices were dried in the vacuum. Thiol groups were reduced by incubation with 10 mM DTT in 100 mM ammonium bicarbonate (30 min at 56°C). Gel slices were shrunk, and thiol groups were alkylated by incubation in 55 mM iodoacetamide in the dark (20 min at rt). Gel slices were washed with 100 mM ammonium bicarbonate (15 min at rt), shrunk as above, and rehydrated with 20-24 µL of 20 ng/µL trypsin (Trypsin Gold, Promega, Madison, USA) in 40 mM ammonium bicarbonate (40 min at 0°C). With the exception of 12 µL, the liquid was removed, and samples were incubated at 37°C overnight (Funk *et al.*, 2014). Alternative to trypsin, elastase or thermolysin were used with the same protocol and incubated at 25°C (elastase) or 37°C (thermolysin) (Communication by mass spectrometry facility of the BZH).

LC-MS and sample analysis

The digested peptides present in the supernatant were analyzed online using a LC-MS setup at a nanoAcquity UPLC system (Waters, Milford, USA; 90 min gradient run) coupled with an LTQ Orbitrap XL™ ETD Hybrid Ion Trap-Orbitrap Mass Spectrometer (Thermo Scientific™ by Thermo Fisher Scientific Inc., Waltham, USA) (Communication

by mass spectrometry facility of the BZH and by the ZMBH Core facility for mass spectrometry and proteomics).
All MS/MS samples were analyzed using Mascot (Matrix Science, London, UK; version 2.1.0.81). Mascot was set up assuming the digestion enzyme non-specific (elastase, trypsin) or assuming the digestion enzyme trypsin. Mascot was searched with a fragment ion mass tolerance of 0,50 Da and a parent ion tolerance of 10,0 PPM. Carbamidomethyl of cysteine was specified in Mascot as a fixed modification. Deamidated of asparagine, oxidation of methionine and phosphorylation of serine, threonine and tyrosine were specified in Mascot as variable modifications.
Scaffold (version Scaffold_4.5.3, Proteome Software Inc., Portland, OR) was used to validate MS/MS based peptide and protein identifications. Peptide identifications were accepted if they could be established at greater than 95,0% probability by the Peptide Prophet algorithm (Keller *et al.*, 2002) with Scaffold delta-mass correction. Protein identifications were accepted if they could be established at greater than 95,0% probability and contained at least 2 identified peptides. Protein probabilities were assigned by the Protein Prophet algorithm (Nesvizhskii *et al.*, 2003). Proteins that contained similar peptides and could not be differentiated based on MS/MS analysis alone were grouped to satisfy the principles of parsimony. (Information provided via Scaffold software; Communication by mass spectrometry facility of the BZH and by the ZMBH Core facility for mass spectrometry and proteomics).

2.2.3. DNA, RNA and cloning methods

2.2.3.1. Extraction of genomic DNA from *N. crassa*

500 µL pre-warmed 60°C 2xCTAB buffer were added to 300 µL frozen *N. crassa* mycelia powder and mixed immediately with a spatula. The suspension was incubated at 60°C and 400rpm for 30 min (ThermoMixer, Eppendorf AG, Hamburg, Germany). An equal volume (800 µL) of chloroform/isoamylacohol (24:1) was added at rt and the mix was incubated with frequent inverting (on a turning wheel) for 10 min. The mix was centrifuged at 2000 g and rt for 10 min (Centrifuge 5415 D, Eppendorf AG, Hamburg, Germany). The upper, aqueous phase of the supernatant was transferred to a fresh tube, 1 µL RNase A (10 mg/mL stock) was added and the solution was incubated at 37°C for 30 min (ThermoMixer, Eppendorf AG, Hamburg, Germany). 0,7 volumes of isopropanol were added (350 µL isopropanol for 500 µL supernatant) to precipitate the genomic DNA (gDNA), the solution was inverted 4-6 times and centrifuged at 14000 g and rt for 30 min. The supernatant was discarded, the pellet was washed with 1 mL -20°C cold 70% EtOH and centrifuged again at 14000 g and rt for 5 min. The pellet was dried at 37°C for 10 min (ThermoMixer, Eppendorf AG, Hamburg, Germany) and resuspended in 250 µL ultrapure water. The pellet was resolved o/n at 4°C. The gDNA concentration was measured with the NanoDrop ND-1000 UV-Vis Spectrophotometer (NanoDrop Technologies LLC by Thermo Fisher Scientific Inc., Waltham, USA) and set to 150 ng/µL. For PCR, 1 µL gDNA 150 ng/µL were used per 25 µL PCR reaction mix.

2.2.3.2. Extraction of Plasmids from *E. coli*

For the extraction of Plasmids from *E .coli*, 3 mL fresh culture in LB medium (see 2.2.3.10) were used and processed with the GeneJET Plasmid Miniprep Kit (Thermo Scientific™ by Thermo Fisher Scientific Inc., Waltham, USA) according to the manufacturer´s instructions. The concentration of the plasmid DNA solution was measured with the NanoDrop ND-1000 UV-Vis Spectrophotometer (NanoDrop Technologies LLC by Thermo Fisher Scientific Inc., Waltham, USA).

2.2.3.3. PCR

PCR was performed with Q5 Polymerase (New England Biolabs Inc., Ipswich, USA) according to the manufacturer´s instructions. Primers were designed using the SerialCloner 2.6.1 software (http://serialbasics.free.fr/Home/Home.html), the Oligonucleotide Properties Calculator (http://biotools.nubic.northwestern.edu/OligoCalc .html) and the NEB T_m calculator (http://tmcalculator.neb.com/#!/main). Thermocycling was performed in Labcyclers with and without gradient (SensoQuest GmbH, Göttingen, Germany).

When PCR from a plasmid was performed, the template plasmid was digested after PCR reaction by addition of 1 µL DpnI (New England Biolabs Inc., Ipswich, USA) per 50 µL PCR reaction mix and incubation at 37°C for 1 h.

The PCR product was purified with the Wizard®SV Gel and PCR Clean-Up System (Promega GmbH, Walldorf, Germany) according to the manufacturer´s instructions.

2.2.3.4. Sequencing of DNA

Sequencing primer were designed using the SerialCloner 2.6.1 software (http://serialbasics.free.fr/Home/Home.html), the Oligonucleotide Properties Calculator (http://biotools.nubic.northwestern.edu/OligoCalc.html) and the NEB T_m calculator (http://tmcalculator.neb.com/#!/main).

Sequencing results were analyzed using the SerialCloner 2.6.1 software and the MultAlin online tool (Corpet, 1988).

2.2.3.5. Restriction digestion of DNA

Plasmids and PCR products were digested with restriction enzymes for the purpose of linearization and transformation in *N. crassa* or for the purpose of cloning in *E. coli*. At maximum 6000 ng DNA per 100 µL total reaction volume were incubated with the required restriction enzymes and the corresponding buffer (both purchased from New England Biolabs Inc., Ipswich, USA) at 37°C for 2 h (incubator, BINDER GmbH, Tuttlingen, Germany). In the rare case, that a restriction enzyme required a temperature different from 37°C, the incubation was performed in a ThermoMixer (Eppendorf AG, Hamburg, Germany). Appropriate restriction enzymes were identified and selected based on the respective DNA sequence with the SerialCloner 2.6.1 software (http://serialbasics.free.fr/Home/Home.html). The reaction mix was purified via an agarose gel or directly with the Wizard®SV Gel and PCR Clean-Up System (Promega GmbH, Walldorf, Germany) according to the manufacturer´s instructions.

2.2.3.6. Agarose gels

Agarose gel electrophoresis was performed to either analyse or purify DNA. The gels were casted with either 1 % or 0.7 % agarose in TAE buffer, supplemented with ethidium bromide (Cat.-No. A2273, Applichem GmbH, Darmstadt, Germany). Prior to loading, gel loading dye (Cat.-No. B7024S, New England Biolabs Inc., Ipswich, USA) was added to the DNA samples. The electrophoresis was performed in TAE buffer at 110 V for 30 – 45 min. The separation of DNA molecules in the gel was visualized using UV light (wavelength 312 nm, Intas transillumninator, Intas Science Imaging Instruments GmbH, Göttingen, Germany) and pictures were taken with a camera. DNA bands were excised in UV light with a scalpel and the DNA was extracted using the Wizard®SV Gel and PCR Clean-Up System (Promega GmbH, Walldorf, Germany) according to the manufacturer´s instructions.

2.2.3.7. Ligation of DNA

DNA fragments were ligated using T4 DNA ligase (Cat.-No. M0202, New England Biolabs Inc., Ipswich, USA). The reaction was set up according to the manufacturer´s protocol. 70 ng vector backbone were used, the corresponding volume (µL) of insert was calculated according to the following formula.

$$\frac{insert\ length\ (bp)}{vector\ length\ (bp)} \times 70\ ng\ \div concentration\ insert\ \left(\frac{ng}{\mu L}\right) \times multiplication\ factor$$

The multiplication factor was derived from the vector-to-insert ratio. Usually, the ration 1:2 was tried first and depending on the success of the ligation, different ratios (1:1, 1:4, etc.) were tried. The ligation reaction mix was incubated at rt for 30 min and either transformed in *E. coli* or stored at -20°C.

2.2.3.8. PCR-based cloning

For PCR-based cloning, overlapping DNA-fragments were generated by PCR. Residual PCR template in 2000-2500 ng of purified PCR product (Wizard®SV Gel and PCR Clean-Up System, Promega GmbH, Walldorf, Germany) was removed by digestion with DpnI in NEBuffer™ 2.1 (both New England Biolabs Inc., Ipswich, USA) acc. to manufacturer´s instruction. T4 DNA Polymerase (New England Biolabs Inc., Ipswich, USA) was added and reaction was performed acc. to manufacturer´s instruction to fill the ends of the PCR products. The ligation of the overlapping DNA-fragments was performed *in vivo* in *E. coli*. The amount of vector and insert was calculated as described in 2.2.3.7 but 2100-2500 ng instead of 70 ng vector in 51 µL final volume were used. The transformation of *E. coli* described in 2.2.3.10 was slightly modified: 25 min incubation of DNA and cells on ice, 60 min incubation in SOC.

2.2.3.9. Site-directed mutagenesis

This protocol for site-directed mutagenesis was kindly provided by Dr. Linda Lauinger. The primers were designed acc. to the following criteria: 25-45 bp in length, melting temperature of ≥78°C, minimum GC content of 40 %, mutations in the middle of the primer, full overlap of the forward and reverse primer. The melting temperature was

calculated acc. to the formula T_m = 81,5 + (0.41* x % GC content) – (675 / N - x % mismatch) with N= primer length in bases and values for % = whole numbers. The reaction was set up as in Table 2.9 and PCR was run acc. to Table 2.9 overnight. 1 µL of the PCR mix was kept for transformation control. 1 µL DpnI (New England Biolabs Inc., Ipswich, USA) was added to the remaining 50 µL PCR mix, mixed well and incubated at 37°C for 1 h. Transformation of *E. coli* was performed with 1 µL transformation control, 1 µL and 2 µL of DpnI-treated PCR mix. The remaining solution was stored at -20°C. In case the transformation of *E. coli* was not successful, 5 µL of DpnI-treated PCR mix were transformed.

Table 2.9: Reaction set up, template preparation and thermocycling protocol for site-directed mutagenesis.

Mutagenesis Reaction set up	**stock**	**final conc.**	**final vol.**
Pfu Buffer	10 x	1 x	5,00 µl
dNTPs	10 mM	0,1 mM	1,50 µl
Forward primer	125 ng/µl	2,5 ng/µl	1,00 µl
Reverse primer	125 ng/µl	2,5 ng/µl	1,00 µl
DMSO	100%	2%	3,00 µl
DNA	see template below		1,00 µl
Pfu Ultra polymerase	5 U/µl	0,1 U/µl	0,15 µl
H_2O	-	add to 51 µl	38,00 µl

Polymerase purchased from Bioron International (Ludwigshafen, Germany)

Mutagenesis template	**stock**	**final conc.**	**elongation**
Vector DNA	10 ng/µl	0,2 ng/µl	70 sec/1 kb

Mutagenesis Cycle step	**temperature**	**time**	**Cycle**
Initial denaturation	94°C	2 min	1
Denaturation	94°C	50 sec	
Annealing	60°C	50 sec	18
Extension	68°C	see template	
Final extension	68°C	15 min	1
Storage	12°C	∞	1

2.2.3.10. Transformation and cultivation of *E. coli*

50 µL chemically competent *E. coli* DH5α cells were thawed on ice and at maximum 5 µL DNA were added and gently mixed with the cells. The cells were incubated 15-20 min on ice, heat-shocked at 37°C for 30 sec (ThermoMixer, Eppendorf AG, Hamburg, Germany) and cold-shocked on ice for 2 min. If a transformation failed once, the heat shock and the cold shock were repeated once. For the retransformation of plasmids, the cells were directly added to 50 mL LB medium supplemented with antibiotics (usually ampicillin) and incubated gently shaking at 37°C o/n. For colony selection, 200 µL SOC medium were added and the cells were incubated gently shaking at 37°C for 45 min. The cell suspension was plated on a pre-warmed solid LB medium plate supplemented with the respective antibiotics and incubated at 37°C o/n (incubator, BINDER

GmbH, Tuttlingen, Germany). The next day, clones were picked, transferred to 3 mL LB medium supplemented with antibiotics (usually ampicillin), and grown gently shaking at 37°C o/n. The cells were harvested and the plasmids were extracted for further analysis (sequencing, restriction digestion, PCR) as described above (see 2.2.3.2).

2.2.3.11. Extraction of RNA from *N. crassa*

500 µL peqGOLD Trifast (Cat.-No. 30-2010, peqlab, VWR International GmbH, Darmstadt, Germany) were added to 50 µL frozen *N. crassa* mycelia powder and mixed immediately by vortexing. The samples were incubated at 37°C and 800 rpm for 5 min (ThermoMixer, Eppendorf AG, Hamburg, Germany). The samples were transferred on ice, 100 µL chloroform were added and mixed vigorously by vortexing for 15 s per sample. The samples were incubated again at 37°C and 800 rpm for 5 min and then centrifuged at 12000g, 4°C for 10 min (Centrifuge 5417 R, Eppendorf AG, Hamburg, Germany). The upper phase was transferred to a fresh tube, 250 µL isopropanol (4°C / ice-cold) were added mixed by inverting. The precipitation was performed on ice for 10 min and the precipitate was pelleted at 12000g, 4°C for 10 min. The samples were transferred on ice and the supernatant was removed thoroughly. The pellet was washed twice with 500 µL 75 % ethanol (vortexing, then pelleting at 12000g, 4°C for 10 min). The supernatant was removed thoroughly and the pellet was dried for 3-10 min at rt. The RNA pellet was resolved in 150 µL RNAse-free water at 60°C, 800 rpm for 10 min (ThermoMixer, Eppendorf AG, Hamburg, Germany). The concentration of the RNA solution was measured with the NanoDrop ND-1000 UV-Vis Spectrophotometer (NanoDrop Technologies) and the solution was stored at -80°C.

2.2.3.12. cDNA synthesis and qPCR

Total cDNA from *N. crassa* was synthesized using the Maxima First Strand cDNA Synthesis Kit (Cat.-No. K1642, Thermo Scientific™ by Thermo Fisher Scientific Inc., Waltham, USA) according to the manufacturer's instructions. The minimum reaction volume amounted to10 µL and contained 0,5 µg total RNA. The cDNA was diluted 1:3 in ultrapure water.

Strand specific cDNA of *frq sense* was synthesized using the QuantiTect Reverse Transcription Kit (Cat.-No. 205314, Qiagen N.V., Venlo, Netherlands) with specific primers (final concentration 0.5 µM) according to the manufacturer's instructions. cDNA was diluted 1:4 in ultrapure water.

Primer and TaqMan probes were for quantitative real-time PCR (qPCR) designed using the SerialCloner 2.6.1 software (http://serialbasics.free.fr/Home/Home.html), the Oligonucleotide Properties Calculator (http://biotools.nubic.northwestern.edu/OligoCalc.html) and the NEB T_m calculator (http://tmcalculator.neb.com/#!/main). qPCR was performed using the qPCRBIO Probe Mix Hi-ROX (Cat.-No. PB20.22-51, PCR Biosystems Ltd., London, UK) in 96-well plates. The reaction mix qPCR was set up as shown in Table 2.10.

Table 2.10: Reaction set up for qPCR

Component	Volume
cDNA	4 µL
2x qPCRBIO Probe Mix Hi-ROX	10 µL
Forward primer 10 µM	0,8 µL
Reverse primer 10 µM	0,8 µL
Probe (TaqMan) 5 µM	0,8 µL
Water	3,6 µL
	Σ 20 µL

Thermocycling was performed in the StepOnePlus real-time PCR system (Applied Biosystems® by by Thermo Fisher Scientific Inc., Waltham, US) under conditions shown in Table 2.11. The mean cycle threshold values (C_t values) were calculated from triplicates.

Table 2.11: qPCR thermocycling protocol.

Step	Temperature	Time	Cycles
Initial denaturation	95 °C	2 min	-
Denaturation	95 °C	5 s	40
Annealing and extension	60 °C	20 s	

2.2.4. Chromatin Immunoprecipitation (ChIP)

The data generated with Chromatin Immunoprecipitation and subsequent analysis of the samples were kindly provided by Michael Oehler. See the method section of the PhD thesis of Michael Oehler, title “Light-induced White Collar Complex has a dual function as combined transcriptional activator and repressor”, Heidelberg University, Heidelberg, Germany for further details (Oehler, 28.02.2020).

3. Results

3.1. Mapping of phosphorylation sites of WC-1 and WC-2

So far, only 10 phosphorylation sites of WC-1 and only one phosphorylation site of WC-2 was known. In previous studies (He *et al.*, 2005; Sancar *et al.*, 2009), the purified proteins were digested with trypsin for the analysis by mass spectrometry. However, trypsin cleavage sites are rare in the amino acid sequence of both WC-1 and WC-2, so the sequence coverage is low.

The aim of this experiment was to identify dark- and light specific phosphorylation sites by using the unspecific cleaving enzymes elastase and thermolysin. To evaluate the raw data, it was necessary to take details of the respective methods into account (see Table 3.1). Initially, a tandem (two-step) affinity purification of dark-grown and light-induced samples was performed in January 2014 (Figure 3.1) as well as in March 2014 (5.1Figure 5.1). By using the same biological material twice, numerous phosphorylation sites were mapped but also limitations of the sample preparation and the mass spectrometry were uncovered.

Table 3.1: Overview over the four experiments used to map the phosphorylation sites of WC-1 and WC-2.
See also Figure 3.1, Figure 5.1, Figure 5.2 and Figure 5.3.

PURIFICATION	JANUARY 2014	MARCH 2014	JANUARY 2016	JULY 2016
BIOLOGICAL MATERIAL	Δ*wc-2, bd, qa-2 tap- wc-2* (same experiment used for both purifications)		*wt, bd*	*wt, bd*
DARK / LIGHT	DD24, LI 15 min		DD24, LI 30 min	LL
CROSSLINKING	10 min formaldehyde		-	-
PURIFICATION METHOD	Tandem affinity purification (TAP) of tagged WC-2	Tandem affinity purification (TAP) of tagged WC-2	IP with anti-WC-2 antibody	IP with anti-WC-2 antibody
PURPOSE	Phosphorylation sites of WC-1 and WC-2, Interaction partners	Phosphorylation sites of WC-1 and WC-2, Interaction partners	Phosphorylation sites of WC-2 (Search for T473, S476, S484)	Search for phosphorylation on WC-2 T473, S476, S484
MS METHOD	ESI, Orbitrap	ESI, Orbitrap	ESI, Orbitrap	ESI, Orbitrap
ENZYME 1	Elastase	Elastase	Elastase	-
ENZYME 2	Thermolysin	Thermolysin	Thermolysin	-
ENZYME 3			Trypsin	Trypsin
SEQUENCE COVERAGE WC-1	95,5 %			
SEQUENCE COVERAGE WC-2	100 %			

For further identification of phosphorylation sites of WC-2, the protein was enriched by immunoprecipitation with an anti-WC-2 antibody (see Figure 5.2 and Figure 5.3 in the appendix) and trypsin was used in addition to the unspecific proteases to increase the specificity of the mass spectrometry by searching for predictable peptides. However, the sequence coverage of trypsin amounts to only approx. 50% in case of WC-2 whereas elastase and thermolysin cleavage products cover approx. 80-90% of WC-1 and 80-99% of WC-2. Taken all samples together, 95,5 % of the sequence of WC-1 were covered and 100% of the sequence of WC-2 were covered (Table 3.1).
In the first experiment, yielding the material for the purifications in January and March 2014, samples were harvested after 24 h in dark (0 min sample) and after 24 h in dark followed by 15 min light-induction (15 min sample). After 15 min in light, the phosphorylation of WC-1 and WC-2 is on an intermediate level (see Figure 1.7). This phosphorylation status was chosen to allow both the mapping of phosphorylation sites and the pull-down of a kinase. After 15 min in light, the phosphorylation of WCC is high in comparison to hypophosphorylated WCC in darkness but after 15 min in light WCC is still further phosphorylated meaning that kinases should interact with WCC and could be trapped by crosslinking. In the third experiment, samples were harvested after 24 h in dark and after 24 h in dark followed by 30 min light-induction to analyze WC-2 at the time point of maximum phosphorylation. For a very specific analysis of WC-2 in the fourth experiment, samples were grown in constant light, when the phosphorylation of WC-2 is also at the maximum.

3.1.1. Limitations of the methods used to map phosphorylation sites

When using the unspecific cleaving enzymes elastase and thermolysin, the comparability of samples is limited and the quantification of results is not possible. This became obvious by comparing a dark- and a light sample as well as by comparing the two purifications of the same biological material in January and March 2014. When two peptides from two samples differ by only one amino acid in length, the elution properties from the chromatography column, the electron spray ionization properties, the flight properties and the fragmentation pattern change. Also, the automatic selection of peptides in the first MS for the fragmentation in the second MS is changed. Thus, conclusions from the comparison of samples have to take these limitations into account.
Furthermore, the absolute number of phosphorylation sites is questionable because of numerous putative phosphorylation sites. These are sites that were found together with other possible phosphorylation sites in a peptide but couldn´t be located exactly due to an incomplete fragmentation spectrum of the peptide.

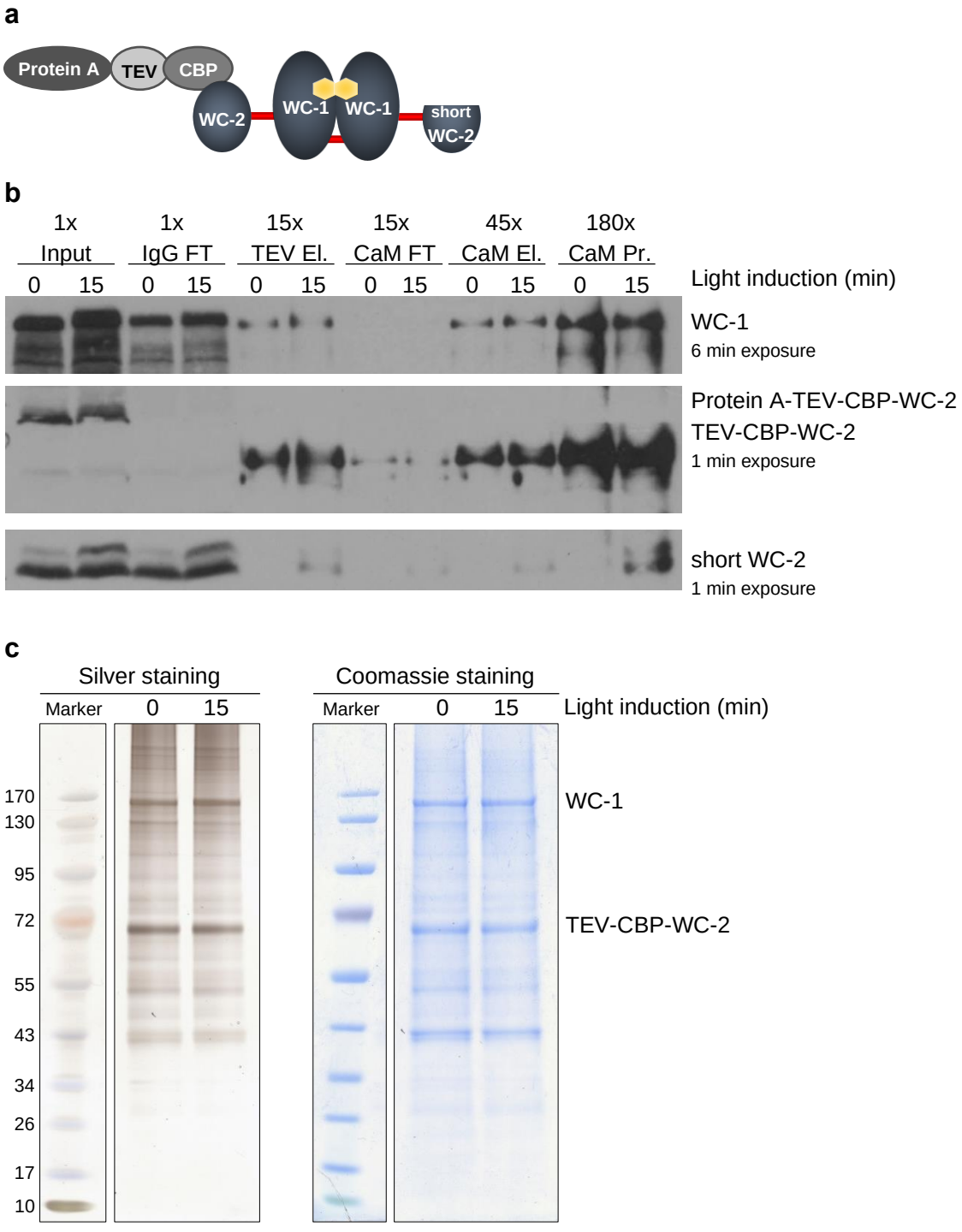

Figure 3.1: Result of the tandem affinity purification (TAP) of tagged WC-2
in January 2014 (see Figure 5.1 in the appendix for March 2014). **3.1a:** Schematic presentation of the cross-linked (red bars) complex that is pulled down in light. Protein A = first part of the TAP tag; TEV = cleavage site for TEV protease; CBP = calmodulin binding protein, second part of the TAP tag. **3.1b**: Western blot showing the different stages of TAP: the input, the IgG flow through (IgG FT), the TEV elution (TEV El), the Calmodulin flow through (CaM FT), the Calmodulin elution (CaM El) and the precipitation of the total protein from Calmodulin elution (CaM Pr). **3.1c**: Silver staining and Coomassie staining of the SDS gels. The Calmodulin precipitation (CaM Pr) samples were loaded. Molecular weight marker in kDa.

3.1.2. Phosphorylation sites of WC-1

In this study, 34 phosphorylation sites were mapped (see Table 3.2, Figure 3.2, Figure 3.3, see Table 5.1 and Table 5.2 in the appendix). Among these 34 sites, 27 are new phosphorylation sites of WC-1. In total, 10 phosphorylation sites of WC-1 are known from previous studies (He *et al.*, 2005; Sancar *et al.*, 2009), but only 7 of these sites were confirmed in this study. Out of 34 phosphorylation sites, 19 sites were found unique on a peptide and 15 sites remain putative phosphorylation sites.

Table 3.2: Detailed list of phosphorylation sites of WC-1 found in this and in previous studies.
Remarks indicated by asterisks are explained in chapter 3.1.2.

SITES FOUND IN THIS STUDY

no.	aa	S, T	aa+1	putative?	LI	DD	Remark	found previously
1	111	S	V	single	LI	DD		
2	200	**S**	**P**	**single**	LI	-	*1	
3	315	**S**	**P**	**single**	LI	DD		Sancar *et al*., 2009 (LL)
4	*317*	*S*	*L*	*putative*	LI	-	*2	Sancar *et al*., 2009 (LL)
5	334	S	V	single	LI	DD		
6	336	T	N	single	LI	DD		
7	340	**T**	**P**	**single**	LI	DD		
8	*346*	*S*	*T*	*putative*	-	DD	*3	
9	347	**T**	**P**	**single**	LI	DD		
10	536	**T**	**P**	**single**	LI	-	*4	
11	*824*	*S*	*P*	*putative*	LI	DD	*5	
12	831	**S**	**P**	**single**	LI	DD		Sancar *et al*., 2009 (LL)
13	*863*	*S*	*A*	*putative*	-	DD	*6	
14	*866*	*S*	*S*	*putative*	-	DD	*7	
15	867	S	A	single	LI	DD		
16	967	T	G	single	LI	-	*8	
17	971	**S**	**P**	**single**	LI	DD		
18	*988*	*S*	*N*	*putative*	LI	-	*9	He *et al.*, 2005 (in DD), Sancar *et al*., 2009 (LL)
19	990	**S**	**P**	**single**	LI	-	*10	He *et al.*, 2005 (in DD), Sancar *et al*., 2009 (LL)
20	1005	**S**	**P**	**single**	LI	DD		Sancar *et al*., 2009 (LL)
21	*1007*	*S*	*T*	*putative*	-	DD	*11	
22	*1008*	*T*	*T*	*putative*	-	DD	*12	
23	*1009*	*T*	*T*	*putative*	LI	DD	*13	
24	*1010*	*T*	*A*	*putative*	LI	DD	*14	
25	*1012*	*T*	*K*	*putative*	LI	DD	*15	
26	1015	**S**	**P**	**single**	LI	DD		Sancar *et al*., 2009 (LL)
27	1017	S	L	single	LI	DD		
28	1021	S	S	single	LI	-	*16	
29	*1022*	*S*	*T*	*putative*	LI	-	*17	
30	*1023*	*T*	*T*	*putative*	LI	-	*18	

31	*1024*	*T*	*A*	*putative*	LI	-	*19	
32	*1071*	*S*	*G*	*putative*	LI	-	*20	
33	1074	**S**	**P**	**single**	LI	DD		
34	1166	S	V	single	LI	DD		

SITES FOUND PREVIOUSLY BUT NOT IN THIS STUDY								
no.	**aa**	**S, T**	**aa+1**	**putative?**	**LI**	**DD**	**Remark**	**found previously**
(35)	992	S	H	-	-	-	-	He *et al.*, 2005 (in DD)
(36)	994	S	S	-	-	-	-	He *et al.*, 2005 (in DD)
(37)	995	S	P	-	-	-	-	He *et al.*, 2005 (in DD), Sancar *et al*., 2009 (LL)

SUMMARY	
single, not followed by proline:	8 sites
single, followed by proline:	11 sites
putative sites:	15 sites
confirmed previous studies:	7 sites
found new in this study:	27 sites
found in previous studies, but not here:	3 sites

No light- or dark-specific sites on WC-1

Giving the high number of phosphorylation sites of WC-1 and the huge shift of the WC-1 signal in the SDS-gel due to increasing phosphorylation, it was expected to identify light- and may be also dark-specific phosphorylation sites. Surprisingly, the majority of phosphorylation sites were detected in the dark as well as in the light (see Table 3.2). Several sites appear to be either light- or dark-specific, but detailed analysis of the peptides rejects this conclusion.

Phosphorylation sites like S315, S831 and S1015 were found unique on up to six peptides and additionally on more peptides where the phosphorylation couldn´t be located exactly. They were found in both purifications of the same biological material in January 2014 and in March 2014. Interestingly, such phosphorylation sites were found in the dark- as well as in the light-sample (see Table 5.1 and Table 5.2 in the appendix).

In contrast to that, the phosphorylation sites S200, T536 and T967 (*1, *4 and *8 in Table 3.2), were found unique on only one peptide in the light-sample of only one out of two purifications of the same biological material. Hence, these are most likely peptides that hardly elute from the column or hardly ionize. The phosphorylated peptides in the respective dark-samples have rather not be found for technical reasons then are not existent. The loss of phosphorylation due to storage of the biological material at -80°C can be excluded as root cause since S200 and T536 were found in March 2014, approx. two months after the first purification in January 2014. Whereas S200, T536 and T967 were found unique on only one peptide in light in one purification, other unique phosphorylation sites like S971 were found on one peptide in light and on one peptide in dark in only one out of two purifications of the same biological material. This indicates

that some peptides are either rare or, most likely, difficult to detect by mass spectrometry due to their molecular properties. The analysis of the sequence coverage of WC-1 in the 8 individually digested samples (January / March, 0 min / 15 min, elastase / thermolysin = 8 samples) showed that all phosphorylation sites were found in regions of high sequence coverage (Figure 3.2). Thus, numerous peptides were found that cover the respective site but it might be a rarely phosphorylated site or the phosphorylated peptide may have unfavorable chemical properties that interfere with fragmentation and detection during mass spectrometry.

Other examples are the potential light-specific phosphorylation sites S1021, S1022, T1023, T1024 (*16-*19 in Table 3.2). Three peptides were found: S1021 was found unique on the first peptide, one out of the four potential phosphorylation sites must be phosphorylated on the second peptide and on the third peptide, either S1022 or T1023 are phosphorylated. All the three peptides were found in light in the purification in March 2014, but not in the purification in January 2014. Thus, S1021 is definitely phosphorylated and either S1022 or T1023 is phosphorylated as well. Whether three or four sites are phosphorylated in vivo cannot be concluded from this data. Since no phosphorylated sites S1021, S1022, T1023, T1024 were found in the dark sample in March 2014, these sites might be light-specific sites. But since not even S1021 was found phosphorylated in the purification of the light-sample in January 2014, it is highly doubtful, whether this is a true light-specific phosphorylation site.

In many cases, putative phosphorylation sites occur in close vicinity on the same peptide as phosphorylation sites that were also found unique on a peptide. These putative sites appear in a light- or a dark-sample only because the fragmentation pattern of a peptide is incomplete and the phosphorylation cannot be located exactly. But in the same sample, several peptides are detected with higher fragment coverage that prove the existence of the unique phosphorylation site both in light and in dark. Thus, the existence of these putative phosphorylation sites is doubtful and the light- or dark-specificity is even more doubtful. Examples are the putatively phosphorylated S317 in vicinity to S315 (*2 in Table 3.2), the putatively phosphorylated S346 before T347 (*3 in Table 3.2), the putatively phosphorylated sites S863 and S866 appearing on peptides together with S867 (*6 and *7 in Table 3.2), and the putatively phosphorylated S1071 in vicinity to S1074 (*20 in Table 3.2). This evaluation is supported by the fact that the putative phosphorylation site S824 (*5 in Table 3.2) was found once in light and once in dark on the same peptide as the unique site S831.

Another special case is the S,T-rich stretch comprising the unique phosphorylation sites S1005, S1015, S1017 and the putative phosphorylation sites S1007, T1008, T1009, T1010 and T1012 (*11-*15 in Table 3.2). Most of these sites were found in light as well as in dark. Some of the peptides contained putative phosphorylation sites together with unique sites, indicating that the unique site is the actual phosphorylation site. But some of the peptides contained the putative sites S1007 - T1012 only. Thus, some of these putative sites are actually phosphorylated *in vivo*.

Remarkably, the previously found phosphorylation sites S988 and S990 (*9, *10 in Table 3.2) were hardly confirmed in this study. Only two peptides were found in light in only one out of two purifications of the same biological material. On the first peptide, S990 was located exactly and on the second peptide, either S988 or S990 are phosphorylated. Since S988 is only a putative phosphorylation site and since in total only two peptides were found in one sample in light, it is very doubtful that these are true light-specific phosphorylation sites.
The observation that there are neither dark- nor light-specific phosphorylation sites leads to the conclusion that there is a pool of poorly and differently phosphorylated WC-1 molecules in the cell in darkness so that every phosphorylation site can be detected in the dark-sample. The kinases are active in darkness but the efficiency of the phosphorylation is low. Light strongly enhances the efficiency of the kinase activity and creates a pool of highly phosphorylated WC-1 molecules.

No phosphorylation of known protein domains of WC-1

Interestingly, no phosphorylation sites were found in one of the known protein domains of WC-1 like the LOV-, the PAS B, the PAS C and the ZnF- domain (Figure 3.2). The two PolyQ domains of WC-1 were not covered by peptides but there are no serine, threonine or trypsin residues in these domains anyway. As a consequence, phosphorylation of WC-1 does obviously not alter the function of one of the known protein domains. There are accumulations of phosphorylation sites upstream of the LOV-domain and especially downstream of the zinc finger DNA-binding domain indicating a regulatory impact on the activity of WCC. However, the phosphorylation sites of WC-1 were not further investigated in this study.

SP/TP sites are overrepresented on WC-1

The arrangement of phosphorylation sites of WC-1 in Figure 3.2 clearly shows that SP and TP sites are overrepresented. Among 34 phosphorylation sites of WC-1, 15 sites are putative phosphorylation sites, 8 unique sites are followed by other amino acids than proline and 11 unique sites are followed by proline. S824P is the only putative site followed by proline, so, there might be in total 12 phosphorylation sites followed by proline. The result that 11 out of 12 SP, TP sites are unique sites covered by multiple peptides indicates that proline-directed kinases are key-components of the mechanism of the phosphorylation of WC-1. Interestingly, the distribution of SP, TP sites over the protein sequence of WC-1 follows the overall pattern of an N-terminal and C-terminal cluster.
Proline-directed phosphorylation by proline-directed kinases of the group MAPKs and CDKs often serve as priming phosphorylation for phospho-directed kinases as CK1 and GSK3 (Pinna and Ruzzene, 1996). Since the SP, TP phosphorylation sites on WC-1 occur along with SX, TX sites, the SP, TP might serve as priming phosphorylation for FRQ-mediated phosphorylation by CK1a.

As shown in the amino acid sequence in Figure 3.3, numerous SP, TP sites of WC-1, especially in the N-terminal region, were not found phosphorylated. Also, numerous serine and threonine over the whole amino acid sequence of WC-1 residues were not found phosphorylated indicating that the 34 phosphorylation sites mapped in this study may not represent the all possible phosphorylation sites of WC-1.
Despite the large number of phosphorylation sites and the obvious activity of proline-directed kinases, no conserved phosphorylation motifs were identified that would give information about the kinases acting on WC-1.

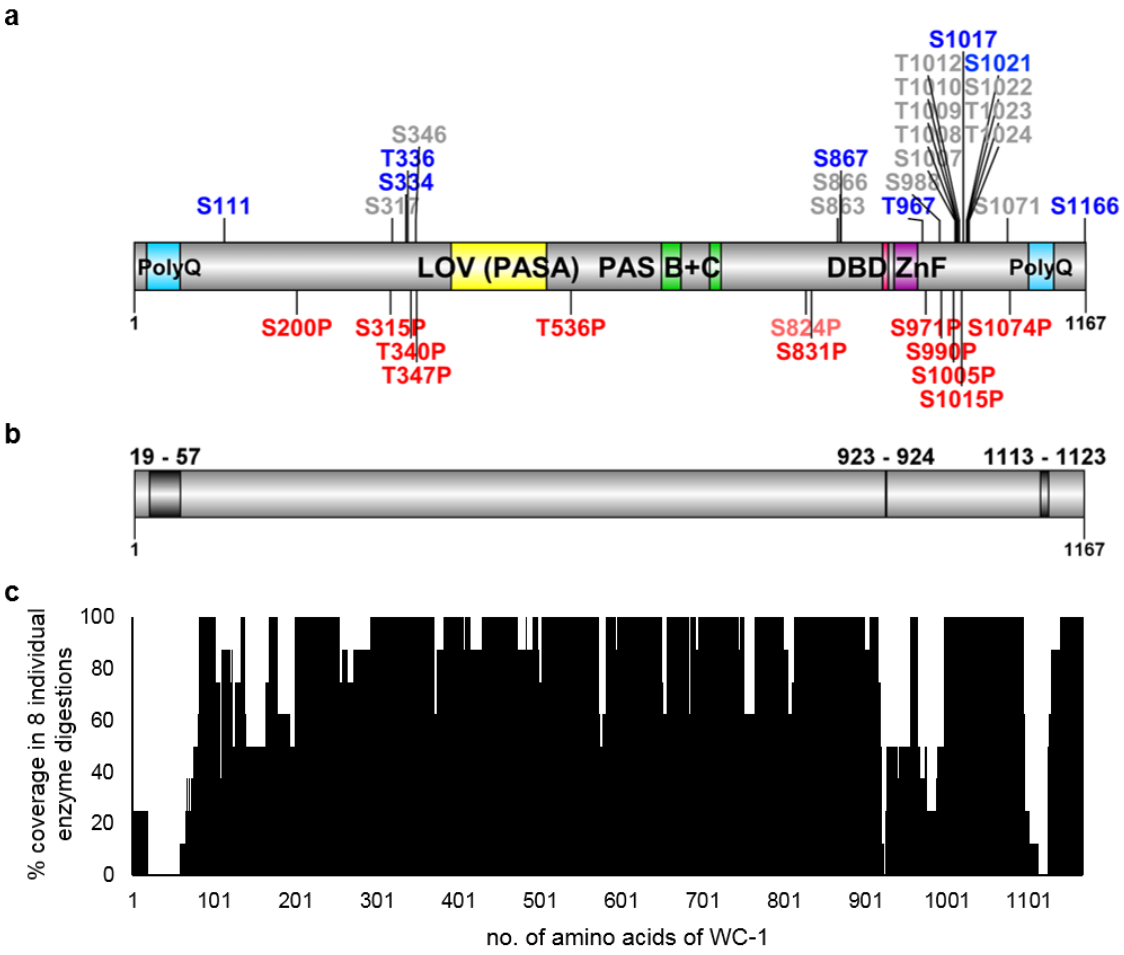

Figure 3.2: Phosphorylation sites of WC-1 in context of the known protein domains and the sequence coverage.
3.2a: Phosphorylation sites of WC-1 in context of the known protein domains. **3.2b:** The sequence coverage of WC-1 amounts to 95,5 %. Mainly the PolyQ domains were not covered. **3.3c:** The sequence coverage of 8 individual digested samples were summed up to identify regions of high- and of low coverage.

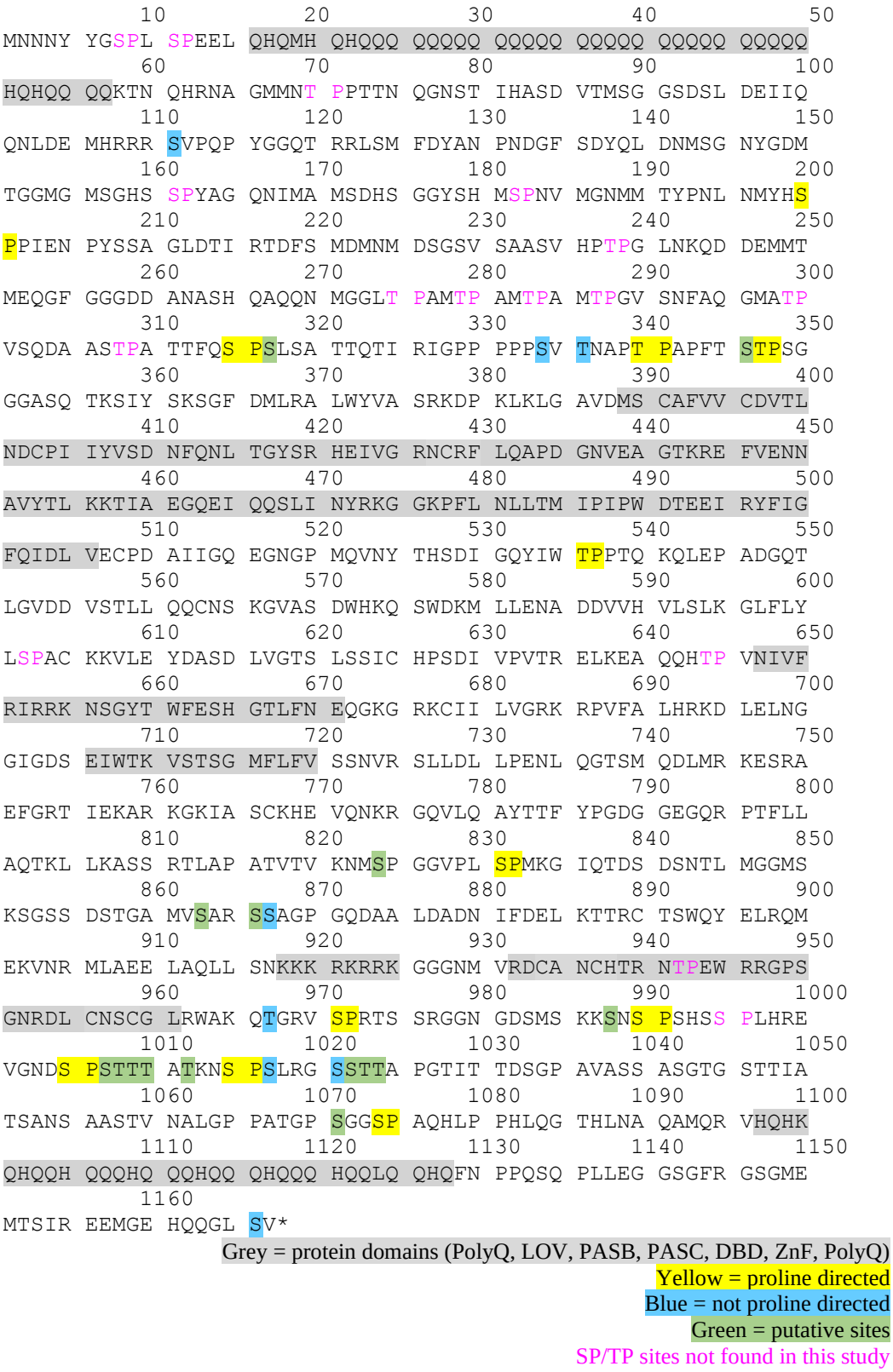

Figure 3.3: The distribution of phosphorylation sites of WC-1 over the amino acid sequence.

3.1.3. Phosphorylation sites of WC-2

Table 3.3: Detailed list of phosphorylation sites of WC-2 found in this and in a previous study. Results from this study are obtained from two tandem-affinity-purifications of the same biological material and two immunoprecipitations of different biological material.

no.	aa	S, T	aa+1	putative?	LI	DD	Remark	found previously
1	*80*	*S*	*M*	*putative*	LI	DD		
2	82	S	N	single	LI	DD		
3	86	**T**	**P**	**single**	LI	DD		
4	118	**S**	**P**	**single**	LI	DD		
5	*128*	*S*	*S*	*putative*	-	DD	*1	
6	*129*	*S*	*A*	*putative*	-	DD	*2	
7	136	**T**	**P**	**single**	LI	DD		
8	138	T	T	single	LI	DD		
9	*139*	*T*	*T*	*putative*	LI	DD		
10	*140*	*T*	*T*	*putative*	LI	DD		
11	*141*	*T*	*S*	*putative*	LI	DD		
12	*142*	*S*	*G*	*putative*	LI	-	*3	
13	287	T	K	single	-	DD	*4	
14	331	S	Q	single	LI	DD		
15	*336*	*S*	*D*	*putative*	LI	DD		
16	339	**T**	**P**	**single**	LI	DD		
17	341	S	D	single	LI	DD		
18	*344*	*T*	*A*	*putative*	-	DD	*5	
19	*390*	*S*	*R*	*putative*	-	DD	*7	
20	394	S	I	single	LI	DD		
21	433	**S**	**P**	**single**	LI	DD		Sancar *et al*., 2009 (LL)
22	435	T	L	single	LI	DD		
-	*473*	*T*	*L*	*putative*	LI	DD	*artefacts from first experiment (purifications in January and March 2014)*	
-	*476*	*S*	*P*	*putative*	LI	DD		
-	*484*	*S*	*G*	*putative*	-	DD		
23	523	**T**	**P**	**single**	LI	DD		

SUMMARY	
single, not followed by proline:	7 sites
single, followed by proline:	6 sites
putative sites:	10 sites
found in previous studies:	1 site
found new in this study:	22 sites
found in previous studies, but not here:	0 sites

In total, 23 phosphorylation sites were mapped on WC-2 (see Table 3.3, Figure 3.4, Figure 3.5, see Table 5.3, Table 5.4, Table 5.5 in the appendix). In Table 3.3, three additional phosphorylation sites (T473, S476, S484) are listed but these sites were an artefact of the

first experiment, as outlined later. So far, only one phosphorylation site of WC-2 was known (Sancar *et al.*, 2009), this site was confirmed in this study and 22 new sites were identified. Out of 23 phosphorylation sites, 13 sites were found unique on a peptide and 10 sites remain putative phosphorylation sites.

No light- or dark-specific sites on WC-2

As in case of WC-1, the majority of phosphorylation sites of WC-2 was found both in dark and in light. Some sites that appear to be either dark- or light-specific will be reviewed in detail.

S128 and S129 (*1, *2 in Table 3.3) are putative phosphorylation sites found on only one peptide in the dark-sample in January 2016 (see Table 3.1). In this experiment, immunoprecipitation was used to purify WC-2, and the phosphorylation sites found by tandem-affinity-purification of tagged WC-2 in January and March 2014 were confirmed but S128 and S129 were found for the first time. Thus, this peptide seems to be rare and phosphorylated S128 or S129 was not found in the light-sample for technical reasons rather than biological reasons. This evaluation is supported by the example of T523 clearly showing the limitations of the phosphorylation site mapping methods used in this study. T523 was found phosphorylated on numerous peptides in light and in dark in the experiments in January and March 2014. However, in January 2016, a phosphorylated T523 was found on only one peptide in the light-sample highlighting the necessity of cautious interpretation of the results.

Phosphorylation site T287 (*4 in Table 3.3) is a similar example. T287 was found as single site on two peptides in the dark-sample in January 2014, but not again in the purification of the same biological material in March 2014 and not by the different experimental approach in January 2016.

Most likely, either the phosphorylation or the peptide is rare and the corresponding phosphorylated peptide was not detected in the light-induced sample. Thus, it is unlikely that this site represents a dark-specific phosphorylation.

S142 (*3 in Table 3.3) is a putative phosphorylation site occurring on a long S, T stretch in peptides in light along with the putative sites T141, T140, T139 and the unique sites T138 and T136. Since all the neighboring sites to S142 were found in dark as well as in light, the light-specificity of S142 is most probably just implied by the incomplete fragmentation of the respective peptides from the light-sample. The same conclusion applies to T344 (*5 in Table 3.3) and S390 (*6 in Table 3.3) that were found as putative sites on peptides in dark-samples together with the unique sites S341 and S394, respectively.

Overall, 14 individually digested samples of WC-2 were analyzed by mass spectrometry. The analysis of the sequence coverage in each sample revealed that all phosphorylation sites were found in regions that were highly represented in each sample (Figure 3.4). Thus, numerous peptides were found that cover the respective phosphorylation site but it might be a rarely phosphorylated site or the phosphorylated peptide may have unfavorable

chemical properties that interfere with fragmentation and detection during mass spectrometry.
Taken together, the phosphorylation sites of WC-2 are neither light-, nor dark-specific like the phosphorylation sites of WC-1. The model created for WC-1 can be extended to the whole WCC: in dark, there is a pool of poorly and differently WCC molecules in the cell, the activity of kinases is massively increased in light yielding a pool of highly phosphorylated WCC molecules.

No phosphorylation of protein domains of WC-2

As shown in Figure 3.4 and like in WC-1, no phosphorylation sites were found in the known domains of WC-2, namely the PAS domain and the zinc finger DNA-binding domain. Thus, neither the interaction of WC-2 with WC-1, nor the binding to DNA are directly impaired. The phosphorylation sites of WC-2 are roughly distributed in two clusters: a N-terminal cluster before the PAS domain and a C-terminal cluster beyond the PAS-domain.
In Table 3.3, three putative phosphorylation sites in the zinc finger DNA-binding domain of WC-2 are listed as artefacts. In the purification in January 2014, one peptide with a phosphorylation either on S476 or on S484 in zinc finger DNA-binding domain was found. In the purification in March 2014, two peptides with a phosphorylation either on T473 or on S476 were found. S476 and S484 were mutated to aspartate to mimic constitutive phosphorylation and the function of WC-2 S476D was severely impaired (data not shown). Since this would have been an on/off-switch-like mechanism, it was crucial to confirm the putative phosphorylation site S476 *in vivo*. However, the general mapping of phosphorylation sites in January 2016 did not confirm the previous result. The digestion of WC-2 with trypsin yields a peptide from the WC-2 zinc finger DNA-binding domain that comprises T473, S476 and S484. The specific search for this peptide in July 2016 (see Table 3.1), gave no evidence for a phosphorylation on this peptide. Thus, the previous result is an artefact and phosphorylation of the WC-2 zinc finger DNA-binding domain is not part of the mechanism of the light-induced phosphorylation of WCC.

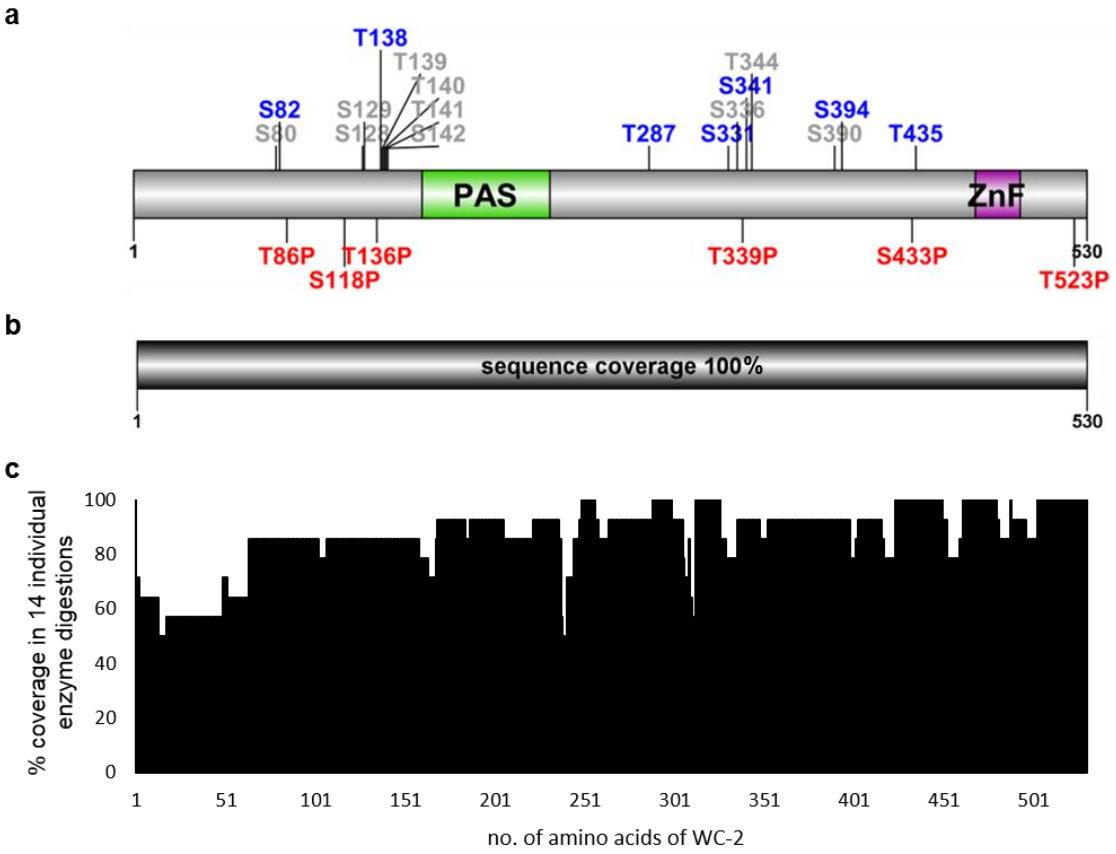

Figure 3.4: Phosphorylation sites of WC-2 in context of the known protein domains and sequence coverage.
3.4a: Phosphorylation sites of WC-2 in context of the known protein domains. **3.4b:** The sequence coverage of WC-2 amounts to 100 %. **3.4c**: The sequence coverage of 14 individual digested samples were summed up to identify regions of high- and of low coverage.

SP/TP sites are overrepresented on WC-2

Like in WC-1, SP and TP sites are also overrepresented in WC-2 (see Figure 3.4). Out of 23 phosphorylation sites of WC-2, 10 sites are putative phosphorylation sites, 7 sites are unique phosphorylation sites followed by other amino acids than proline and 6 sites are unique sites followed by proline. Like all phosphorylation sites of WC-2, the SP and TP sites cluster roughly into an N-terminal cluster and into a C-terminal cluster with three SP, TP sites each. Thus, the conclusions drawn from WC-1 can be extended to the whole WCC: the abundance of SP, TP sites indicates the activity of proline-directed kinases and the clustering of phosphorylation sites implies the hypothesis of priming phosphorylation at SP, TP sites and subsequent phosphorylation of other SX, TX sites.
In contrast to WC-1 (see Figure 3.3), almost all SP, TP sites of WC-2 were found phosphorylated in this study (see Figure 3.5). Yet, numerous SX, TX sites were not found phosphorylated in this study so that the 23 phosphorylation sites of WC-2 may not represent the all possible phosphorylation sites.
Remarkably and exactly like WC-1, no conserved phosphorylation motifs were identified that would give information about the kinases acting on WC-2.

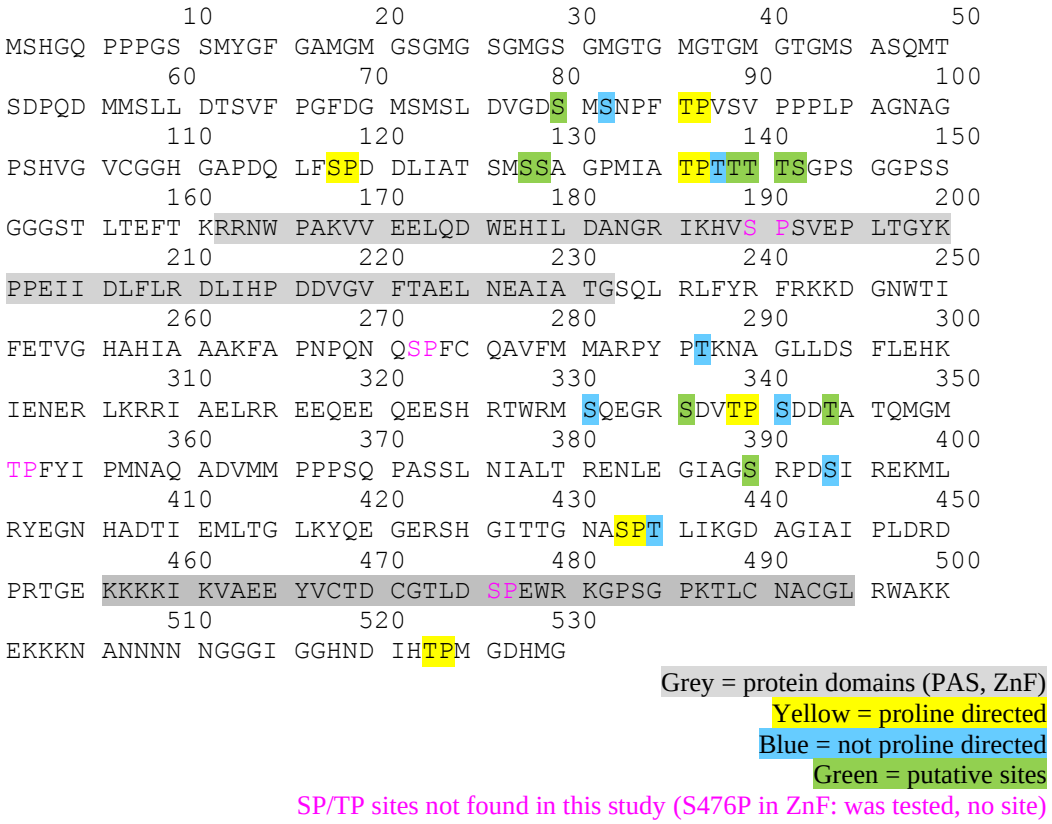

Figure 3.5: The distribution of phosphorylation sites of WC-2 over the amino acid sequence.

3.1.4. Summary of the phosphorylation sites of WC-1 and WC-2

The analysis of the phosphorylation sites of WC-1 and WC-2 revealed that both proteins share all characteristics. This finding isn´t surprising since both proteins act together as WCC. No light- or dark-specific phosphorylation sites were found on both WC-1 and WC-2. SP, TP sites are overrepresented and occur in clusters with other phosphorylation sites on both proteins indicating the activity of proline-directed kinases that might set priming phosphorylation. However, no conserved phosphorylation motifs were found that would give a hint for the kinases involved in the mechanism. The large number of phosphorylation sites of both WC-1 and WC-2 points to an hour-glass-like mechanism meaning that rather the increasing number of phosphorylation than the exact position of the phosphorylation site modifies the function of the protein.

3.2. The composition of L-WCC

The light-triggered formation of L-WCC connects two WC-1 molecules directly via their LOV domains but the number of WC-2 molecules involved in L-WCC is still under debate (Malzahn *et al.*, 2010; Wang *et al.*, 2015).

To clarify this, an N-terminally TAP-tagged *wc-2* under control of an qa-inducible promoter was used to compare the pull-down of a non-tagged, short isoform of WC-2 in

light and in dark. Due to an internal start codon in the ORF of *wc-2* (Neiss *et al.*, 2008), an N-terminally truncated, non-tagged, short isoform of WC-2 (sWC2) is expressed independently from qa-induction of the tagged full-length WC-2 at sufficient levels. It has been shown previously that sWC-2 forms the WCC with WC-1, that sWC-2 can fully rescue the ability of Neurospora WCC to be entrained by light and that sWC-2 can rescue the circadian rhythm in constant darkness to some extent (Neiss *et al.*, 2008).

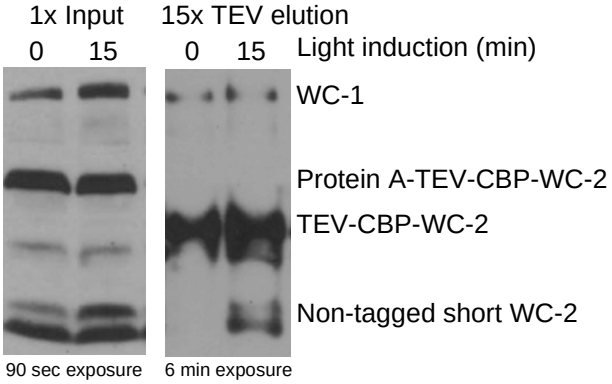

Figure 3.6: *In vivo* proof of the composition of the light-induced WCC.
Non-tagged short WC-2 appears in the input in the dark- as well as in the light-sample. After the first purification and elution step of the tandem affinity purification, short WC-2 is pulled-down only in the light-sample indicating that L-WCC consists of two WC-1 and two WC-2 molecules.

To show the composition of L-WCC, the expression of the tagged full-length WC-2 was induced in the mutant strain. To stabilize protein-protein interactions by crosslinking, the samples were treated with formaldehyde before harvest in dark or after 15 min light-induction.

By pulling on the N-terminal tag of full-length WC-2, WC-1 was pulled-down both in dark and after light-induction. Interestingly, the non-tagged sWC-2 was pulled-down only after light-induction, but not in dark (see Figure 3.6). Thus, non-tagged sWC-2 can only be precipitated if it is associated with WC-1 and if WC-1 forms a light dimer with a WCC consisting of WC-1 and tagged full-length WC-2. Thus, L-WCC must be a tetramer consisting of two molecules WC-1 and two molecules WC-2.

3.3. CK-1a is the only known L-WCC-phosphorylating kinase

3.3.1. Pull-down of kinases together with WCC not above background level

A tandem affinity purification (TAP) of tagged WC-2 (Δ*wc-2, bd, qa-2 tap- wc-2*) was performed aiming at the enrichment of kinases that phosphorylate WCC. To stabilize protein-protein-interaction, the material was cross-linked with formaldehyde. It was expected to pull-down kinases at a time point of intermediate light-induced phosphorylation of WCC after 15 min of light-induction (after growth in dark for 24 h). As control, material grown in constant darkness for 24 h was used. See chapter 3.1, Table 3.1 for further details of the experiments. The light- and the dark-sample of the purification were separated by size in an SDS gel. This was necessary since WC-1 and

WC-2 required further purification for the detection of phosphorylation sites by mass spectrometry. As expected, WC-1 and WC-2 appeared as prominent bands of expected size in the SDS gel (Figure 3.1). In the rest of the gel, numerous bands of different intensities were visible. After excision of WC-1 and WC-2 for phosphorylation site analysis, the whole gel was cut into slices and analyzed for protein identification. Light- and dark samples were analyzed separately. Each analyzed gel band yielded a long list of protein hits at different scores. Since there was no sample with a dominant protein beside WC-1 or WC-2, further analysis of the data was performed based on the protein score of each hit in each sample.

The protein score is as measure for the probability of the identity of a protein or a peptide detected by mass spectrometry. The higher the score of a protein, the higher the probability that the mass computationally assigned to the protein was assigned correctly and the protein truly occurs in the sample. The protein score does not provide reliable quantitative information but can be used for limited interpretations regarding the abundance of a protein in the sample. The protein score contains some quantitative information because the more peptides are assigned with a certain protein, the higher is the probability that this protein really has been in a sample. If a protein is highly abundant in a sample analyzed by mass spectrometry, many peptides of this protein will be measured, will be assigned to that protein and will give a high score for that protein. But on the other hand, there are several reasons why a highly abundant protein in a sample is represented by only a few peptides and a low score. First, a highly abundant protein might have only very few cleavage sites of the proteases used for digestion. Second, the resulting peptides might have unfavorable molecular properties (length, sequence) for the chromatography, the electron spray ionization and the further fragmentation following the detection in the first MS. The selection criteria during first MS (Top-10-method) and the sequence coverage of a peptide after second MS further bias the overall protein score.

To search for potential interaction partners of WCC, several proteins of interest and control proteins were selected for the data analysis, the results are shown in Figure 3.7. As control and example for high scores, WC-1 and WC-2 are shown since these were the most prominent proteins in each sample. But since the actual WC-1 and WC-2 were excised from the gel and used for the mapping of phosphorylation sites, the protein score shown here represent only the smear of WC-1 and WC-2 over the gel. The protein scores of WC-2 range roughly between 100 and 2000. The longer protein WC-1 is known as stable interaction partner of WC-2 and was pulled down at score up to 6000. Thus, a stable interaction partner of WCC is expected to appear in the protein identification at high score above 1000. However, the known interaction partner FRQ was found at score only up to 600; FRH at up to 800 and CK1a at up to 600. Since there were numerous unspecific proteins found at the same or much higher scores, it is doubtful whether the experimental conditions allowed the pull-down of other WC-2 interaction partners than WC-1. As unspecific controls of high score, actin, translation elongation factor 3 (EF3) and the metabolic enzymes 6-PFK, Lysine-5 and ADH are shown. All control samples (including

WC-1 and WC-2) show that these proteins were found in the dark- and the light sample at roughly the same score (Figure 3.7). But there are also exceptions: 6-PFK and Lysine-5 appear to be enriched in the dark-sample. Of course, these data have no biological significance since it is very unlikely that these metabolic enzymes are degraded in response to light within only 15 min. The highest score of each control protein (except from WC-1 and WC-2) were found in the gel band that corresponds to the molecular mass of the protein. This observation was expected and reflects the limited quantitative information contained in the protein score.

The highest score of the proteins of interest also correlates with the molecular mass of the respective protein. Except, the highest score does not correspond to the molecular mass for FRQ, FRH, PKC and RCM1 since these proteins are of similar sizes as WCC and the major population of these proteins was likely excised from the gel together with WC-1. So, the highest score of these large proteins is found in the smear of large, crosslinked protein complexes above 170 kDa. The proteins FRQ, FRH, RCM1 and RCO1 appear to be more abundant in the light-sample than in the dark-sample (Figure 3.7). This is expected since the FRQ-FRH-CK1a complex was shown to phosphorylate WCC in response to light (He *et al.*, 2006). However, CK1a does not show an enrichment in the light-sample (Figure 3.7). RCM1 and RCO1 are known to be regulators of light-induced gene expression (Liu *et al.*, 2015; Olmedo *et al.*, 2010; Ruger-Herreros *et al.*, 2014), the enrichment in the light-sample is an interesting observation (Figure 3.7). Similar observations for FRQ, FRH, CK1a and RCM1 were made in the purification of January 2014 (see Figure 5.4 in the appendix). The comparability of the two purifications is limited since in January 2014, some gel bands of the light- and the dark-sample had to be pooled. Thus, for RCO1, the light- and dark-abundance cannot be assessed. In contrast to the March 2014 experiment, three gel bands of very high molecular weight were analyzed the January 2014 experiment. The molecular weight of this gel section is above the molecular weight marker was assigned arbitrarily with 300, 400 and 500 kDa. These high molecular weight data of FRQ, FRH and RCM1 suggest high abundance in the light sample (see Figure 5.4 in the appendix). However, large protein aggregates, very likely artifacts of the crosslinking, migrate slowly in the gel and the digestion and further sample processing for mass spectrometry might be highly biased.

Taken together, the two data sets based on the same biological material show a tendency of enrichment of known WCC interaction partners in the light-sample despite the intense and different processing of the samples. But the data also show the limitations of the interpretation of protein scores and no conclusion about other interaction partners except from the know proteins can be drawn. The pull-down assay did not reveal a new WCC phosphorylating kinase but suggests that new WCC interaction partners could be identified in a quantitative experimental approach.

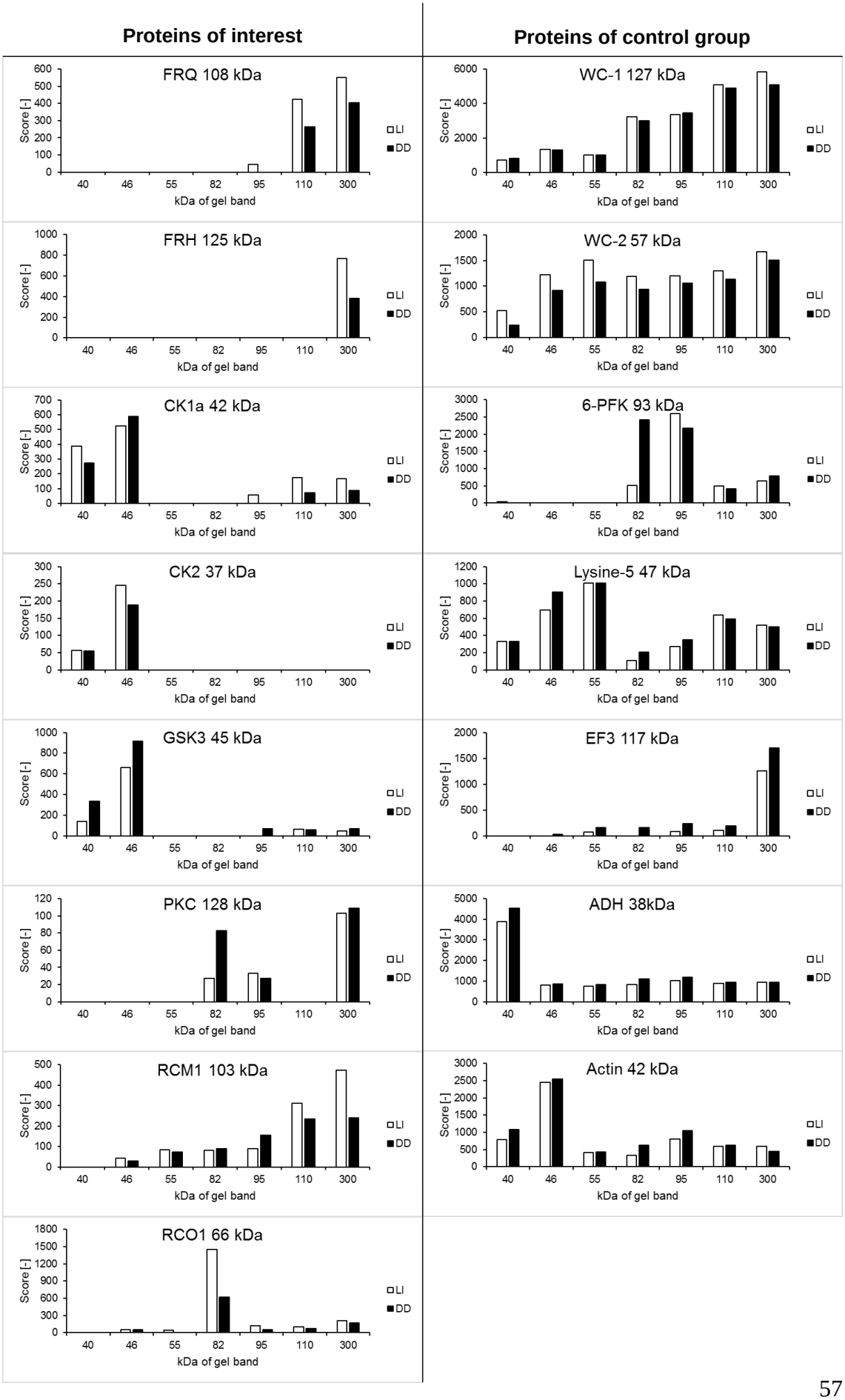
Proteins of interest
Proteins of control group
FRQ 108 kDa
WC-1 127 kDa
FRH 125 kDa
WC-2 57 kDa
CK1a 42 kDa
6-PFK 93 kDa
CK2 37 kDa
Lysine-5 47 kDa
GSK3 45 kDa
EF3 117 kDa
PKC 128 kDa
ADH 38kDa
RCM1 103 kDa
Actin 42 kDa
RCO1 66 kDa
Score [-]
kDa of gel band
40
46
55
82
95
110
300
LI
DD

Figure 3.7: Selected proteins identified by mass spectrometry in the tandem affinity purification of tagged WC-2 in March 2014
The light- and the dark-sample were separated by size in an SDS-gel. Tagged WC-2 and its very stable interaction partner WC-1 were pulled down at high concentrations and appeared as prominent bands in the gel (refer to Figure 3.1 and Figure 5.1). These bands were excised and analyzed for protein phosphorylation. The rest of the gel was cut into several bands that comprise a certain mass range. The intermediate mass of each band is indicated on the x-axis. The mass of 300 kDa is only a very rough estimation since this band was excised from the gel over the upper band of the molecular weight marker (170 kDa). Light- and dark-bands (**LI and DD, respectively**) were analyzed independently. The MS method used was not quantitative mass spectrometry, so the protein score distribution over the whole mass range was analyzed instead for selected target proteins and for selected control proteins. Since the protein score contains some information about the abundance of the protein in the sample, the aim was to search for a light-induced enrichment of interaction partners of WCC. As control, WC-1 and WC-2 are shown. As outlined above, the actual WC-1 and WC-2 band are not part of the identification analysis shown here. The proteins scores of WC-1 and WC-2 shown here represent the smear of these proteins over the whole gel. As further controls, two very abundant proteins, ADH and actin, are shown. The metabolic enzymes 6-PFK and lysine-5 and the translation elongation factor 3 (EF3) represent unspecific protein hits of various size. As proteins of interest and known interactors of WCC, FRQ, FRH, CK1a and CK2 are shown. GSK3 and PKC were suggested to phosphorylate WCC previously. RCM1 and RCO1 were shown to also bind to LRE, the target sequence of WCC in light-inducible genes (Liu *et al.*, 2015; Olmedo *et al.*, 2010; Ruger-Herreros *et al.*, 2014).

The absence of dominant kinase in the pull-down assay supports the mechanistic model created based on the mapping of phosphorylation sites. Kinases phosphorylated both WC proteins selectively and differently rather than sequentially. Kinases attach to and detach from the WC proteins leaving mostly only one phosphorylation. This generates a pool of differentially, poorly phosphorylated WC proteins in dark and a pool of higher but also differential WC-proteins in light.

3.3.2. Testing of kinase knock out mutants did not reveal a candidate for the light-induced phosphorylation

The accumulation of phosphorylation at SP/TP sites on both WC proteins pointed to the activity of proline-directed kinases. Among the proteins pulled-down together with WCC, several proline-directed kinases were found even though not at an enrichment above background level. The candidates are glycogen-synthase kinase 3 (GSK3), Mitotic division kinase-1 (MDK-1), Serine/threonine protein kinase-47 (STPK47), Mitogen-activated protein kinase-1 (MAPK-1), Mitogen-activated protein kinase-2 (MAPK-2).

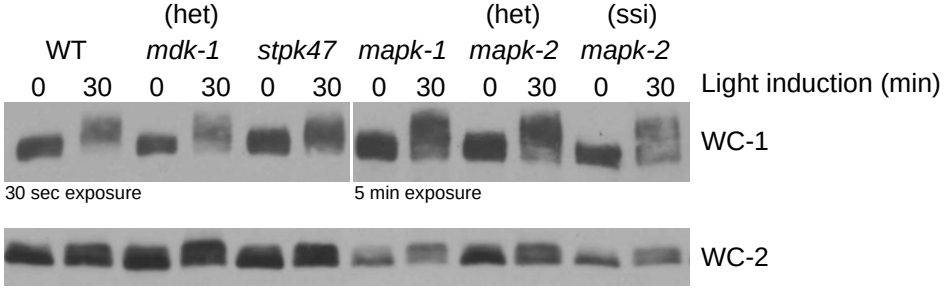

Figure 3.8: Light induction of selected kinases knock out mutants.
Knock out strains of Mitotic division kinase-1 (*mdk-1*, heterokaryon), Serine/threonine protein kinase-47 (*stpk47*), Mitogen-activated protein kinase-1 (*mapk-1*), Mitogen-activated protein kinase-2 (*mapk -2*) do not show an altered pattern of light-induced WCC phosphorylation. het = heterokaryon, ssi = single spore isolate. Samples were taken after growth for 24 h in dark (0 min) and after light induction (30 min).

GSK3 is probably not the kinase catalyzing the light-induced phosphorylation of WCC because this was excluded already in a previous study (Tataroglu *et al.*, 2012). Knock out strains of the other proline-directed kinases were screened for a changed phosphorylation pattern of WC-1 and WC-2 in a light induction experiment but no phenotype deviating from the wild type was found (see Figure 3.8). One possible reason is that the right kinase was not tested. Another possible reason is that several kinases phosphorylated WCC and that there is a functional compensation of the knock out of a single kinase. And when a kinase is essential, the screening of knock out mutants is not the suitable method to identify the kinase. The tested kinases Mitotic division kinase-1 (MDK-1) and Mitogen-activated protein kinase-2 (MAPK-2) are most likely essential kinases since the respective knock out strains are available only as heterokaryon or single spore isolate strains. The kinases activity in such strains might be less than in wild type but is not fully abolished.

3.3.3. FRQ-dependent CK1a is known to phosphorylated L-WCC

A previous study found that FRQ-recruited CK-1a partially contributes to the light-induced phosphorylation of WCC (He *et al.*, 2006). However, this study showed the light-induced phosphorylation of WC proteins on Western blots only in constant light (LL).

Here, the previous findings were confirmed for WC-2, but not for WC-1 by light induction experiments with a *frq* knock out strain and with a CK-1a binding-deficient FRQ mutant (see Figure 3.9). WC-1 was found to be phosphorylated transiently with the same pattern in response to light both in the wild type and in a *frq* knock out strain (see Figure 3.9a).
This contradicts the previous study (He *et al.*, 2006). In a *frq* knock out strain, no light-induced phosphorylation of WC-2 was detectable. Since FRQ is not a kinase itself, it must be a mediator of the light-induced phosphorylation. Previous studies (He *et al.*, 2006) have shown that FRQ recruits CK-1a and CK-II to phosphorylate WCC. The *frq* mutant ΔFCD1-2 lacking the two FRQ - CK-1a interaction domains was compared to the wild type in a light induction experiment (see Figure 3.9b). As expected from the *frq* knock out strain, the light-induced phosphorylation of WC-1 was not impaired in the mutant but the light-induced phosphorylation of WC-2 was abolished in ΔFCD1-2. This result proved that CK-1a is at least one kinase that phosphorylates WC-2 in an FRQ- and light-dependent manner.

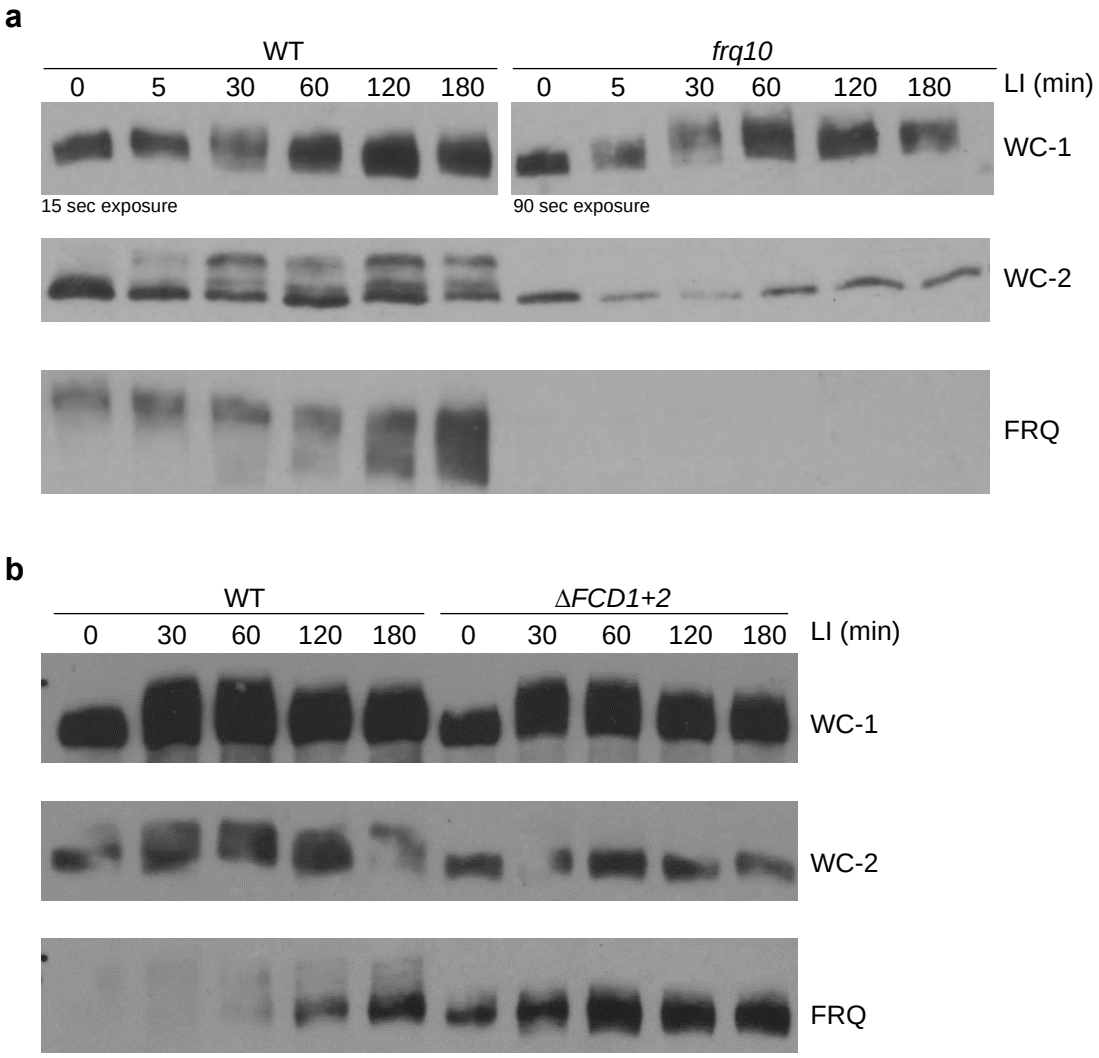

Figure 3.9: The FRQ- and CK1a-dependent light-induced phosphorylation of WC-2.
3.9a LI = Light induction (DD24, DD24 + min in light as indicated) experiment in wild type (WT) and *frq* knock out (*frq10*) mutant. **3.9b** Light induction (DD24, DD24 + min in light as indicated) experiment in wild type (WT) and in an FRQ mutant that lacks the two FRQ-CK1a-interacting domains (Δ*FCD1+2*).

3.4. Phosphorylation attenuates the activity of WCC

To investigate the function of the phosphorylation sites of WCC, this study focused on the smaller subunit WC-2 for two reasons: First, WC-2 seems to be the subunit of WCC that is more relevant for the light-induced activity of WCC. Wang *et al*. have shown that only WC-2 is required for DNA-binding of WCC for light-induction but DNA-binding for circadian functions requires both the DNA binding domains of WC-1 and WC-2 (Wang *et al.*, 2015). Second, the genetic manipulation of WC-2 was easier than the genetic manipulation of WC-1 at that time, when the experiments of this study were performed.

All the 23 phosphorylation sites of WC-2 presented in Table 3.3 (except from T473, S476, S484 that turned out to be artefacts) were mutated either to alanine to prevent

phosphorylation on these sites (A, the respective *wc-2* mutant of is referred to as *wc-2 allA*) or to aspartate to mimic constitutive phosphorylation (D, the respective *wc-2* mutant of is referred to as *wc-2 allD*).

3.4.1. WC-2 allA is hypophosphorylated but possibly post-translationally modified, WC-2 allD mimics artificial hyperphosphorylation

In *wc-2 allA*, any light-induced phosphorylation was abolished (see Figure 3.10). However, WC-2 allA appeared as two distinct bands on the SDS gel at every time point of a light induction. The upper band of WC-2 allA migrated on the same level as the lowest band of the wild type WC-2. The lower band of WC-2 allA migrated even faster than the lowest band of the wild type WC-2 in the SDS-gel (see Figure 3.10b, especially time point 180 min). The observation of these two bands suggested that WC-2 allA occurred as a non-modified and as a post-translational modified species, the wild type WC-2 occurred only as the unknown post-translational modified species.

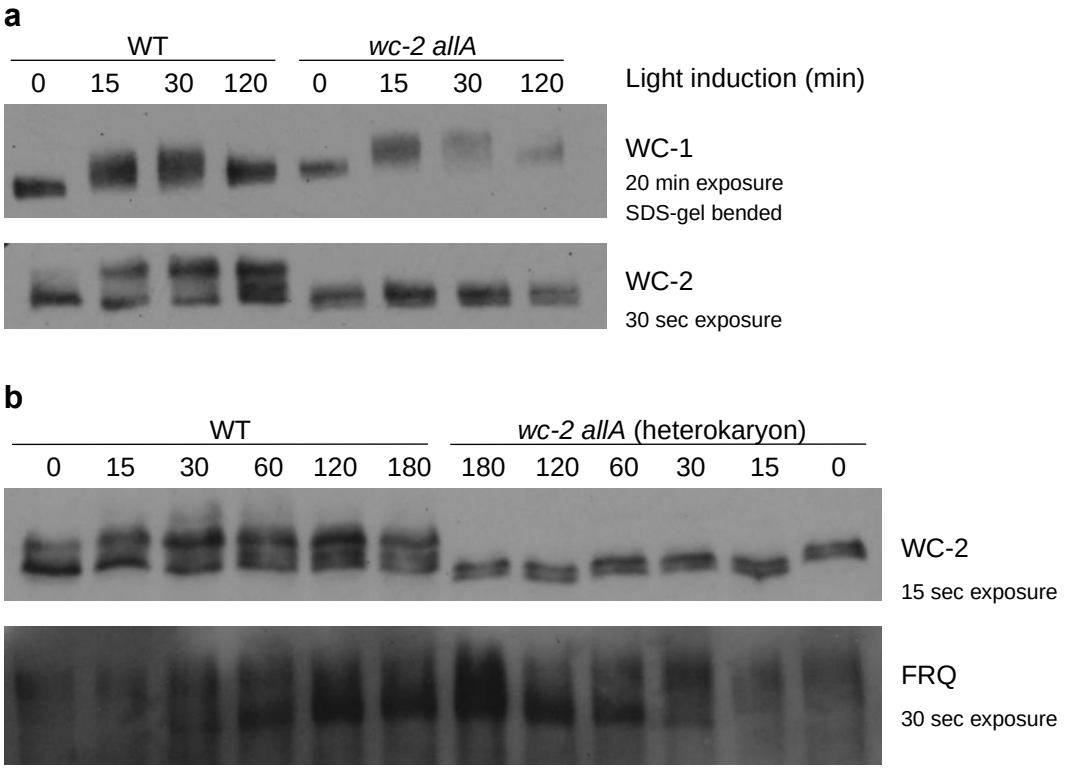

Figure 3.10: Light induction of *wc-2 allA* in comparison to the retransformed *wc-2 wild type* (WT). **3.10a** Light induction experiment (DD24h, DD24h + min in light as indicated) of a *wc-2 allA* homokaryon mutant, WC-1 and WC-2 are shown. The upper part of the gel showing WC-1 is slightly bended. **3.10b** Light induction experiment (DD24h, DD24h + min in light as indicated, WT and *wc-2 allA* were loaded in opposed order) of a *wc-2 allA* heterokaryon mutant, better resolution of WC-2 and FRQ expression are shown.

A dephosphorylation assay was performed to test whether this unknown post-translational modification was phosphorylation. The Western Blot of the dephosphorylation assay did not show the resolution of the two bands of WC-2 allA very well (see Figure 3.12). Despite the low resolution, it was visible that the migration of two distinct bands of WC-2 allA was not altered by the treatment with phosphatase. The direct

comparison of the dephosphorylated wild type WC-2 and WC-2 allA showed, that dephosphorylated WC-2 allA was still migrating faster. Thus, the appearance of WC-2 allA as two distinct bands in the SDS-gel is most likely due another post-translational modification than phosphorylation. The mutation of numerous serine and threonine residues of WC-2 to alanine might interfere with this post-translational modification so that the fast migrating, unmodified WC-2 becomes detectable. The investigation of this hypothesis remains to be done.

The dark-level and the light-induced expression of FRQ were not impaired in *wc-2 allA*. Thus, there was no light-induced phosphorylation of WC-2 allA detectable although sufficient levels of FRQ were available to recruit CK-1a to WC-2. CK-1a could obviously not find a target phosphorylation site on WC-2 allA.

The light-induced phosphorylation of WC-1 in *wc-2 allA* was not affected. Since also the expression of FRQ was not affected in *wc-2 allA*, WC-1 seemed to compensate for the lacking regulation of WC-2.

In *wc-2 all D*, any light-induced phosphorylation was abolished and the migration of WC-2 allD in the SDS-gel was dramatically slowed down compared to wild type WC-2 (Figure 3.11).

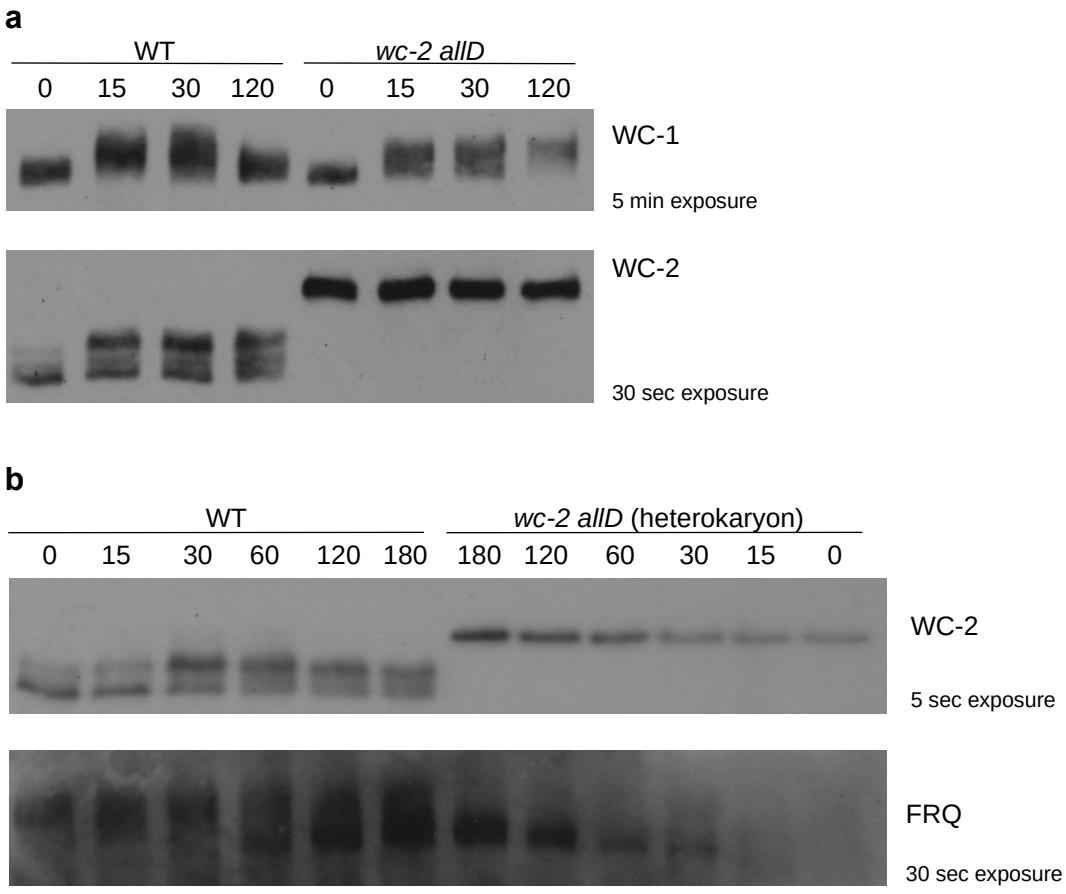

Figure 3.11: Light induction of *wc-2 allD* in comparison to the retransformed *wc-2 wild type* (WT). **3.11a** Light induction experiment (DD24h, DD24h + min in light as indicated) of a *wc-2 allD* homokaryon mutant, WC-1 and WC-2 are shown. **3.11b** Light induction experiment (DD24h, DD24h + min in light as

indicated, WT and *wc-2 allD* were loaded in opposed order) of a *wc-2 allD* heterokaryon mutant, WC-2 and FRQ expression are shown.

The mutation of all phosphorylation sites to aspartate obviously represents an artificial hyperphosphorylation of WC-2 that is never reached *in vivo*. In conclusion, full phosphorylation on the same WC-2 molecule never occurs *in vivo* or might occur rarely but the small number of fully phosphorylated WC-2 molecules cannot be detected by Western Blot. This finding strongly supports the model of a pool of differentially phosphorylated WCC species outlined in chapter 3.1. In the phosphatase assay, no dephosphorylation of WC-2 allD was observable confirming that most likely all phosphorylation sites of WC-2 were mapped in this study (see Figure 3.12).
Compared to the wild type, the dark-level of FRQ was lower in WC-2 allD but the light-induced expression of FRQ was not affected. Hence, the activity of WC-2 allD seems to be affected to some extent.
The light-induced phosphorylation of WC-1 was affected in *wc-2 allD* (see Figure 3.11a). In the dark, WC-1 in *wc-2 allD* was hypophosphorylated and did not differ from the wild type. But in response to light, the hyperphosphorylation of WC-1 was less pronounced in *wc-2 allD* than in the retransformed *wc-2 wild type* and was persistent rather than transient. This phenotype is known from a DNA-binding deficient mutant of *wc-2* lacking any expression of WCC target genes like *vvd*. To explain the phenotype of WC-1 in *wc-2 allD*, the activity of WCC in this mutant needs to be investigated (see following chapter 3.4.2).

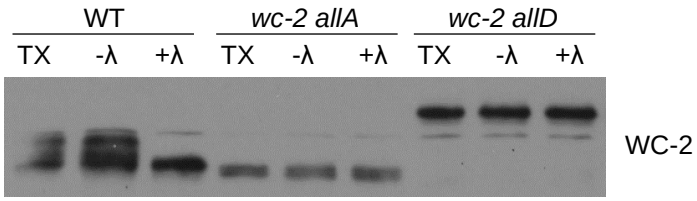

Figure 3.12: Dephosphorylation of WC-2 in WT (retransformed *wc-2 wild type*), in *wc-2 allA* and *wc-2 allD*.
TX = total protein extract; -λ = control sample in Lambda phosphatase buffer without enzyme; +λ = sample treated with Lambda phosphatase.

3.4.2. Phosphorylation gradually reduces the activity of WCC

During handling of *wc-2 allA* and *wc-2 allD* cultures in light induction experiments, it was observed that *wc-2 allA* strains change their color from white to orange in response to light like the wild type but *wc-2 allD* strains remain white (no photos shown). The characteristic orange color of *Neurospora crassa* is due to the synthesis of carotenoids in response to light. Genes involved in the biosynthesis of carotenoids are targets of the light-activated WCC (Harding and Turner, 1981). The measurement of the expression of the carotenoid synthesis gene *al-2* confirmed the observation described above (see Figure 3.13). Both the retransformed wild type and *wc-2 allA* showed light-induced expression

of *al-2*, whereas the expression of *al-2* in *wc-2 allD* was strongly reduced. Notably, a slight increase in *al-2* mRNA levels in *wc-2 allD* was still observable.

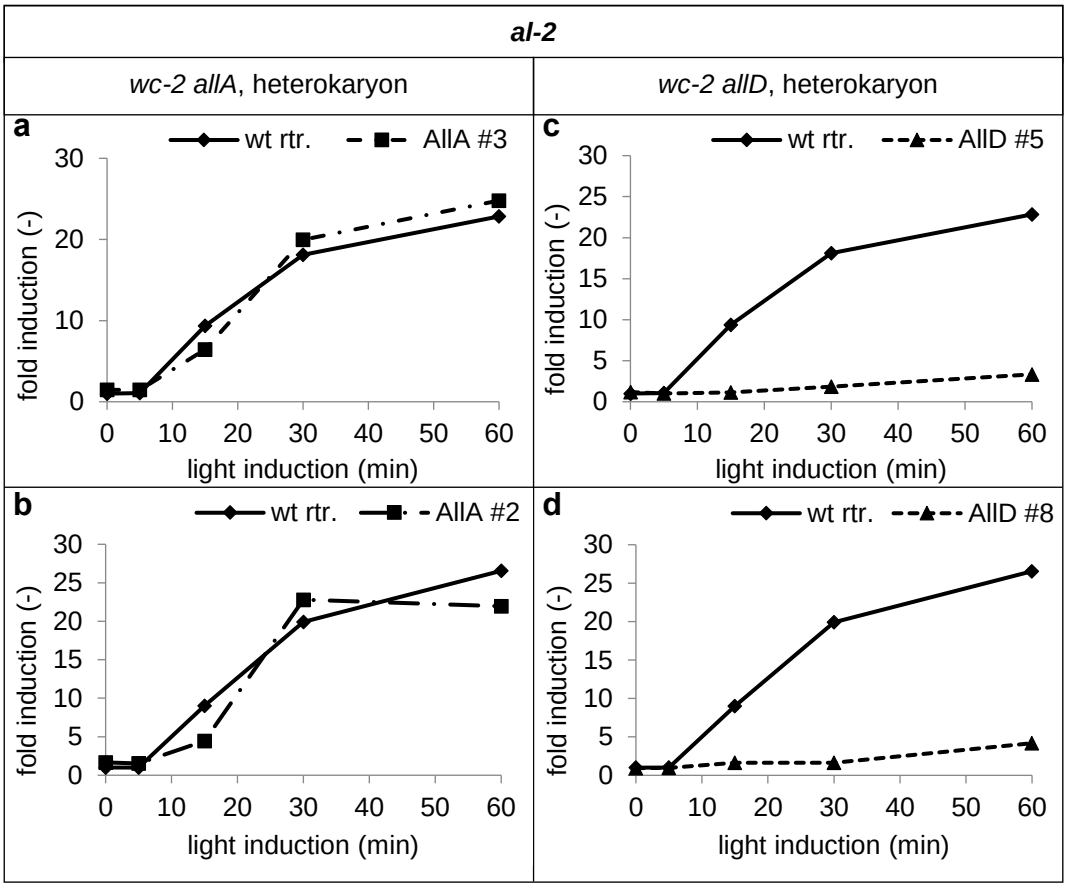

Figure 3.13: mRNA expression of *al-2* in response to light.
N=1 **3.13a, 3.13b** For *wc-2 allA*, two heterokaryon clones are shown in comparison to the retransformed *wc-2 wild type*. **3.13c, 3.13d** For *wc-2 allD*, two heterokaryon clones are shown in comparison to the retransformed *wc-2 wild type*. All measurements were performed once but in different clones.

Like *al-2*, the light-inducible gene *vvd* was expressed in response to light in the retransformed wild type and *wc-2 allA*, but the expression of *vvd* was strongly reduced in *wc-2 allD* (see Figure 3.14). Also like *al-2*, zooming in the curve of the vvd expression in *wc-2 allD* revealed that there was still light-induced expression at a very low level (see Figure 3.14 d and e).

The strong reduction of the *vvd* expression explains the persistence of the light-induced phosphorylation of WC-1 in *wc-2 allD* (Figure 3.11). Light-activated VVD molecules are known to dimerize with light-activated WCC, to disrupt the WCC light dimers and thereby inactivate WCC. Thus, the VVD-WCC dimers should not be a target of phosphorylation and this mechanism is thought to explain the transience of the light-induced phosphorylation of WC-1. Since there is no or not sufficient expression of *vvd* in a DNA-binding deficient mutant of *wc-2* (*wc-2 RD/DD*, data not shown) as well as in *wc-2 allD*, the light-induced phosphorylation of WC-1 is persistent in both strains (data for *wc-2 RD/DD* not shown). Nevertheless, the lack of VVD cannot explain why the

hyperphosphorylation of WC-1 is less pronounced in a DNA-binding deficient mutant of *wc-2* as well as in *wc-2 allD*. This will be investigated and discussed later in chapter 3.6.

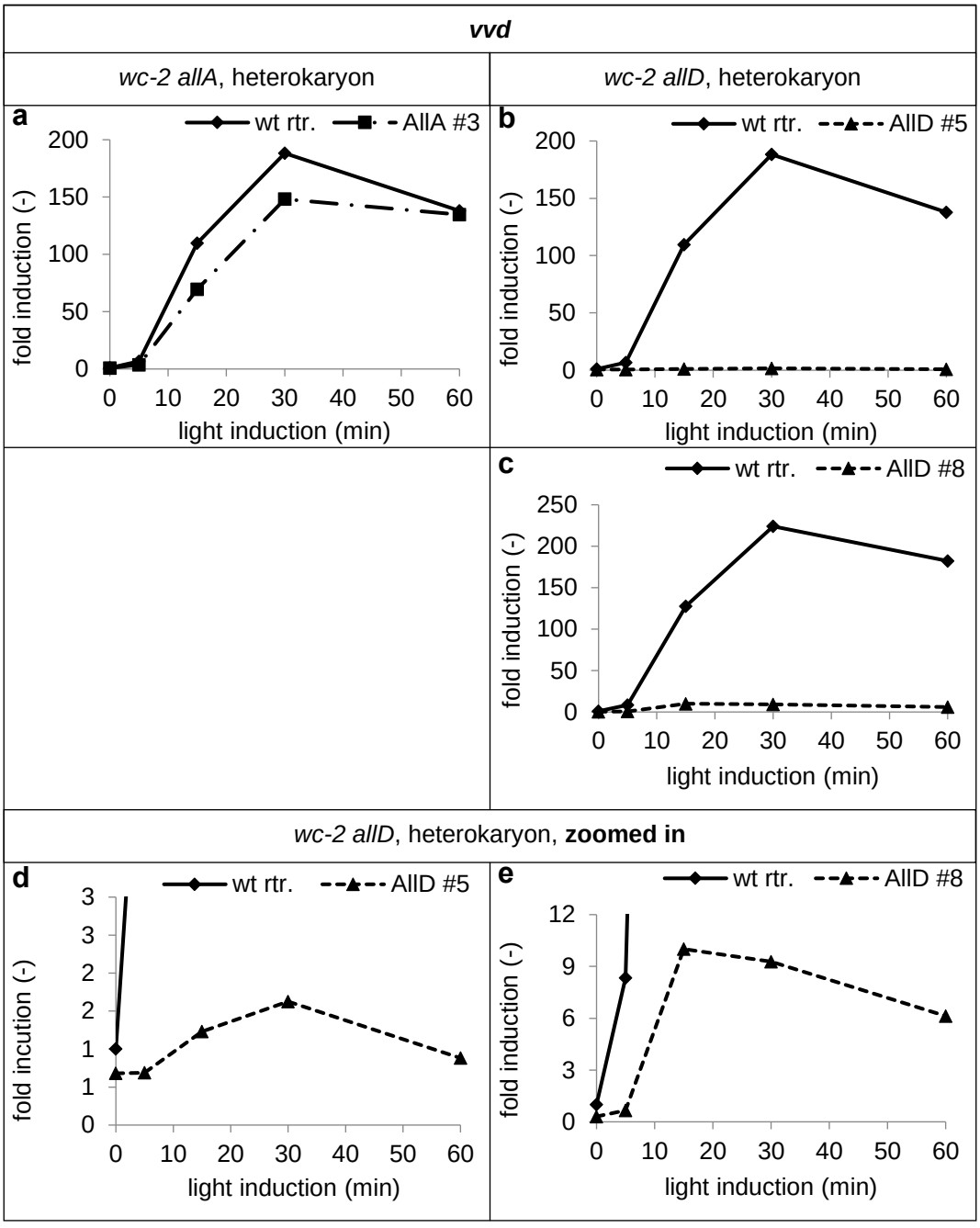

Figure 3.14: mRNA expression of *vvd* in response to light.
N=1; **3.14a** For *wc-2 allA*, one heterokaryon clone is shown in comparison to the retransformed *wc-2 wild type*. **3.14b, 3.14c** For *wc-2 allD*, two heterokaryon clones are shown in comparison to the retransformed *wc-2 wild type*. **3.14d** Zoom of **3.14b** to show the curve shape of the *vvd* expression in *wc-2 allD* clone #5. **3.14e** Zoom of **3.14c** to show the curve shape of the *vvd* expression in *wc-2 allD* clone #8. All measurements were performed once but in different clones (except from *wc-2 allA*).

Like *al-2* and *vvd*, the light-induced expression of *frq* total mRNA was not affected in *wc-2 allA*. However, the light-induced expression of *frq* in *wc-2 allD* revealed a special feature of the *frq* locus. The standard *frq* qPCR primer and probes detect *frq* total mRNA,

comprising *frq* sense and *frq* antisense mRNA. The *frq* total mRNA expression was reduced in *wc-2 allD* but was less strong reduced than the expression of *al-2* and *vvd*. The strand-specific measurement of *frq* sense mRNA explained that result. The light-induced expression of *frq* sense mRNA is even higher in *wc-2 allD* than in the wild type, more detailed explanation is given below. The *frq* antisense mRNA was not measured here but it is most likely strongly reduced like *vvd* and *al-2* leading to an overall intermediate expression of *frq* total mRNA as seen in Figure 3.15b. The measurement of the light-induced expression of *frq* (sense) in both *wc-2 allA* and *wc-2 allD* correlates with the detection of light-induced expression of FRQ in both *wc-2 allA* and *wc-2 allD* (see Figure 3.10 and Figure 3.11).

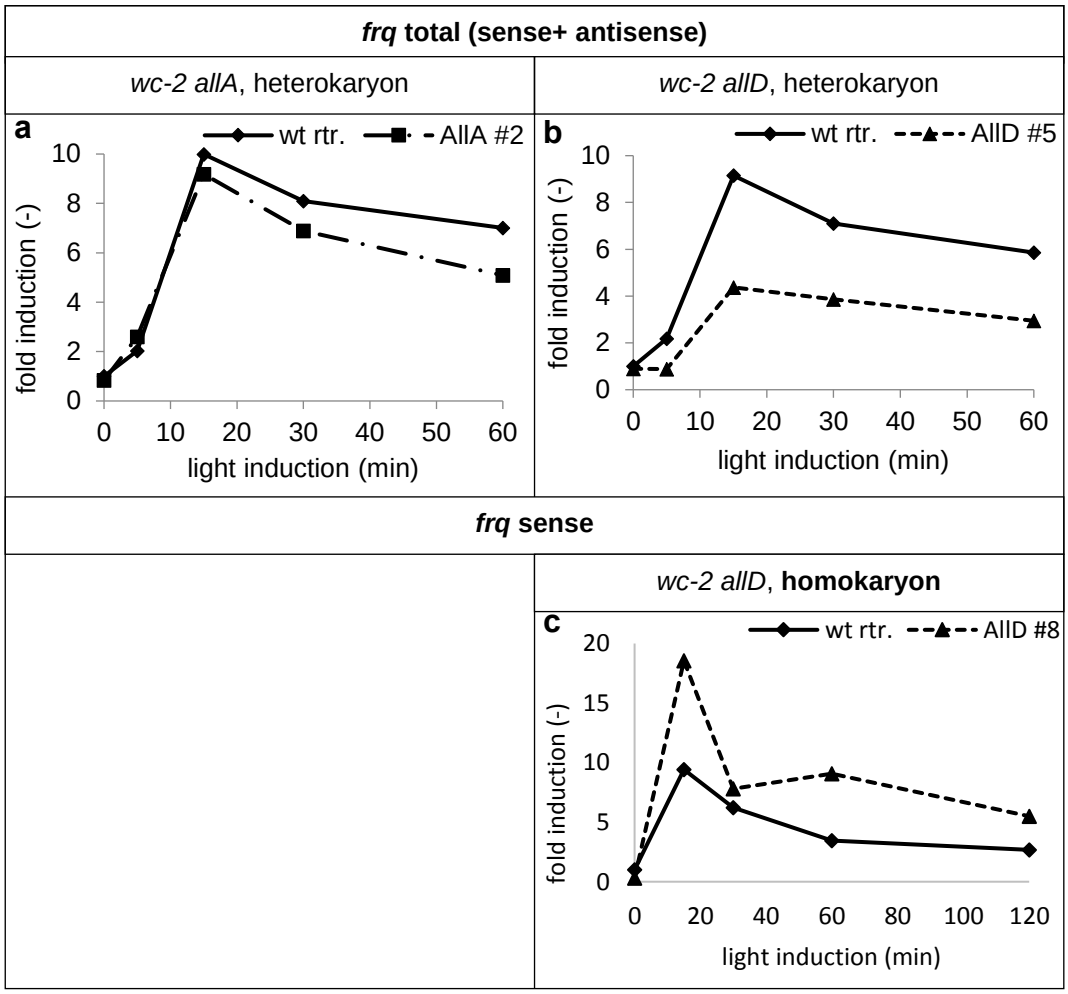

Figure 3.15: mRNA expression of *frq* total mRNA and of *frq sense* mRNA in response to light. N=1; **3.15a** For *wc-2 allA*, *frq* total mRNA of one heterokaryon clone is shown in comparison to the retransformed *wc-2 wild type*. **3.15b** For *wc-2 allD*, *frq* total mRNA of one heterokaryon clone is in comparison to the retransformed *wc-2 wild type*. **3.15c** For *wc-2 allD*, *frq sense* mRNA of one homokaryon clone is shown in comparison to the retransformed *wc-2 wild type*. All measurements were performed once.

ChIP experiments performed by Michael Oehler confirmed the results of the qPCR data presented above. In these experiments, a short light pulse was performed instead of light induction. The light intensity used in this experiment was sufficient to induce WCC

activity and phosphorylation. WC-2 allA was found to bind to the LREs of the light-inducible genes *vvd* and *frq* like WC-2 WT. The DNA binding of WC-2 allD could still be measured but was strongly reduced compared to WC-2 WT (Figure 3.16).

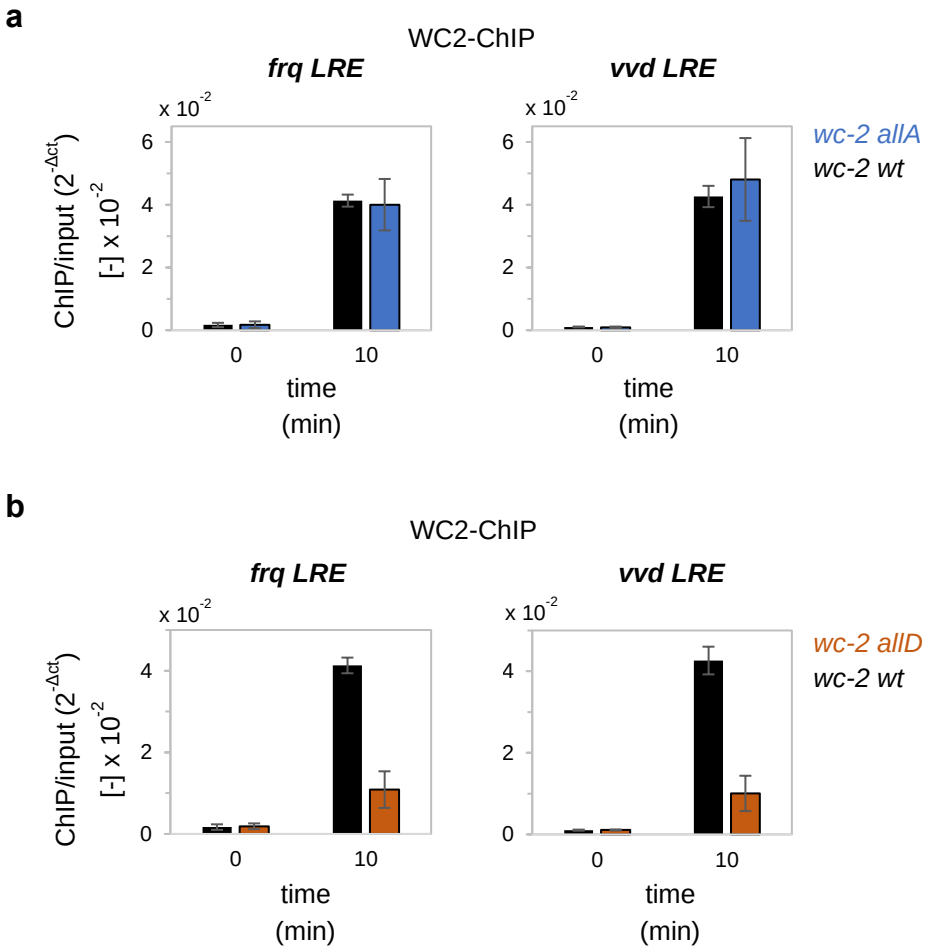

Figure 3.16: α-WC2 ChIP-qPCR of *wc-2 allA* and *wc-2 allD* on *frq LRE* and *vvd LRE*.
The experiment was performed by Michael Oehler using strains from Linda Ebelt. *wc2 wild type* and *wc-2 allA* **(3.16a)** or *wc-2 allD* **(3.16b)** cultures were grown in liquid medium. After 24 h in darkness, a sample was taken (0 min), the culture was subjected to a light pulse (1 min, 85 µM $m^{-2} s^{-1}$) and after 10 min, another sample was taken. WC2 was immunoprecipitated and bound DNA was extracted. Purified DNA was measured by qPCR and normalised to DNA levels in the input sample. (mean values ±SEM, *n* = 3)

Taken together, these results showed that the activity of WCC is unaffected in *wc-2 allA* but the activity of WCC is strongly reduced in *wc-2 allD*. WC-2 allD can still bind to target gene promoters and induce residual expression of *al-2* and *vvd*. Since *frq* sense is expressed under control of a very sensitive promoter *frq* sense LRE, the binding of less active WC-2 allD delays the inactivation of the promoter and allows the synthesis of more transcripts. These results show that phosphorylation attenuates the activity of WCC. Phosphorylation of WCC is not an on/off switch, it´s rather a gradual reduction of the transcriptional activity.

Since *wc-2 allD* is less active, shouldn´t *wc-2 allA* be more active and deregulated? Phosphorylation and thus inactivation are not possible in *wc-2 allA*, but the results show

that there must be a regulatory compensation by WC-1. WC-1 is not mutated in *wc-2 allA* and is still a target for phosphorylation.

3.4.3. Phosphorylation also attenuates the circadian activity of WCC

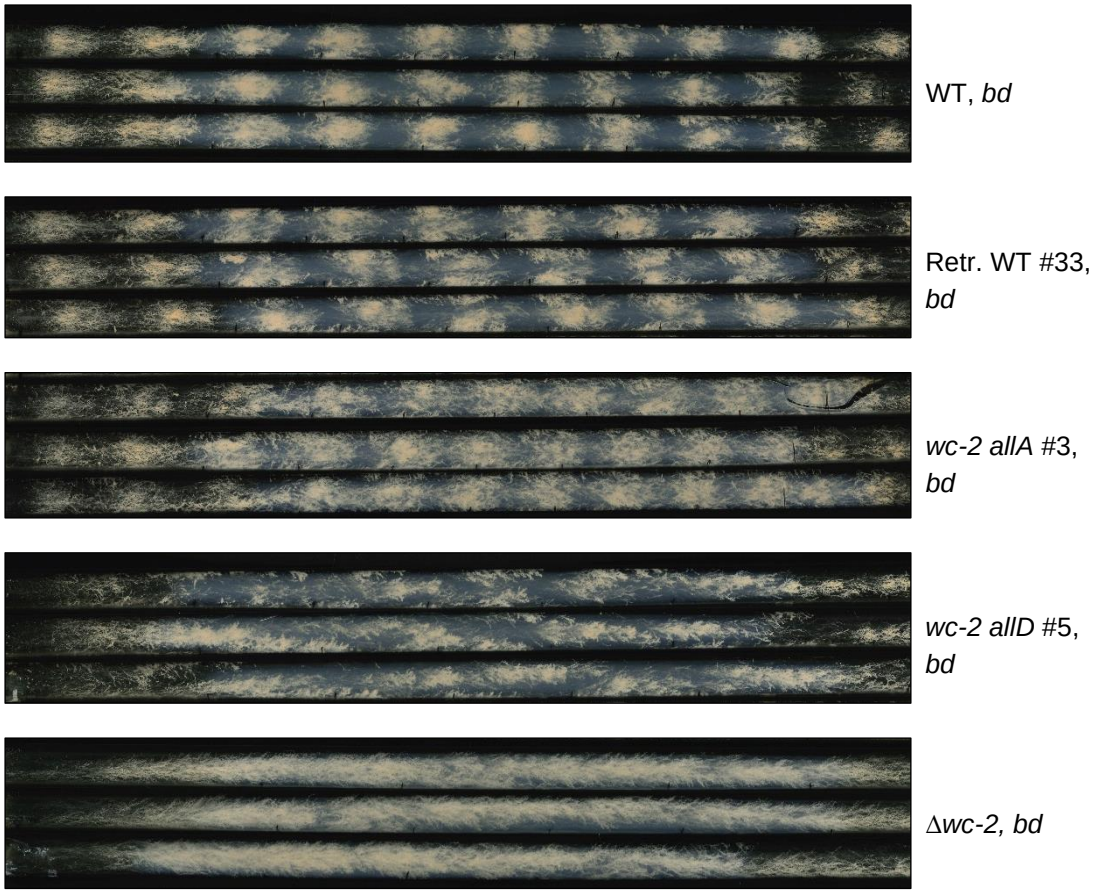

Figure 3.17: Race tube assay of *wc-2 allA* and *wc-2 allD*.
Growth in constant darkness to visualize the circadian clock in wild type *bd*, retransformed *wc-2 wild type bd* (retr. WT, clone #33), *wc-2 allA bd*, *wc-2 allD bd* and Δ*wc-2 bd*. Three race tubes of the same sample were grown in parallel.

Previous studies have shown that the circadian phosphorylation of WCC attenuates its activity (He *et al.*, 2005). Since phosphorylation on the WC-2 sites mapped in this study strongly attenuates the activity of WCC, it was checked whether the same phosphorylation sites also affect the circadian activity of WCC. A racetube assay in constant darkness revealed that *wc-2 allA* shows rhythmic conidiation like the wild type and the retransformed wild type (see Figure 3.17 and Figure 3.18). As observed for the light-induced activity, WC-1 obviously compensates for the lacking regulation of WC-2 allA during the circadian activity. But the conidiation of *wc-2 allD* was arrhythmic like in Δ*wc-2* (see Figure 3.17 and Figure 3.18). Hence, the circadian activity of WCC is strongly attenuated in *wc-2 allD*. This result is in accordance with the observation that the dark-level of FRQ is reduced in *wc-2 allD* (see Figure 3.11b). When the FRQ level is too low, the feedback loop of the clock is not maintained and there is no circadian rhythm.

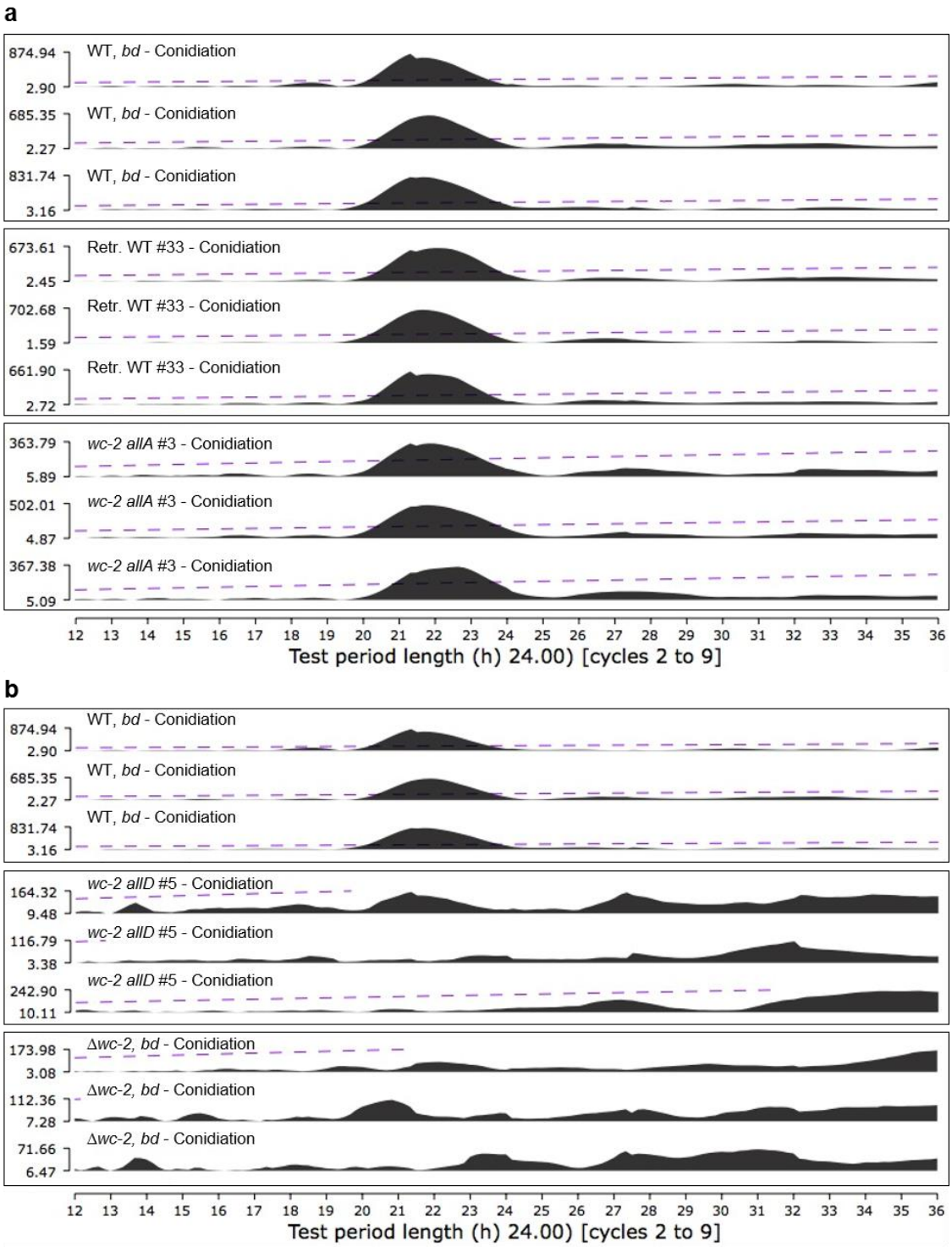

Figure 3.18: Analysis of the race tube assay of *wc-2 allA* and *wc-2 allD*.
Strains: wild type *bd*, retransformed *wc-2 wild type bd*, *wc-2 allA bd* **(3.18a)**, *wc-2 allD bd* **(3.18b)** and Δ*wc-2 bd*. Three race tubes of the same sample were grown in constant darkness in parallel (n=3). For analysis, the conidiation density of each circadian cycle was aligned to visualize graphically the period length.

3.4.4. Conclusion: circadian and light-induced phosphorylation do very likely not differ in phosphorylation sites

The circadian and the light-induced expression of *frq* are controlled by two distinct promoter elements, the clock-box (c-box) and the light-responsive element (LRE). The investigation of both the light-induced and the circadian activity of *wc-2 allD* suggested that phosphorylation attenuates both activities of WCC. Mimicking phosphorylation on WC-2 allD led to an arrhythmic phenotype most likely caused by very low FRQ levels due to a reduced expression of *frq* sense from the clock-box. Mimicking phosphorylation on WC-2 allD also led to reduced expression of *frq* antisense from the antisense LRE but to an enhanced expression of *frq* sense from the sense LRE. Taken together, these results imply that the same phosphorylation sites regulate both the dark and the light-activity of WCC. This conclusion correlates with the finding, that all the phosphorylation sites of WC-1 and WC-2 were found in light as well as in dark.

3.5. SP, TP pre-phosphorylation enhances phosphorylation of WC-2

The prevalence of SP, TP phosphorylation sites on both WC-1 and WC-2 points to the activity of proline-directed kinases and to an important function of these phosphorylation sites. To investigate the function of the in total six SP, TP phosphorylation sites of WC-2, the serine or threonine residues were mutated to either alanine or aspartate to either prevent or mimic constitutive phosphorylation. Based on the distribution of the SP, TP phosphorylation sites on WC-2 (see Figure 3.4), an N-terminal and a C-terminal cluster comprising three SP, TP phosphorylation sites each were identified (see Table 3.4).

Table 3.4: Overview of the SP, TP phosphorylation site mutants of WC-2.

WC-2 phosphorylation sites SP, TP	Alanine mutant	Aspartate mutant
T86, S118, T136, T339, S433, T523	*wc-2 6**A**P*	*wc-2 6**D**P*
T86, S118, T136	-	*wc-2 3**D**P N-terminal*
T339, S433, T523	-	*wc-2 3**D**P C-terminal*

3.5.1. The phenotype of WC-2 6DP and WC-2 3DP C-terminal

The mutation of all six SP, TP sites to DP (*wc-2 6DP*) and the mutation of the three C-terminal SP, TP sites to DP (*wc-2 3DP C-terminal*) resulted in a gradually accelerated phosphorylation of WC-2 (Figure 3.19a). WC-2 in *wc-2 6DP* was almost fully hyperphosphorylated in dark (0 min light induction) already, WC-2 in *wc-2 3DP C-terminal* showed an equal distribution of hypo- and hyperphosphorylated species in dark whereas the wild type was mostly hypophosphorylated. In response to light, WC-2 in *wc-2 6DP* reached full phosphorylation, WC-2 in *wc-2 3DP C-terminal* was almost hyperphosphorylated similar to the wild type but the hyperphosphorylation was more pronounced in *wc-2 3DP C-terminal* (Figure 3.19a). The light-induced phosphorylation of WC-1 was not affected.

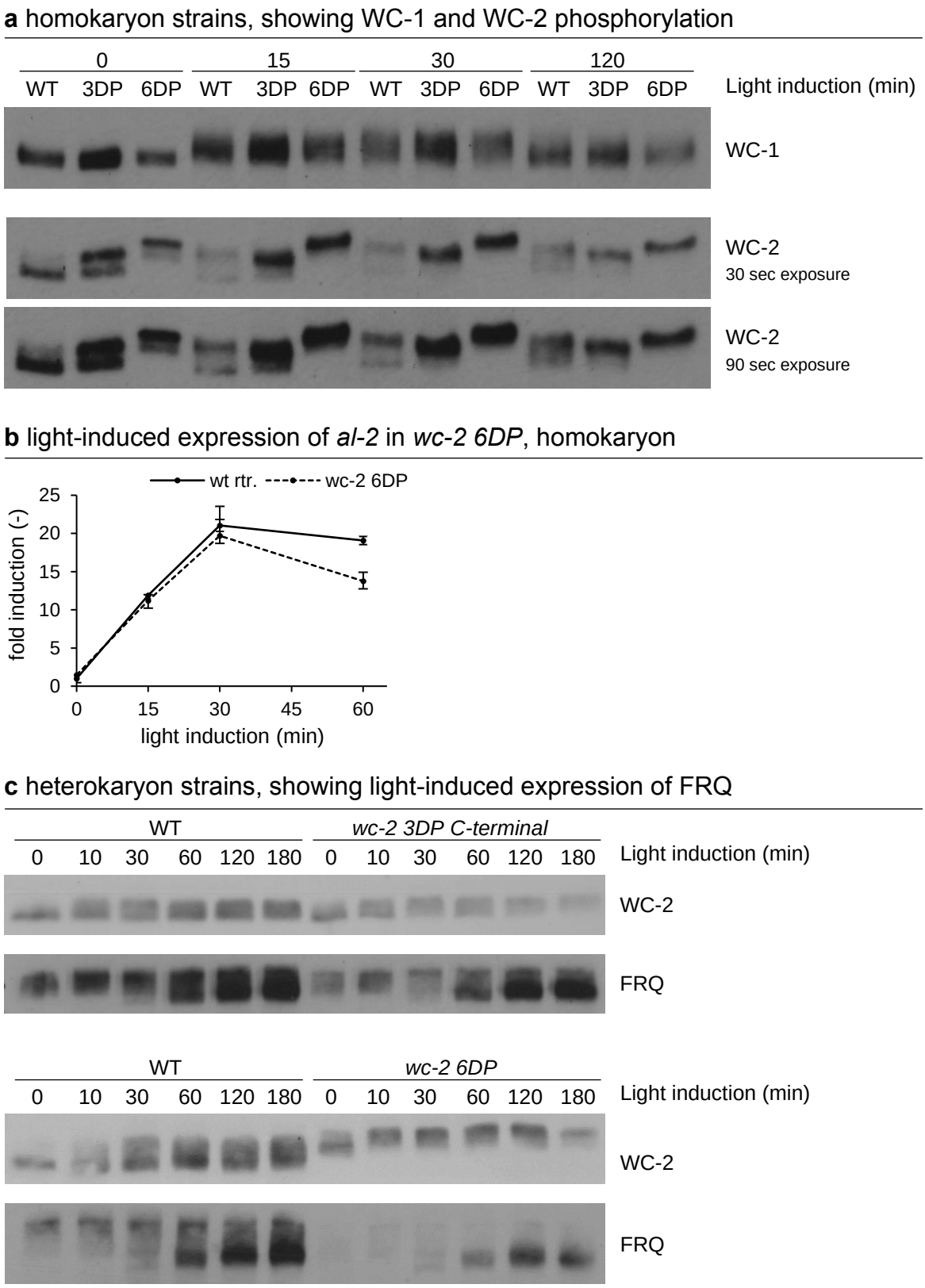

Figure 3.19: Light induction experiments of retr. *wc-2 wild type*, *wc-2 3DP C-terminal* and *wc-2 6DP*. **3.19a** High resolution of the phosphorylation of WC-1 and WC-2 in denaturing protein extracts of the respective homokaryon strains. **3.19b** Light-induced expression of *al-2*, data are available for *wc-2 6DP* only. The retransformed *wc-2 wild type* is shown as N=2, *wc-2 6DP* is shown as N=3 based on 3 different clones that behaved very similar. **3.19c** FRQ expression in response to light in native protein extracts of the

respective heterokaryon strains. The resolution of the phosphorylation of WC-2 is lower, since these were native protein extracts.

Interestingly, accelerated phosphorylation of WC-2 in the DP mutants was observed already in the dark and also in response to light. As outlined in chapter 3.1, the phosphorylation of WCC occurs already in dark and the efficiency of the phosphorylation reaction is enhanced in response to light. It seems that SP, TP phosphorylation also enhances the efficiency of the phosphorylation reaction similar to light.
The light-induced expression of *al-2* mRNA in *wc-2 6DP* and the light-induced expression of FRQ protein in both *wc-2 6DP* and *wc-2 3DP C-terminal* were similar to the retransformed *wc-2 wild type* (see Figure 3.19b and c). Remarkably, the FRQ level in dark was lower in the hyperphosphorylated mutant *wc-2 6DP* but the light-induced expression of FRQ was not affected. This is as similar phenotype as observed in *wc-2 allD* (see Figure 3.11b) but in contrast to *wc-2 allD*, the expression of *al-2* is not reduced in *wc-2 6DP*. Very likely, the modification of WC-2 in *wc-2 6DP* is compensated by WC-1 and the overall regulation of WCC by phosphorylation is not affected. However, the experiments shown in Figure 3.19 have to be repeated in homokaryon strains (light-induced expression of FRQ) or more often, in the same clone and for other targets of WCC (qPCR data). ChIP analysis of *wc-2 6DP* and *wc-2 3DP C-terminal* would also be required to detect small changes in WCC activity.
In *wc-2 6DP,* the replacement of six serine, threonine residues by six negatively charged aspartate residues resulted in a slower migration of WC-2 in the SDS gel. In contrast to that, the replacement of the three C-terminal serine, threonine residues by three negatively charged aspartate residues in *wc-2 3DP C-terminal* caused a similar migration pattern of WC-2 as in the wild type. This observation is further discussed in the following chapter.

3.5.2. The phenotype of WC-2 3DP N-terminal and WC-2 6AP

The mutation of the three N-terminal SP, TP sites to DP (*wc-2 3DP N-terminal*, see Table 3.4) resulted in a light-induced phosphorylation of WC-1 and of WC-2 and in a light-induced expression of FRQ that did not differ from the retransformed *wc-2 wild type* (see Figure 3.20a). However, these findings need to be confirmed by SDS-gels at higher resolution and by the measurement of the light-induced expression of target genes of WCC by qPCR.
Interestingly, the three aspartate residues introduced to *wc-2 3DP N-terminal* caused already the slower migration of WC-2 in the SDS gel as seen in *wc-2 6DP*. Thus, at least one of the N-terminal DP sites causes the strong shift of the WC-2 signal. Since these phosphorylation sites are found *in vivo* but the strong shift is not observed *in vivo*, it remains questionable, whether the strong shift is an artefact caused by the artificially introduced aspartate residue.
As 6DP residues accelerate the phosphorylation of WC-2, the mutation of these residues to alanine was assumed to slow down the phosphorylation of WC-2 since a posttranslational signal might be missing. However, the light-induced phosphorylation of WC-1 and of WC-2 and the light-induced expression of FRQ in *wc-2 6AP* did not differ

from the retransformed *wc-2 wild type* (see Figure 3.20b). The lack of regulatory sites on WC-2 in *wc-2 6AP* is very likely compensated by the regulation of WC-1.

Taken together, the phosphorylation of SP, TP sites of WC-2 are an important regulatory signal for further phosphorylation of WC-2. Since SP, TP phosphorylation sites are overrepresented on WC-1 as well, the regulation of both WC-1 and WC-2 is very likely redundant to some extent.

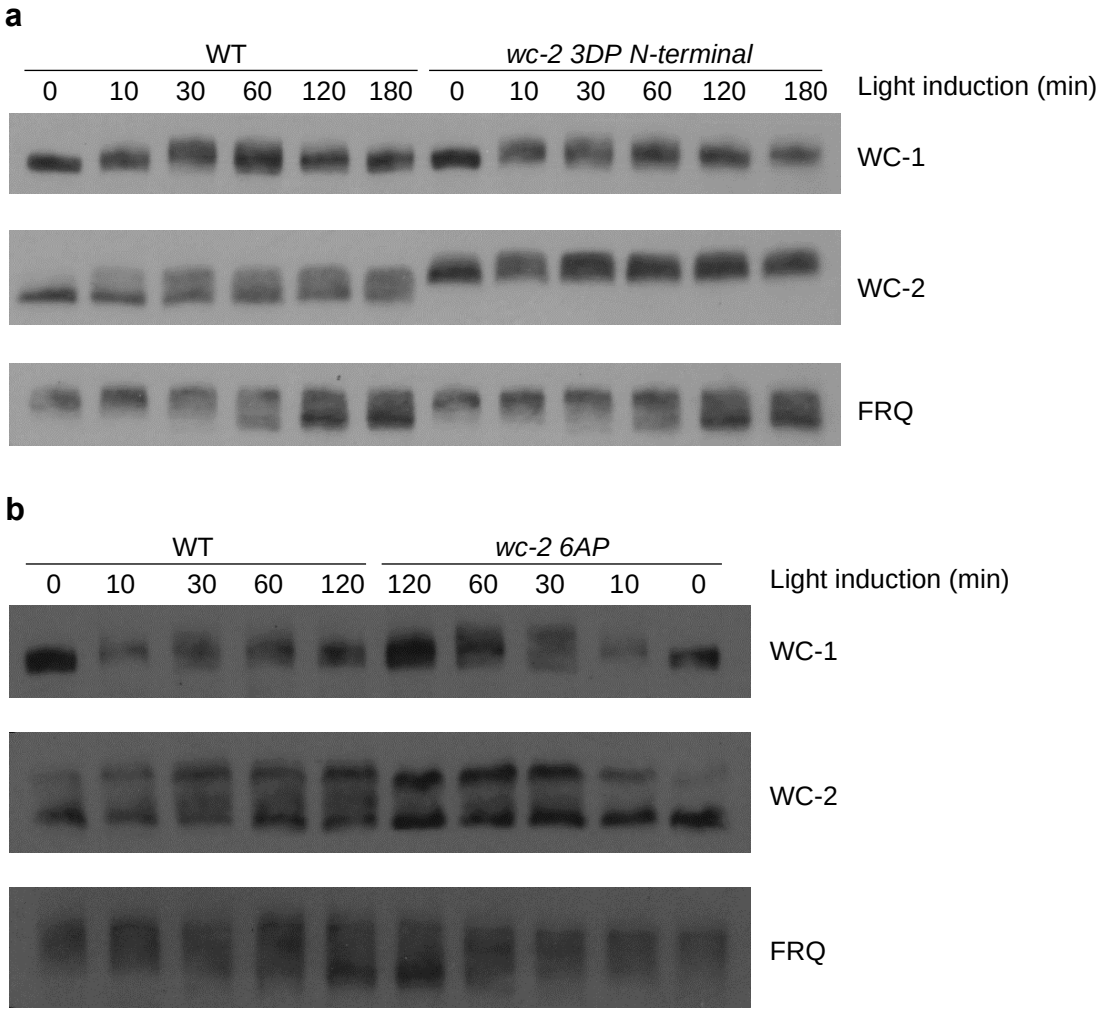

Figure 3.20: Light induction experiment of *wc-2 3DP N-terminal* and *wc-2 6AP*.
3.20a Light induction experiment of the retransformed *wc-2 wild type* and wc-2 *3 DP N-terminal*. Native protein extracts of the heterokaryon strains are shown. **3.20b** Light induction experiment of retransformed *wc-2 wild type* and *wc-2 6AP*. Native protein extracts of the heterokaryon strains are shown. The cloning of *wc-2 6AP* and the design of the experiment was done by Linda Ebelt, the experiment was performed by Justus Hardegen under supervision of Linda Ebelt.

3.6. DNA binding and dimerization of WCC are two triggers of the light-induced phosphorylation of WCC

So far, it was found that increasing phosphorylation reduces the activity of WCC, that FRQ mediates the light-induced phosphorylation of WC-2 by CK-1a and that SP, TP sites trigger further phosphorylation of WC-2. But what is actually the trigger of the light-induced phosphorylation of WCC? Are there differences between WC-1 and WC-2? Three molecular events occur during light induction: the conformational change in the WC-1 LOV domain, WCC dimerization at the WC-1 LOV domain, and binding of WCC to DNA creating contact to numerous potential interaction partners of the transcriptional machinery.

3.6.1. The triggers of the phosphorylation of the small subunit WC-2

A light-induction experiment in a DNA-binding-deficient mutant of WCC (*wc-2 RK/DD*) revealed that WC-2 was not phosphorylated in response to light (see Figure 3.21). The reason was that there was no FRQ expression in *wc-2 RK/DD* since the transcriptional activity is impaired. To compensate for this, FRQ was overexpressed artificially in *wc-2 RK/DD* and in the wild type. In the wild type, the overexpression of FRQ strongly increased the phosphorylation of WC-2 already in dark and of course also in light. In *wc-2 RK/DD*, the overexpression of FRQ resulted in some hyperphosphorylation of WC-2 in dark and further increased hyperphosphorylation in response to light. However, the hyperphosphorylation of WC-2 was not as pronounced in *wc-2 RK/DD* as in the wild type (see Figure 3.21). In conclusion, there is light-induced phosphorylation of WC-2 possible in the DNA-binding deficient mutant, the trigger is most likely the light-induced dimerization of WCC. But since the hyperphosphorylation of WC-2 cannot be restored in *wc-2 RK/DD* to the same extent as in the wild type, DNA-binding is also a trigger of the light-induced phosphorylation.

In a *wc-2* mutant that is DNA-binding deficient but constitutive phosphorylation on the six SP, TP sites is mimicked (*wc-2 6DP RK/DD)*, a slight hyperphosphorylation in response to light was detectable. Thus, the mimicked pre-phosphorylation on the SP, TP sites was sufficient to cause further phosphorylation of WC-2 even in the absence of FRQ. The overexpression of FRQ in *wc-2 6DP RK/DD* strongly increased the phosphorylation of WC-2. The hyperphosphorylation of WC-2 in *wc-2 6DP RK/DD* was as pronounced as in the wild type when FRQ was artificially overexpressed in both strains. Since hyperphosphorylation of WC-2 is more pronounced in *wc-2 6DP RK/DD* strains than in *wc-2 RK/DD* strains, it seems that the mimicked SP, TP phosphorylation can compensate the missing contact to DNA.

Regarding the DNA-binding capacity of WC-2 in *wc-2 RK/DD* and *wc-2 6DP RK/DD*, Figure 3.21 shows that there is some light-induced expression of FRQ. Obviously, the DNA-binding capacity of WCC is strongly reduced due to the RK/DD mutation and the resulting low activity WCC induces expression of the very sensitive *frq* sense LRE as described for *wc-2 allD* in chapter 3.4.2. Previous studies (Schafmeier *et al.*, 2008) and

numerous experiments in this study have shown that the DNA-binding capacity of *wc-2 RK/DD* and *wc-2 6DP RK/DD* is sufficiently low to refer to as DNA-binding deficient strain.

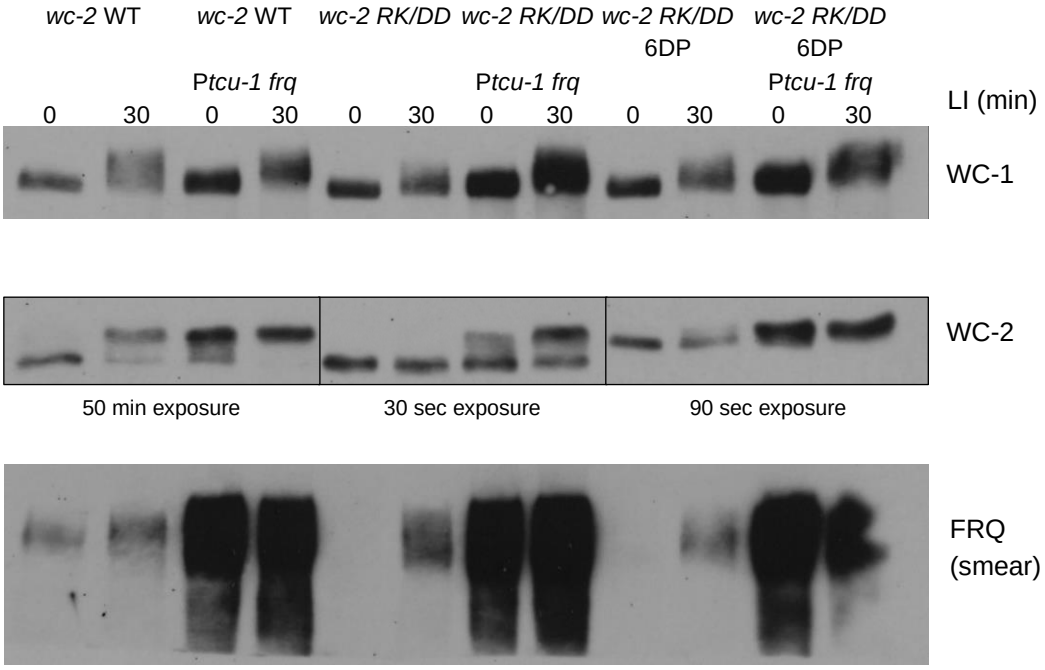

Figure 3.21: Overexpression of FRQ increases phosphorylation of WC-1 and WC-2.
Light induction (LI) experiment of retransformed *wc-2 wild type*, retransformed *wc-2 wild type* $P_{tcu\text{-}1}$ *frq*, *wc-2 RK/DD*, *wc-2 RK/DD* $P_{tcu\text{-}1}$ *frq*, *wc-2 RK/DD 6DP* and *wc-2 RK/DD 6DP* $P_{tcu\text{-}1}$ *frq*. FRQ is overexpressed under control of the $P_{tcu\text{-}1}$ promoter (see lower panel). In this experiment, the WC-2 and the FRQ signal was unusually low in retransformed *wc-2 wild type*. Interestingly, there is still light-induced expression of FRQ in *wc-2 RK/DD* and *wc-2 RK/DD 6DP* although these mutants are DNA-binding deficient. DNA-binding is heavily impaired and not sufficient to initiate transcription beside the very sensitive promoter of *frq*. The very low dark- level of FRQ in *wc-2 RK/DD* is not sufficient to mediate light-induced phosphorylation of WC-2.

3.6.2. The triggers of the phosphorylation of the large subunit WC-1

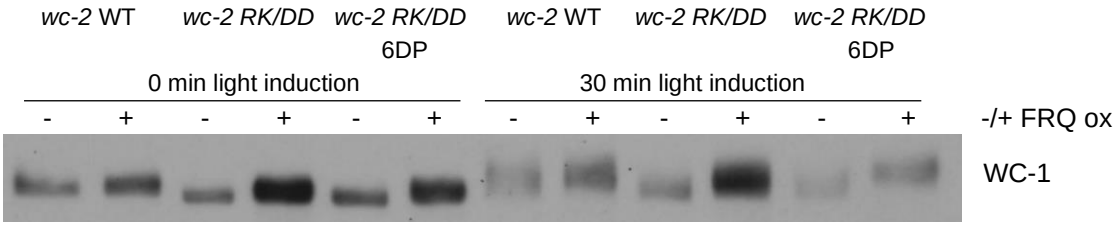

Figure 3.22: Triggers of the light-induced phosphorylation of WC-1.
Different loading scheme of the light induction experiment shown in Figure 3.21 to highlight the light-induced phosphorylation of WC-1 in retransformed *wc-2 wild type*, retransformed *wc-2 wild type* $P_{tcu\text{-}1}$ *frq*, *wc-2 RK/DD*, *wc-2 RK/DD* $P_{tcu\text{-}1}$ *frq*, *wc-2 RK/DD 6DP* and *wc-2 RK/DD 6DP* $P_{tcu\text{-}1}$ *frq* (FRQ ox = FRQ overexpression).

In contrast to the hypophosphorylated WC-2, WC-1 was phosphorylated in response to light in the DNA-binding-deficient mutant *wc-2 RK/DD* (see Figure 3.21). Since there is

still light-induced phosphorylation of WC-1 although DNA-binding is impaired, the trigger of the phosphorylation is very likely the light-induced dimerization of WC-1 at the LOV domain. However, the maximum hyperphosphorylation of WC-1 after 30 min in light was not as high in *wc-2 RK/DD* as in the retransformed *wc-2 wild type* (see Figure 3.22). The same effect was observed in the DNA-binding-deficient mutant *wc-2 6DP RK/DD*. Interestingly, the artificial expression of FRQ in both *wc-2 RK/DD* and in *wc-2 6DP RK/DD* increased the maximum hyperphosphorylation of WC-1 to the level of the retransformed *wc-2 wild type* (see Figure 3.22). Thus, dimerization triggers the light-induced phosphorylation of WC-1 but FRQ-mediated phosphorylation is also required to reach the full hyperphosphorylation of WC-1. The maximum hyperphosphorylation of WC-1 in *wc-2 6DP RK/DD* P_{tcu-1} *frq* was even more pronounced than in the retransformed *wc-2 wild type* P_{tcu-1} *frq* confirming the facilitating function of the SP, TP phosphorylation. In sum, these results indicated that dimerization is a trigger of the WC-1 phosphorylation, that there is a contribution of FRQ to the light-induced phosphorylation of WC-1 and that SP, TP phosphorylation on WC-2 enhance the light-induced phosphorylation of WC-1.

WC-1 hyperphosphorylation below the maximum was also observed in *wc-2 allD* (Figure 3.11). In *wc-2 allD*, DNA-binding of WCC is strongly reduced and there is hardly any FRQ detectable in the dark but there are sufficient FRQ levels reached after more than 60 min in light. So, the absence of sufficient FRQ levels during the first 30 min of light induction explain the reduced hyperphosphorylation phenotype of WC-1 in accordance with the conclusions drawn from *wc-2 RK/DD* and in *wc-2 6DP RK/DD*.

In *wc-2 allD* (see Figure 3.11), the light-induced phosphorylation remains below the maximum and is persistent, whereas the light-induced phosphorylation of WC-1 in the *wild type* is transient. The persistence of the WC-1 phosphorylation over a time range of at least 2 h was also observed in a *vvd* non-function mutant (vvd^{SS692}, Heintzen *et al.*, 2001) and in *wc-2 RK/DD* (data not shown). These mutants, *wc-2 allD*, *vvd* non-function and *wc-2 RK/DD*, have in common that VVD is not expressed or not functional and cannot interfere with the light-induced dimerization of WCC. It seems that WCC-VVD dimer is not a target of kinases and that WCC-VVD dimerization thus impedes WCC phosphorylation. These observations are another strong argument that WCC dimerization is a trigger of the light-induced phosphorylation.

In contradiction to these conclusions, WC-1 was as high phosphorylated in a *frq knock out* mutant as in the wild type (see Figure 3.9) although FRQ is missing as mediator of the WC-1 phosphorylation. The mutants showing intermediate hyperphosphorylation of WC-1 in the absence of FRQ, *wc-2 RK/DD, wc-2 6DP RK/DD* and *wc-2 allD*, have in common that both FRQ and DNA-binding are missing. In the *frq knock out* mutant, WCC does still bind to DNA and initiates transcription, just the *frq* gene is knocked out. Thus, DNA-binding and light-induced dimerization of WC-1 at the LOV domain must be the triggers that induce maximum hyperphosphorylation of WC-1 in the *frq knock out* mutant. Since FRQ overexpression and light-induced dimerization of WC-1 at the LOV domain

can induce maximum hyperphosphorylation of WC-1 in *wc-2 RK/DD* $P_{tcu\text{-}1}$ *frq*, the two triggers, DNA-binding and FRQ, can compensate for each other to some extent. But there is also the possibility that the differences in the phosphorylation of WC-1 cannot be resolved by SDS-gel as it was used in this study. On the other hand, compensation seems to be a general fail-safe mechanism in the regulation of the activity of WCC as it was also observed that the two subunits WC-1 and WC-2 can compensate for each other.

Taken together, the two subunits of WCC, WC-1 and WC-2, have different features and are phosphorylated differentially. But the separate investigation of WC-1 and WC-2 with the mutants shown in this chapter and in this study lead independently to the same conclusions:

- FRQ mediates the phosphorylation of both WC-1 and WC-2.
- DNA-binding is a trigger of the phosphorylation of both WC-1 and WC-2.
- SP, TP phosphorylation enhances further phosphorylation of both WC-1 and WC-2.
- The light-induced dimerization of WCC is a trigger of the phosphorylation of both WC-1 and WC-2. However, direct proof is pending.
- Whether the conformational change in the WC-1 LOV domain is a trigger of light-induced phosphorylation could not be dissected with the experimental approaches used here.

3.7. Hypothesis: feedback of the transcriptional machinery on WCC

As described above, DNA-binding is a trigger of the phosphorylation of WCC and phosphorylation on SP, TP of WC-2 enhances further phosphorylation of WCC. The occurrence of DNA-binding and proline-directed phosphorylation is hardly a coincidence because several proline-directed kinases are components of the transcriptional machinery: CDK7, CDK8, CDK9.

These proline-directed kinases are brought in close vicinity to the specific transcription factor WCC by the transcriptional machinery and might phosphorylate WCC. The phosphorylation of the SP, TP sites of WCC could be checkpoint of transcription. It could be a feedback of the correctly assembled (pre)initiation complex on WCC marking WCC with the message „Transcription factor was active!“ (Figure 3.23). The phosphorylation on SP, TP sites would enhance further phosphorylation mediated by FRQ that deactivates WCC.

With this mechanism, the cell could discriminate between light-activated WCC and light-activated WCC that has actually initiated light-induced transcription. This mechanism would ensure that not all light-dimers of WCC are deactivated immediately by phosphorylation but only transcriptional active WCC molecules are deactivated.

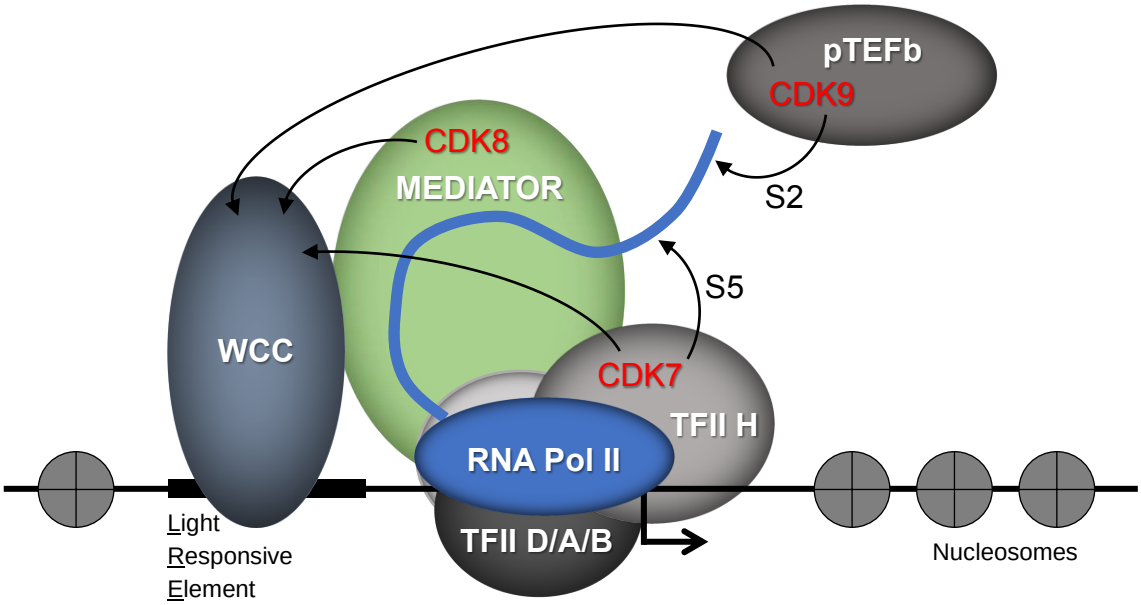

Figure 3.23: Hypothesis of the feedback of the transcriptional machinery on the specific transcription factor White Collar Complex (WCC).
WCC is binding to its target sequence, the light responsive element (LRE), in the promoter region of a light-inducible gene. Nucleosomes are removed from the relevant sequences to initiate transcription. The proline-directed kinases of the transcriptional machinery (highlighted in red) might feedback on WCC and phosphorylate the SP, TP sites.

3.8. Artificial SP, TP phosphorylation rescues WC-2 phosphorylation in the presence of a transcriptional inhibitor.

To investigate the hypothesis of the feedback of the transcriptional machinery, a light-induction experiment was performed in the retransformed *wc-2 wild type* and in *wc-2 6DP* in the presence and absence of the transcription inhibitor thiolutin. In dark, after 0 min light induction, thiolutin suppressed the slight hyperphosphorylation of WC-2 in both the retransformed *wc-2 wild type* and in *wc-2 6DP* (see Figure 3.24). In light (30 min light induction), thiolutin suppressed any light-induced phosphorylation of WC-2 in the retransformed *wc-2 wild type*. After 120 min in light, the suppression was still maintained (data not shown). Unlike the wild type, WC-2 was light-induced phosphorylated in *wc-2 6DP* in the presence of thiolutin. However, thiolutin shifted the fraction of hyper- and hypophosphorylated WC-2 in *wc-2 6DP* towards the hypophosphorylated species (see Figure 3.24). In conclusion, the transcriptional inhibitor thiolutin suppressed the phosphorylation of WC-2 in the wild type but the six phospho-mimicking DP residues in in *wc-2 6DP* restored the phosphorylation of WC-2 to some extent. Thus, phosphorylation at the SP, TP sites seems to mimic active transcription.

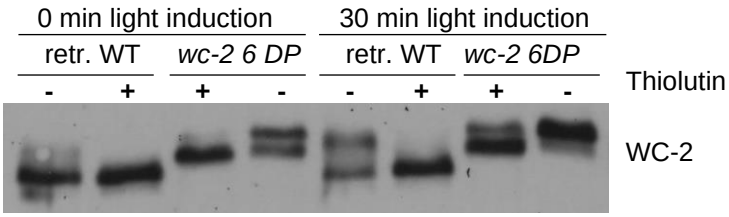

Figure 3.24: Light-induced phosphorylation of WC-2 6DP in the presence of the transcriptional inhibitor Thiolutin.
Light induction experiment in retransformed *wc-2 wild type* and *wc-2 6DP* in the presence and absence of 12 µg/mL thiolutin, a transcriptional inhibitor. The cultures were incubated with thiolutin for 90 min in dark before harvesting the 0 min sample or starting the 30 min light induction.

However, this finding supports but does not prove the hypothesis of the feedback of the transcriptional machinery, since thiolutin was found to have pleiotropic effects in the cell and the mechanism of the transcriptional inhibition by thiolutin is not fully understood so far (Lauinger *et al.*, 2017). It was shown that thiolutin prevents binding of WCC to target genes (Brunner Lab, unpublished data) and that RNAP II transcript levels as well as RNAP II S5-P occupancy at promoters are reduced in the presence of thiolutin (Lauinger *et al.*, 2017). Nevertheless, it cannot be excluded the phosphorylation of WCC is modified in the presence of thiolutin due to pleiotropic effects. Several other transcriptional inhibitors and inhibitors of CDK7 and CDK9 were tested in Neurospora crassa but no effect on transcription was measured (data not shown). Thus, the use of conventional, small inhibitory compounds is no suitable approach to prove the hypothesis of the feedback of the transcriptional machinery.

3.9. Outlook: Proof of the hypothesis with a sensitive CDK7 mutant

If CDK7, CDK8 and CDK9 could be inhibited or knocked out, it is expected to find a reduced phosphoryation of WCC according to the hypothesis of a feedback of the transcriptional machinery. Inhibition with conventional inhibitors is not an option, as outlined above.

CDK8 (stk-8 in *N. crassa*) is available as homokaryon knock out strain indicating that this kinase is not essential *N. crassa*. The *stk-8* knock out strain was tested in a light induction experiment but no impact on the phosphorylation of WC-1 and WC-2 was found (unpublished data, not shown).

For CDK7 and CDK9 (prk-3 and stk-1, stk-47 in *N. crassa*), knock out strains are not available since these kinases are essential. To overcome this, a sensitized mutant of CDK7 (Prk3) was cloned. The mutation makes the active site accessible for a small inhibitory compound but still allows the turn-over of ATP (Figure 3.25). Thus, the mutant is viable but the activity of CDK7 can be inhibited. Additionally, the inhibition CDK7 would also inhibit CDK9 since transcript elongation cannot start as long as transcription is not initiated. After cloning of the sensitive CDK7 (Prk3) mutant, this project was handed over and is still ongoing.

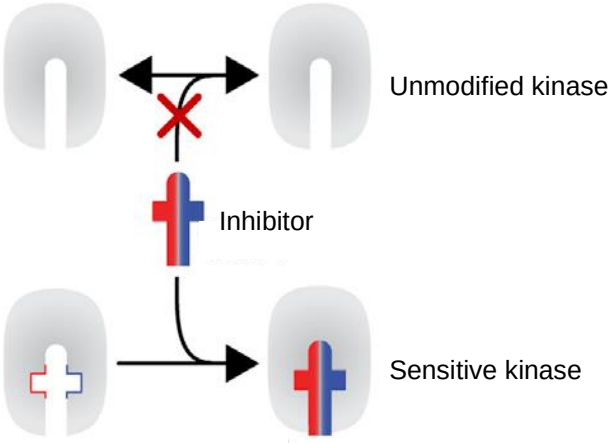

Figure 3.25: Visualization of the principle of a sensitized essential kinase.
One or more amino acids are mutated to enlarge the active site and make it accessible for an inhibitor. ATP can still be processed so that the mutant is viable. Modified acc. to Rodriguez-Molina *et al.*, 2016.

3.10. Conclusion: The mechanism of the light-induced phosphorylation of White Collar Complex

The aim of this project was to unravel the mechanism of the light-induced phosphorylation of WCC. The results of this project imply the following mechanism that is illustrated in Figure 3.26.

In the dark, there is a pool of differently and poorly phosphorylated molecules of WCC. Blue light is received by the LOV domain in WC-1, the large subunit of WCC. Light reception causes a molecular rearrangement in the LOV domain that allows the dimerization of two LOV domains and thus the formation WCC light-dimers. This dimerization is **the first trigger** of the light-induced phosphorylation of WCC.

The WCC light-dimer binds to the LRE in the promoter of light-inducible genes. The forming transcriptional machinery (pre-initiation complex) brings CDK7 and also CDK9 in close vicinity to WCC. At some point of successful initiation of transcription or successful formation of the pre-initiation complex, CDK7 (may be also CDK8, maybe later also CDK9) phosphorylated WCC most likely at the SP, TP residues. This is a feedback of the transcriptional machinery that leaves a mark on WCC telling "transcription factor was active". Thus, DNA-binding is **the second trigger** of the light-induced phosphorylation of WCC.

In the following, the protein complex based on FRQ brings CK1-a to WCC and the accumulating phosphorylation on single WCC molecules gradually reduces the activity. FRQ-mediation is **the third trigger** of the light-induced phosphorylation of WCC. In the following, light-activated WCC molecules are caught by VVD and this inhibits the phosphorylation of WC-1 causing the transience of the WC-1 phosphorylation while WC-2 remains hyperphosphorylated.

Overall, the identification of phosphorylation sites, their function and the identification of triggers and enhancers of the light-induced phosphorylation have shown that this mechanism is rather a balance of kinetics and efficiency than a stringent sequence of switch-like molecular events. This balance as well as several options for compensation ensure the flexibility, the fine-tuning and protection of the system.

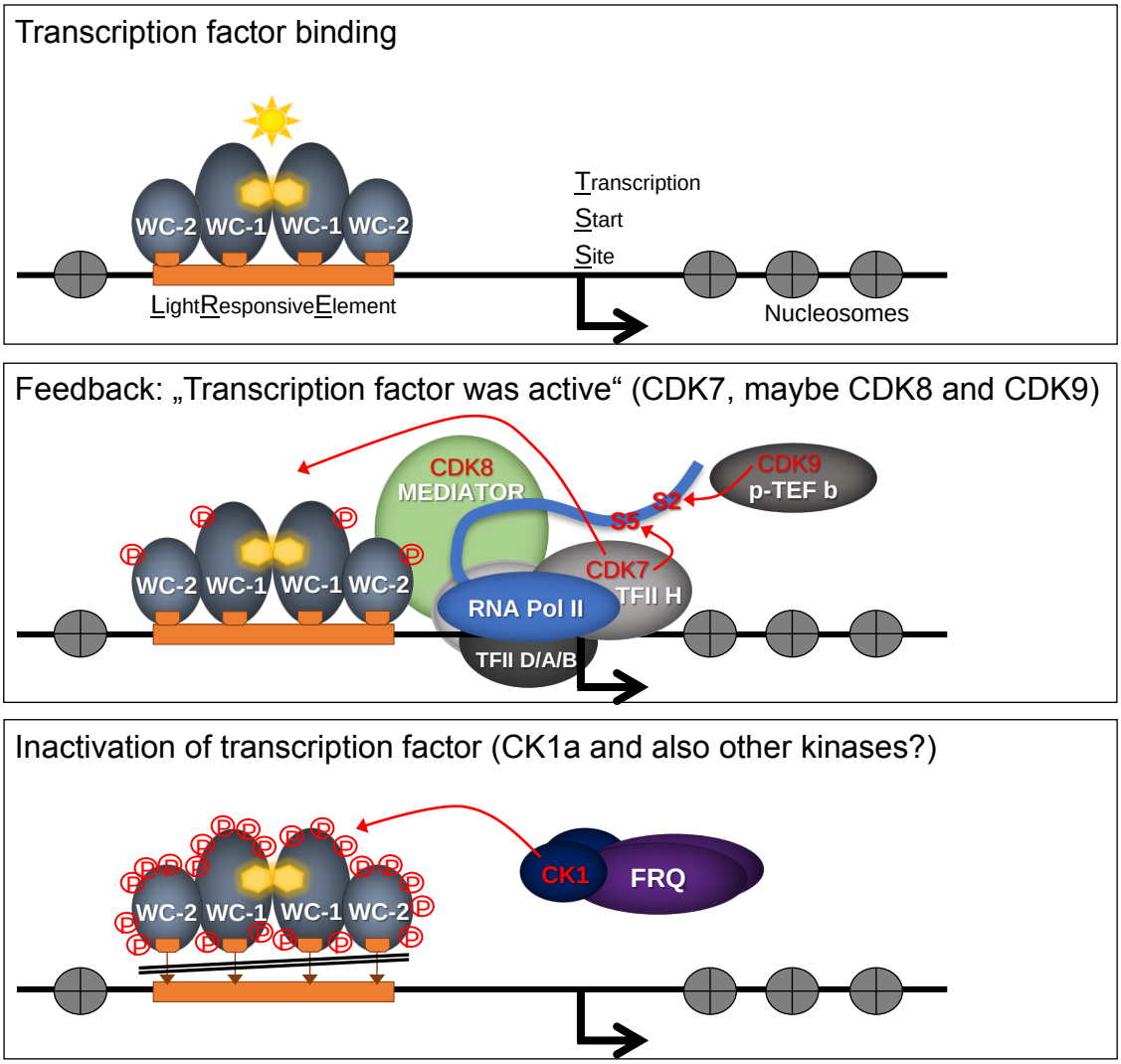

Figure 3.26: Graphical summary of the results of this study.

4. Discussion

4.1. Comparison of this study with a similar study

In May 2019, Wang *et al*. from the research group of Jay C. Dunlap at the Geisel School of Medicine at Darthmouth, Hanover, USA, have published a study very similar to this study (Wang *et al.*, 2019). The experiments and analysis of results for this study were completed in July 2018. Afterwards, only writing and compilation of the thesis was performed. The study of Wang *et al*. is focused on the circadian phosphorylation of WCC while this study is focused on the light-induced phosphorylation. The study of Wang *et al*. brought similar results about, confirming these results to some extent. In the following, the results of this study are discussed in the context of the study by Wang *et al.*, 2019.

Sequence coverage and total number of phosphorylation sites

To map the phosphorylation sites of WCC, a high sequence coverage (100 % or close to 100 %) was achieved in both studies by usage of a combination of proteases. Wang *et al.* used Trypsin and Protease K while this study used Trypsin, Thermolysin and Elastase. Overall, the similar phosphorylation sites were found, but some differences are obvious. For WC-1, Wang *et. al*. found more phosphorylation sites in total and found 3 tyrosine (Y) residues phosphorylated whereas this study found only S, T phosphorylation (see Table 4.1). For WC-2, Wang *et. al*. found less phosphorylation sites in total, tyrosine phosphorylation wasn´t found in both studies (see Table 4.1).

Table 4.1: Comparison of the number of phosphorylation sites of WC-1 and WC-2 found in this study and in the study of Wang et al. 2019.

		Phosphorylation sites
WC-1	**This study**	34 S, T
	Wang *et al*. 2019	80 S, T, Y
WC-2	**This study**	23 S, T
	Wang *et al*. 2019	15 S, T

Wang *et. al*. concluded from experiments with their WC-1 109A mutant (109 S, T sites mutated collectively to alanine to prevent phosphorylation; 77 phosphorylation sites that were found by mass spectrometry and 32 additional S or T to alanine were mutated), and with their WC-2 15pA mutant (all 15 phosphorylation sites mutated collectively to alanine) that all relevant phosphorylation sites were covered by the mass spectrometry. For WC-2, this study draws the same conclusion from the WC-2 allA mutant (all 23 phosphorylation sites mutated collectively to Alanine). However, Wang *et. al*. state that WC-2 phosphorylation is fully covered by 15 phosphorylation sites whereas this study relies on 23 phosphorylation sites. This discrepancy might be explained by the fact, that 10 out of the 23 phosphorylation sites of this study are putative phosphorylation sites. Thus, the true number of WC-2 phosphorylation sites ranges between 15 and 23 sites.

Since the difference in the number of phosphorylation sites of WC-1 and WC-2 was less pronounced in this study (WC-1: 34 sites; WC-2: 23 sites), the decision to focus the investigation on WC-2 seems reasonable. Whereas the high number of phosphorylation sites of WC-1 in the study of Wang *et. al*. obviously drew the attention to the larger subunit of WCC.

The regulation of WCC requires phosphorylation of both WC-1 and WC-2

When analyzing the phenotype of the WC-1 109A mutant and the WC-2 15pA, Wang *et. al*. found a wild type-like phenotype for both mutants. The WC-2 15pD mutant (mimicking constitutive phosphorylation) was arrhythmic. This study found the same circadian phenotype for *wc-2 allA* and *wc-2 allD*, proving that the results are right. However, this study did not generate phosphorylation site mutants of WC-1. In this study, only phosphorylation sites of WC-2 were mutated and based on several results the hypothesis of the regulatory compensation by WC-1 was developed. The results of this study indicate that both subunits of WCC, WC-1 and WC-2, can compensated for each other although these two molecules have a different structure and different functions to some extent. By creating double mutants of WC-1 and WC-2, Wang *et al*. showed that the regulation of WCC requires phosphorylation of both WC-1 and WC-2. Wang *et al*. analyzed specific phosphorylation site mutants of WC-1 (S, T, Y to A) in the background of wc-2 mutants (S, T to A) and *vice versa* to detect the true phenotype. Thus, the study of Wang *et al*. confirms the hypothesis of compensation from this study.

SP, TP phosphorylation sites of WC-1 and WC-2

This study found SP, TP phosphorylation sites to be overrepresented and focused on the investigation of this finding whereas Wang *et. al*. didn´t touch this topic at all. Table 4.2 shows that the overrepresentation of SP, TP sites is more obvious in this study than in the study of Wang et al., at least for WC-1.

Table 4.2: The overrepresentation of SP, TP sites in this study in comparison to the study of Wang *et al.*

		SP, TP sites	**S, T sites**	**Percentage SP, TP**
WC-1	**This study**	12	34	35 %
	Wang *et al*. 2019	21	77	27 %
WC-2	**This study**	6	23	26 %
	Wang *et al*. 2019	4	15	27 %

The data shown by Wang *et. al*. include the number of peptides on which the phosphorylation site was found. Interestingly, SP, TP sites are overrepresented in the group of WC-1 phosphorylation sites that were found on numerous peptides: 15 sites out of 80 sites were mapped on a high number of peptides (**S8**, **S11**, S92, **S111**, **S200**, S234, **S315**, **S824**, **S831**, **S971**, S988, **S990**, **S1005**, **S1015**, **S1074**) and 11 out of these 15 sites are SP sites (highlighted in bold letters). In this way, the WC-1 data of Wang *et. al*.

support the importance of SP, TP sites identified in this study as a mechanistical aspect of the WCC phosphorylation.

No light- and dark-specific phosphorylation sites on WC-1 and WC-2

Wang *et. al*. analyzed the phosphorylation of WC-1 and WC-2 also under different growth conditions in dark and in light (Wang *et. al*.: LL, LP15, DD15, DD24, this study: LI15, LI30, DD24; see explanation below in Table 4.3). Wang *et. al*. describe LP15 as time point when WCC undergoes maximal light-dependent phosphorylation. But acc. to the results of this study, LP15 as well as LI15 are the time points of intermediate phosphorylation of WCC. Beside this discrepancy, LP15, LP15 and LP30 are supposed to be sufficient to identify light-specific phosphorylation sites.

Table 4.3: Short explanation of the growth conditions in dark and in light.

Growth condition		**Physiology**
LL	constant light	WCC constantly induces FRQ expression
LP15	light pulse for 15 min	WCC undergoes maximal light-dependent phosphorylation, independent from the circadian clock (acc. to Wang *et al*., 2019)
LI15	light induction for 15 min	WCC undergoes intermediate light-dependent phosphorylation, independent from the circadian clock (acc. to this study)
LI30	light induction for 30 min	WCC undergoes maximal light-dependent phosphorylation, independent from the circadian clock (acc. to this study)
DD15	constant dark for 15 hours	WCC is active, circadian subjective morning
DD24	constant dark for 24 hours	WCC is inactive, circadian subjective evening

This study aimed at the identification of light-specific phosphorylation sites but came to the conclusion that there is hardly a difference in light- and dark-phosphorylation of WCC although the molecular mechanism of the WCC activity in light and in dark are different. Wang *et. al*. performed the mapping of phosphorylation sites in light and in dark but did not analyze or discuss the specificity of the phosphorylation. Their data (presented in Figure S1 in Wang *et al.*, 2019) show light- and dark-specific phosphorylation sites of both WC-1 and WC-2. But many of these sites were found in this study under both conditions and several sites, that seemed to be light- or dark-specific phosphorylation sites in this study were found under both conditions in the study of Wang *et al.*, 2019.
Furthermore, for both WC-1 and WC-2 it is obvious that light- or dark-specific phosphorylation sites are found on only very few peptides (1-3 peptides). In contrast to that, all phosphorylation site, that were found on numerous peptides, were found in light as well as in dark. The only exception is S971 of WC-1 that was found on 10 peptides at DD24 in the study of Wang *et. al*.. However, S971 was found in this study at LI15 and at

DD24, so is not a dark-specific phosphorylation site. Like the data of Wang *et. al*., the raw data of this study also show some light- or dark-specific phosphorylation sites. The analysis of the data revealed, that these sites were found on peptides or fragmentation products of peptides and that were rare and most likely hardly detectable by mass spectrometry. The observation that the light- or dark-specific phosphorylation sites of the study by Wang *et. al*. were also found on rare peptides supports the interpretation of the data from this study. The light- or dark specificity of most of the phosphorylation sites is chemical-technical artefact of the mass spectrometry.

T339 and S433 of WC-2 are the key target sites

Regarding WC-2, only T339 and S433 were found on numerous peptides (5 peptides and more) in the study of Wang *et. al*, all the other phosphorylation sites were found on less than 5 peptides. And like the observations made for WC-1, T339 and S433 of WC-2 were found in light and in dark and are SP, TP sites. These two sites are part of the cluster that was identified as minimum of mutated phosphorylation sites causing arrhythmia (*wc-2* S331A, T339A, S341A, S433A, T435A). It would be interesting so see the phenotype of a T339, S433 double mutant, but Wang *et al*. did not present such a mutant. In the study of Wang *et al*., the phosphorylation sites were mutated to alanine to prevent phosphorylation. Also, the phenotypes of WC-2 alanine mutants were analyzed in the context of WC-1 alanine mutants and *vice versa* to eliminate the masking of phenotypes by compensation of the other subunit of WCC. In this study, a phenotype related to T339 and S433 of WC-2 was found by using the opposite approach. In the *wc-2 3DP C-terminal* mutant, T339, S433 and T523 (SP, TP sites) are mutated to aspartate to mimic phosphorylation in a *wc-1* wild type background. Mimicking phosphorylation of only one subunit obviously has a stronger effect. The mutation of T339, S433, T523 to aspartate resulted in an accelerated phosphorylation of WC-2. This acceleration was even more pronounced in *wc-2* T86D, S118D, T136D, T339D, S433D, T523D (*wc-2 6DP*) but not visible at all in *wc-2* T86D, S118D, T136D, pointing to the importance of T339 and to S433. In this study, the alanine mutant *wc-2* T86A, S118A, T136A, T339A, S433A, T523A (*wc-2 6AP*) was found to have a wild type-like phenotype and it was concluded that this is due to the compensation by WC-1. The study of Wang *et al*. confirms this conclusion. Taken together, the results of both studies indicate that T339 and S433 of WC-2 are the key target sites of the transcriptional machinery to regulate WC-2 activity in light as well as in dark although the molecular mechanisms of WCC activity in light and in dark are different.

Phosphorylation modulates the strength of WCC DNA binding

Wang *et al*. showed that WC-1 and WC-2 alanine mutants bind stronger to the *frq* c-box than the wild type since the alanine mutation represents an active, hypophosphorylated state of WCC. The WC-2 aspartate mutant was found to bind less strong to the *frq* c-box than the wild type since the aspartate mutation represents a constitutive

hyperphosphorylation. In this study, the same outcome was found for a WC-2 alanine and a WC-2 aspartate mutant, but for the *frq* LRE instead of the *frq* c-box. Thus, both studies came to the conclusion that phosphorylation gradually modulates the DNA binding and thus the activity of WCC. This further proves that the circadian activity and the light-induced activity of WCC are most likely regulated by the same mechanism of phosphorylation. Although the circadian activity and the light-induced activity of WCC are different molecular mechanism, the difference in the mechanism of phosphorylation remains elusive.

The WC-1 S990 cluster

Wang *et al*. identified the cluster of WC-1 phosphorylation sites around S990 (S971, S988, S990, S992, S994, S995) to be crucial for the inactivation of WCC. The respective experiments were conducted in a WC-2 15A or WC-2 10A background to eliminate the compensation by WC-2. Except from S971, this cluster represents the first phosphorylation sites detected on WCC in a study by He *et al.*, 2005 (S988, S990, S992, S994, S995). In contrast to these studies, this study mapped only S971, S988 and S990 and S988 is doubtful since it is a putative phosphorylation site. This contradicts the importance that was assigned to the full cluster around S990 in the other studies. But interestingly, S971 and S990 are both followed by proline. Taken the results of all studies together, the SP sites S971 and S990 might be the only functional relevant phosphorylation sites. If so, this further supports the crucial function of proline-directed phosphorylation the regulation of WCC.

FRQ-mediated phosphorylation of WC-1

Wang *et al*. detected FRQ-promoted phosphorylation events on WC-1 and WC-2. The experimental approach was to mutate all S, T, Y residue on WC-1 or WC-2 to alanine and then to reverse selected sites of interest to the wild type amino acid. Since the FRQ level was very low in these strains, FRQ was overexpressed artificially under control of an inducible promoter. The results showed that FRQ overexpression promotes phosphorylation of WC-1 S971; S990; S1015; S988 + S992 + S994 + S995 and WC-2 S433. The WC-1 site S971 showed phosphorylation even in the absence of FRQ and the overexpression of FRQ strongly increased the phosphorylation. In this study, similar conclusions were drawn from very different experimental approaches. This study has shown that FRQ and CK-1a are not required for but enhance the light-induced hyperphosphorylation of WC-1. Unlike WC-1, FRQ and CK-1a are required for and also enhance the light-induced hyperphosphorylation of WC-2.

Interestingly, the current standard kinase prediction tools predict that most the above-mentioned phosphorylation sites of WC-1 and WC-2 are hardly a target of CK1a or CK2 (see also Table S3 in Wang *et al*. 2019). But if FRQ mediates the phosphorylation of these residues, FRQ may interact with other kinases than CK1a and CK2. Furthermore, the majority of the above-mentioned phosphorylation sites of WC-1 and WC-2 are SP, TP

sites (WC-1 S971; S990; S1015; S995 and WC-2 S433). Again, this implies a strong functional relevance of proline-directed phosphorylation in the regulation of WCC.

The kinases that phosphorylate WCC

Like this study, Wang *et al*. also asked which kinases are involved in the light-induced phosphorylation of WCC. They disconfirmed the previously suggested kinase PKA (Huang *et al.*, 2007) leaving CK1a to be the only kinase known to be essential for the circadian phosphorylation of WCC. CK2 is suggested to compensate for CK1a. In the discussion of the paper, Wang *et al*. mention that no single knock out strains of non-essential kinases show an arrhythmic phenotype. Some kinase knock out strains were screened in this study for altered light-induced phosphorylation of WCC, but no phenotype was detected. Like this study, Wang *et al*. also suggest the redundancy of kinases that regulate the circadian clock. But for the first time, this study suggested the kinases of the transcriptional machinery, CDK7, CDK8, CDK9, to phosphorylate WCC.

The black widow model and WCC phosphorylation

The discussion of the data on Wang *et al*. revealed, that the overrepresentation of SP, TP sites was not recognized. This is surprising since Wang *et al*. use the black widow model to interpret the data and this model obviously suggests proline-directed phosphorylation. The black widow model describes that the appropriate termination of transcription initiation is as important as well-regulated transcription initiation to organize gene transcription activity (Chi *et al.*, 2001; reviewed in Tansey, 2001). The termination of transcription initiation is achieved by controlled activity-associated turnover of transcriptional activators. After initiation of gene transcription, transcription factors are marked and degraded.

Regarding WCC, the negative feedback loop describes that active WCC is hyperphosphorylated in an FRQ-dependent manner to inactivate, but not to degrade WCC. The observation, that hyperphosphorylation stabilizes WCC, is called the positive feedback loop since it maintains the WCC level. In other words, hypophosphorylated, active WCC is instable. Wang *et al*. report that WC-1 and WC-2 mutants that accumulate a critical number or position of alanine mutations, are very active since there is no inactivation by phosphorylation and thus, the WCC levels are low. Wang *et al*. correctly state that this observation is in accordance with the black widow model. They also state correctly, that acc. to the black widow model, the active transcription factor is marked for turnover. However, Wang *et al*. do not mention how WCC gets the mark for turnover. In the black widow model, the transcriptional activator is phosphorylated by CDK 8, the kinase of the mediator complex (homolog *Saccharomyces cerevisiae*: Srb10) to be marked for ubiquitin-mediated proteolysis. CDKs are known to phosphorylate SP, TP motifs.

In contrast to Wang *et. al*., this study suggests that the phosphorylation of WCC is a multistep phosphorylation. Acc. to the black widow model, SP, TP phosphorylation by

the kinases of the transcriptional machinery targets WCC for degradation but also for facilitation of further, inactivating phosphorylation. This hypothesis explains the degradation of active WCC as well as the positive feedback by FRQ. This hypothesis also explains, why the WCC levels are still high in the *wc-2 6DP* mutant. In this mutant, mimicked SP, TP phosphorylation targets for degradation but also strongly facilitates the stabilizing, FRQ-mediated phosphorylation.

The observation that active, hypophosphorylated WCC is instable might be due to the fact that the *in vivo*, only a few phosphorylated SP, TP sites could be sufficient to initiate ubiquitin-mediated proteolysis. The experiments with the *wc-2 6DP* mutant showed that the artificial addition of 6 negative leads to a slowdown in the migration in the SDS-PAGE that is never observed *in vivo*. Furthermore, WC-1 and WC-2 could act together so that a very few phosphorylated SP, TP sites on each protein are hardly detectable by SDS-PAGE or mass spectrometry but are sufficient to initiate degradation. The experimental proof that a kinase of the transcription machinery phosphorylates WCC and the technical realization of a time-resolved detection of WCC phosphorylation would be required to test the hypothesis created in this study. Nevertheless, the time-resolved detection of WCC phosphorylation might be impossible since the SP, TP phosphorylation and the FRQ-mediated phosphorylation are very likely parallel processes similar to the light-induced dimerization of WCC (activating) and of WCC and VVD (inactivating). Also, as outlined in the discussion of the data of Wang *et al*., FRQ might also play a role in the recruitment of other kinases, may be also of the CDKs of the transcriptional machinery. The parallelism of positive and negative regulation of WCC and of different regulatory mechanism is very likely since this allows fine-tuning of the gene expression, compensation in case of malfunction of a certain system and thus creates robustness.

4.2. Serine 433 of WC-2, an important regulatory phosphorylation site

Serine 433 was the first phosphorylation site of WC-2 published (Sancar *et al.*, 2009). This previous study found that the WC-2 S433A mutant is rhythmic like the wild type but the S433D mutant has a period slightly longer than wild type. The study also found that WCC is more active in S433A and less active in S433D. This phosphorylation site was confirmed in this study as well as in the study of Wang *et al*., 2019 and it was the most abundant phosphorylation site of WC-2 in both studies. This study identified S433 as SP site as part of the C-terminal cluster of 3 SP, TP sites that shows a strong phenotype. Wang *et al*., identified S433 as part of the cluster of WC-2 phosphorylation sites that are required to maintain the circadian rhythm. Although this study focused on the light-induced phosphorylation and the study of Wang *et al*. focused in the circadian phosphorylation of WCC, the results of both studies are in accordance with the previous study of Sancar *et al.*, 2009. Alanine (A) mutants of WCC phosphorylation sites show increased activity of WCC and Aspartate (D) mutants show decreased activity. The longer

period of the S433D mutant points to an effect on the circadian rhythm. Taken together, these results imply an important regulatory role of serine 433 of WC-2, very likely more important than other phosphorylation sites of WC-2.

4.3. Phosphorylation of WCC equivalents in mammals and *D. melanogaster*

The molecular clocks of *Drosophila melanogaster* and mammals (*Mus, Homo*) share many molecular similarities with *Neurospora crassa*.

In *Drosophila melanogaster*, the positive element in the feedback loop is the heterodimeric transcription factor CLK/CYC (CLOCK and CYCLE). Like WC-1 and WC-2, CLK and CYC also have PAS domains but have bHLH DNA binding domains instead of a ZnF. The negative element in *D. melanogaster* is the PER/TIM complex (PERIOD / TIMELESS) that interacts with kinases and gets intensively phosphorylated, similar to FRQ in *N. crassa*. The Casein Kinase DBT (DOUBLE-TIME, homolog to mammalian CK1ε) is an important pace maker of the *D. melanogaster* circadian clock that phosphorylates PER but also CLK. In *N. crassa*, CK1a was found to phosphorylate FRQ but also WCC. But in *D. melanogaster*, the kinases CK2, SGG (shaggy, ortholog of GSK3), NMO (NEMO, MAPK) and AMPK were also found to phosphorylate one or more proteins of the circadian feedback loop (Cho *et al.*, 2019; Yu *et al.*, 2011; reviewed in Mehra *et al.*, 2009)

In mammals, the positive element is the heterodimeric transcription factor BMAL1/CLOCK. Both proteins have PAS domains and bHLH DNA binding domains. The negative element of the circadian feedback loop is PER/CRY which is in a complex with and phosphorylated by CK1δ. In mammals, numerous kinases were shown to phosphorylate PER/CRY and especially the positive element BMAL1/CLOCK: AKT, ATM, CK1δ/ε, CK2, Chk1, Chk2, GSK3, PKA, PKC, PKG-II, RACK1 (Aryal *et al.*, 2017; Luciano *et al.*, 2018; Robles *et al.*, 2010; Shim *et al.*, 2007; Spengler *et al.*, 2009; Tischkau *et al.*, 2004; reviewed in Mehra *et al.*, 2009).

Taken together, both positive and the negative elements of the central feedback loop in eukaryotes are regulated and controlled by phosphorylation. In contrast to *D. melanogaster* and mammals, only very few kinases are known to phosphorylate the *N. crassa* clock proteins. CK1 plays a major role in the circadian system of *N. crassa, D. melanogaster* and mammals. Due to the difficult identification of kinases with circadian function in *N. crassa*, several studies including this one presumed the activity and the redundancy of many kinases. Given the large number of kinases with circadian function in *D. melanogaster* and mammals, this assumption seems reasonable. Most likely, different experimental approaches are required to identify other kinases in *N. crassa*.

So far, only a few phosphorylation sites of BMAL1/CLOCK are known (1 site BMAL1, 9 sites of CLOCK, mammalian) (Luciano *et al.*, 2018; Spengler *et al.*, 2009; Tamaru *et al.*, 2009; Yoshitane *et al.*, 2009). The phosphorylation sites were found to have various

effects. S90 of BMAL1 was found to regulate the accumulation of BMAL1/CLOCK in the nucleus and mutation of this single site to alanine was found to disrupt the clock function (Tamaru *et al.*, 2009). S38 and S42 of CLOCK were found to additively weaken the activity of BMAL1/CLOCK, an effect of phosphorylation similar to WCC in *N. crassa* (Yoshitane *et al.*, 2009). The phosphorylation cluster S427-S441 of CLOCK was identified as GSK3-mediated phosphor-degron (Spengler *et al.*, 2009). S845 of CLOCK was found to negatively regulate BMAL1/CLOCK in peripheral tissues (Luciano *et al.*, 2018). Among the phosphorylation sites of mammalian BMAL1/CLOCK, S427 of CLOCK is the only site followed by a proline and was identified as target of the proline-directed kinase GSK3.

Interestingly, numerous phosphorylation sites were found on CLK of the CLK/CYC complex (19 sites, *D. melanogaster*; Lee *et al.*, 2014; Mahesh *et al.*, 2014). Like WC-1 and WC-2 (WCC, *N. crassa)*, single phosphorylation site mutation showed only mild effects, so combined mutants were generated. Also similar to WCC, the CLK-16A mutant (16 phosphorylation sites mutated to alanine) is a functional protein and phosphorylation of CLK does not interfere with the interactions of core clock partners. And also like WCC, phosphorylation of CLK was shown to negatively regulate the activity of CLK/CYC (Lee *et al.*, 2014; Mahesh *et al.*, 2014). Remarkably, among the 19 phosphorylation sites of *D. melanogaster* CLK, 8 sites are followed by a proline which is a clear overrepresentation of SP, TP sites as observed for WCC (*N. crassa*). Since the MAPK NMO was shown to play a role in the circadian clock of *D. melanogaster*, and since MAPKs together with CDKs are typical proline-directed kinases, it was tested whether NMO phosphorylates the SP phosphorylation site S859 of CLK. The tests showed that NMO does not phosphorylate S859 (Mahesh *et al.*, 2014). So far, the proline-directed kinases phosphorylating CLK in *D. melanogaster* are not known.

To sum up, the mechanism and the function of the phosphorylation of BMAL1/CLOCK (mammalian) differs from the phosphorylation of WCC (*N. crassa*). Only a few phosphorylation sites of BMAL1/CLOCK were found to negatively regulate the transcriptional activity like it was found for WCC. However, only a few phosphorylation sites of BMAL1/CLOCK are known to date. Since CLK (*D. melanogaster*) and WCC (*N. crassa*) were found to be highly phosphorylated, the identification of more phosphorylation sites of BMAL1/CLOCK (mammalian) can be expected and might reveal new mechanistic details. As outlined above, the similarities of the phosphorylation of CLK (*D. melanogaster*) and WC-1 and WC-2 (WCC, *N. crassa*) are striking. The overrepresentation of SP, TP phosphorylation sites in CLK (*D. melanogaster*) allows to speculate whether the hypothesis of SP, TP phosphorylation as a feedback of the transcriptional machinery on the transcriptional activator can be extended to the circadian clocks of higher eukaryotes.

4.4. Summary of all mechanisms that regulate the light-induced activity of WCC and the contribution of this study

Light activates the blue light receptor and transcription factor WCC and thereby induces gene transcription to synchronize the internal circadian clock of *N. crassa* with the environment. Furthermore, light-induced gene transcription by WCC initiates physiological processes that enable *N. crassa* to cope with issues associated with daylight like, for example, DNA damage by UV-light. Given the importance of light-induction and given the large variation of environmental light conditions, this process requires tight regulation.

On a molecular level, light-induction begins with the dimerization of two light-activated WCC protomers to form L-WCC. At this point, the first regulatory mechanism is the small light receptor VVD that inhibits L-WCC activity by competing with WCC dimerization. This regulatory mechanism is accurately tuneable since *vvd* itself is a light-inducible target of WCC that reacts very fast to light and is expressed relative to the light intensity.

As a next step in light-induction, L-WCC binds to its target sequence on the DNA. At this point, several regulatory mechanisms associated with chromatin remodeling and general transcription can modulate the L-WCC activity. This study contributed to that stage of regulation by suggesting a direct feedback of the transcriptional machinery on L-WCC via phosphorylation at SP, TP sites. By binding to the promoter of a gene, the gene-specific properties interfere with L-WCC activity. Although different target genes of L-WCC share the same binding sequence for L-WCC, the gene expression profiles vary in time and intensity. Phenomena like promoter refractoriness are very likely gene-specific processes.

Whether phosphorylation of L-WCC is the next, last step of the regulation of L-WCC activity is hard to tell since this study found hints that phosphorylation interferes with the previous stages of regulation. This study revealed that phosphorylation gradually reduces the activity of L-WCC, that DNA-binding is a trigger of the phosphorylation and that SP, TP phosphorylation enhances further phosphorylation of both WC-1 and WC-2. If these observations are really due to the feedback of the transcriptional machinery, phosphorylation would be indeed the last step of regulation. However, the results of this study imply that the light-induced dimerization of WCC alone is also trigger of the phosphorylation of both WC-1 and WC-2. A direct proof is pending but if this is true, phosphorylation would occur in parallel to the previous stages of regulation.

This study did not touch the topic of phosphatases. The investigation of the circadian phosphorylation has shown that phosphorylation of WCC is antagonized by phosphatases. On the Western Blot, the light-induced phosphorylation of WC-1 appears transient but was associated with degradation and new synthesis of WC-1 in previous studies. Nevertheless, the parallel, antagonizing activity of phosphatases in light-induced phosphorylation of WCC cannot be excluded.

The molecular effect of the light-induced phosphorylation of WCC is not fully understood yet. Phosphorylation adds a negative charge to a protein that causes electrostatic repulsion from negatively charged DNA, modifies protein-protein interaction and can change the conformation of a protein. Since no phosphorylation sites were found in the DNA-binding domains of WCC, since the structure of WCC is not known and since transcription is a process that requires interaction of numerous proteins, all the effects of phosphorylation are possible.

This study investigated the light-induced phosphorylation and found hints that light-induced phosphorylation does not differ much from the circadian phosphorylation. The study by Wang *et al*., 2019 analyzed the circadian phosphorylation of WCC and the results share several similarities with this study. Thus, this study significantly contributed to the understanding of the regulation of the positive element in the central oscillator of a circadian clock.

5. Appendix

5.1. SDS-Gel of the tandem affinity purification of tagged WC-2 in March 2014

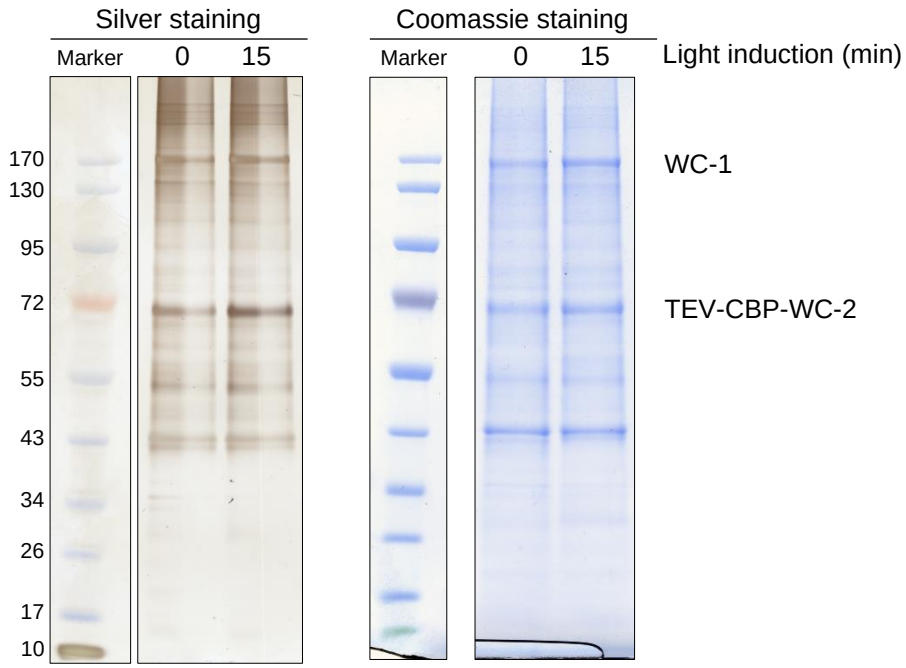

Figure 5.1: Result of the tandem affinity purification (TAP) of tagged WC-2 in March 2014.
Silver staining and Coomassie staining of the SDS gels. The CaM precipitation (CaM Pr) samples were loaded. TEV = cleavage site for TEV protease; CBP = calmodulin binding protein. Molecular weight marker in kDa.

5.2. SDS Gel of the WC-2 IP in January 2016

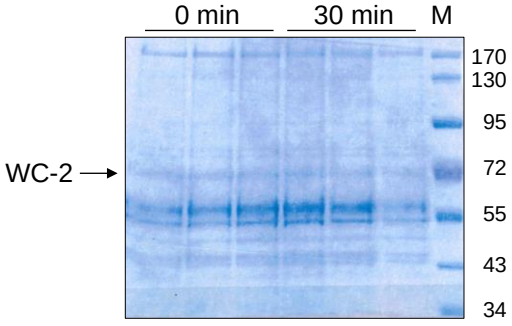

Figure 5.2: Result of the WC-2 Immunoprecipitation in January 2016.
The wc-2 wild type strain was grown in constant dark for 24 h (0 min) and exposed to light for 30 min (light induction). M = molecular weight marker in kDa.

5.3. SDS Gel of the WC-2 IP in July 2016

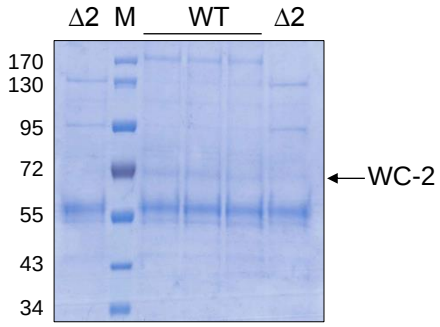

Figure 5.3: Result of the WC-2 Immunoprecipitation in July 2016.
The *wc-2* wild type strain (**WT**) and the *wc-2* knock out mutant (Δ**2**, as control to detect the antibody) were grown in constant light (LL). **M** = molecular weight marker in kDa.

5.4. List of phosphorylated peptides of WC-1

Table 5.1: Phosphorylated peptides of WC-1 that was pulled-down with tagged WC-2 in the tandem affinity purification in January 2014.
0´= samples that were grown in dark for 24 h (DD24); 15´= samples that were exposed to light for 15 min after growth in dark for 24 h.

Position (aa)	**aa +1**	**Peptide**	**Score**	**0´ (DD24) 15´ (LI15)**
S 111	V	RRSVPQPYGGQT	25	0´
		RRSVPQPY	27	15´
		SVPQPYGGQT	33	15´
S 315	P	TTFQSPSLSATTQTI	65	0´
		FAQGMATPVSQDAASTPATTFQSPSLSATTQT	48	15´
		SQDAASTPATTFQSPSLSATTQTI	26	15´
		TTFQSPSLSATTQTI	49	15´
S 315 and/ or S 317	P L	SQDAASTPATTFQSPSLSATTQTI	48	15´
S 334	V	RIGPPPPPSVT	37	0´
		IGPPPPPSVT	40	15´
S 334 or T 336	V N	IRIGPPPPPSVTNAPTPAPFTSTPSGGGASQTKS	45	0´
T 340	P	IRIGPPPPPSVTNAPTPAPFTSTPSGGGASQTKS	70	15´
		NAPTPAPF	23	15´
S 824 and / or S 831	P P	TVKNMSPGGVPLSPMKGIQTDSDSNTLMGGMSK	35	0´
S 831	P	VTVKNMSPGGVPLSPMKG	21	0´
		MSPGGVPLSPMKG	39	15´
		VTVKNMSPGGVPLSPMKG	32	15´
		KNMSPGGVPLSPMKGIQTDSDSNTLMGGMS	55	15´

		TVTVKNMSPGGVPLSPMKGIQTDSDSNTLMGGMS	66	15´
S 863 or S 866 or S 867	A S A	SARSSAGPGQDAALDADNIFDELKTT SARSSAGPGQDAALDADNIFDELKTT	9 46	0´ 0´
S 866 or S 867	S A	VSARSSAGPGQDAALDADNIFDELKTTRCTSWQYE	25	0´
T 967		RWAKQTGRVSPRTS	14	15´
S 988 or S 990	N P	SNSPSHSSPLHREVGNDSPSTT	13	15´
S 990	P	NSPSHSSPLHREVGNDSPSTT	7	15´
S 1005	P	VGNDSPSTTTATKNSPS	20	15´
S 1007 or T 1008 or T 1009 or T 1010 or T 1012	T T T A K	EVGNDSPSTTTATKNSPSLRGSSTTAPGTITTDSGPAVA	12	0´
T 1009 or T 1010	T A	VGNDSPSTTTATKNSPS	19	0´
T 1009 or T 1010 or T 1012	T A K	LHREVGNDSPSTTTATKNSPS	14	15´
T 1010 or T 1012 or S 1015 or S 1017	A K P L	TATKNSPSLRGSSTTAPGTITTDSGPAVA TATKNSPSLRGSSTTAPGTITTDSGPAV	37 62	0´ 15´
T 1012 or S 1015	K P	ATKNSPSLRGSSTTAPGTITTDSGPA ATKNSPSLRGSSTTAPGTITTDSGPAVA TATKNSPSLRGSSTTAPGTITTDSGPAVA	60 30 27	15´ 15´ 15´
S 1015	P	LHREVGNDSPSTTTATKNSPS VGNDSPSTTTATKNSPSLRGSSTTAPGTITTDSGPA TATKNSPSLRGSSTTAPGTITTDSGPAVAS TATKNSPSLRGSSTTAPGTITTDSGPAVAS	54 43 41 41	0´ 0´ 0´ 15´
S 1015 or S 1017	P L	LHREVGNDSPSTTTATKNSPS	23	15´
S 1017	L	TATKNSPSLRGSSTTAPGTITTDSGPAVA TATKNSPSLRGSSTTAPGTITTDSGPAVA	63 52	0´ 15´
S 1071 or S 1074	G P	LGPPATGPSGGSPAQHLPPHLQGTHLNAQAMQR	10	15´
S 1074	P	NALGPPATGPSGGSPAQHLPPHLQGTHLNAQAMQ	22	15´

Table 5.2: Phosphorylated peptides of WC-1 that was pulled-down with tagged WC-2 in the tandem affinity purification in March 2014.
0´= samples that were grown in dark for 24 h (DD24); 15´= samples that were exposed to light for 15 min after growth in dark for 24 h.

Position (aa)	**aa +1**	**Peptide**	**Score**	**0´ (DD24) 15´ (LI15)**
S 111	V	RRSVPQPYGGQT RRSVPQPYGGQT	33 35	0´ 15´

S 200	P	LNMYHSPPIENPYSSAG	29	15´
S 315	P	FAQGMATPVSQDAASTPATTFQSPSLSATTQT	35	0´
		TTFQSPSLSATTQTI	49	0´
		FAQGMATPVSQDAASTPATTFQSPSLSATTQT	71	15´
		TTFQSPSLSATTQTI	62	15´
S 334	V	RIGPPPPPSVT	64	0´
		IRIGPPPPPSVTNAPTPAP	87	15´
		IGPPPPPSVT	38	15´
		RIGPPPPPSVT	42	15´
S 334 or T 336	V N	IRIGPPPPPSVTNAPTPAPFTSTPSGGGASQTKS	69	0´
T 336	N	IRIGPPPPPSVTNAPTPAPFTSTPSGGGASQTKS	89	15´
T 340	P	IRIGPPPPPSVTNAPTPAPFTSTPSGGGASQTKS	40	0´
		IRIGPPPPPSVTNAPTPAPFTSTPSGGGASQTKS	55	15´
		VTNAPTPAPFTSTPSGGGASQTKS	50	15´
		NAPTPAPF	21	15´
S 346 or T 347	T P	FTSTPSGGGASQTKS	21	0´
T 347	P	FTSTPSGGGASQTKS	27	15´
T536	T	IWTPPTQKQLEPADGQT	34	15´
S 824 and S 831	P P	VTVKNMSPGGVPLSPMKG	24	15´
S 831	P	VKNMSPGGVPLSPMKG	59	0´
		KNMSPGGVPLSPMKGIQTDSDSNTLMGGMS	34	0´
		LAPATVTVKNMSPGGVPLSPMKG	53	15´
		VTVKNMSPGGVPLSPMKG	40	15´
		KNMSPGGVPLSPMKGIQTDSDSNTLMGGMS	52	15´
		TVTVKNMSPGGVPLSPMKGIQTDSDSNTLMGGMS	38	15´
S 866 or S 867	S A	VSARSSAGPGQDAA	50	0´
S 867	A	VSARSSAGPGQDAA	31	15´
S 971	P	WAKQTGRVSPRTS	24	0´
		WAKQTGRVSPRTS	20	15´
S 1005 and/or S 1007	P T	VGNDSPSTTTATKNSPS VGNDSP*S*TTTATKNSPS	40 37	0´ 15´
T 1010 or T 1012 or S 1015 or S 1017 or	A K P L	TATKNSPSLRGSSTTAPGTITTDSGPAV TATKNSPSLRGSSTTAPGTITTDSGPAVA (here: two phosphorylated residues, combination not known)	60 28	15´
T 1012 or S 1015 or S 1017	K P L	TATKNSPSLRGSSTTAPGTITTDSGPAV ATKNSPSLRGSSTTAPGTITTDSGPAVA	41 24	0´ 15´
T 1012 or S 1015	K P	TATKNSPSLRGSSTTAPGTITTDSGPAVA	45	15´
S 1015	P	VGNDSPSTTTATKNSPS TATKNSPSLRGSSTTAPGTITTDSGPAVA	40	0´

		VGNDSPSTTTATKNSPS	32	0´
		ATKNSPSLRGSSTTAPGT	68	15´
		ATKNSPSLRGSSTTAPGTITTDSGPAVA	29	15´
		TATKNSPSLRGSSTTAPGTITTDSGPAVAS	44	15´
			48	15´
S 1015 or S 1017	P L	LHREVGNDSPSTTTATKNSPS	66	0´
		VGNDSPSTTTATKNSPS	74	0´
S 1021		KNSPSLRGSSTTAPGTITTDSGPAVA	42	15´
S 1021 or S 1022 or T 1023 or T 1024	S T T A	VGNDSPSTTTATKNSPSLRGSSTTAPGTITTDSGPA	51	15´
S 1022 or T 1023	T T	LRGSSTTAPGTITTDSGPA	41	15´
S 1074	P	LGPPATGPSGGSPAQHLPPH	36	0´
		LGPPATGPSGGSPAQHLPPH	50	15´
		NALGPPATGPSGGSPA	23	15´
S 1166	V	IREEMGEHQQGLSV	21	0´
		IREEMGEHQQGLSV	23	15´

5.5. List of phosphorylated peptides of WC-2

Table 5.3: Phosphorylated peptides of WC-2 purified in the tandem affinity purification in January 2014.
0´= samples that were grown in dark for 24 h (DD24); 15´= samples that were exposed to light for 15 min after growth in dark for 24 h.

Position (aa)	**aa +1**	**Peptide**	**Score**	**0´ (DD24) 15´ (LI15)**
S 80 or S 82 or T 86	M N P	LDVGDSMSNPFTPVSVPPPLPAGNAGPSH	15	15´
S 118	P	VCGGHGAPDQLFSPDDLIATSMSSAGPM	12	15´
T 136	P	IATPTTTTSGPSGGPSSGGGST	63	15´
		MSSAGPMIATPTTT	26	15´
T 287	K	FAPNPQNQSPFCQAVFMMARPYPTKNA	18	0´
		FAPNPQNQSPFCQAVFMMARPYPTKNA	10	0´
S 331	Q	RMSQEGRSDVTPSDDTATQMGMTPFYIPMNA	20	15´
T 339 or S 341	P D	MSQEGRSDVTPSDDTATQMGMTPFYIPMNA	20	15´
		RMSQEGRSDVTPSDDTATQMGMTPFYIPMNA	30	
S 394	I	LTRENLEGIAGSRPDSIREKM	19	0´
		IAGSRPDSIREKM	13	15´
S 433	P	ITTGNASPTLIKGDAG	62	0´
		LKYQEGERSHGITTGNASPTLIKGDAG	26	0´
		HGITTGNASPT	14	0´
		SHGITTGNASPTLI	56	15´
S 476 or	P	IKVAEEYVCTDCGTLDSPEWRKGPSGPKT	30	0´

S 484	G			
T 523	P	AKKEKKKNANNNNNGGGIGGHNDIHTPMGDHMG	31	0´
		NDIHTPMGDHMG	3	0´
		AKKEKKKNANNNNNGGGIGGHNDIHTPMGDHMG	20	15´
		AKKEKKKNANNNNNGGGIGGHNDIHTPMGDHMG	11	15´
		NDIHTPMGDHMG	41	15´

Table 5.4: Phosphorylated peptides of WC-2 purified in the tandem affinity purification in March 2014.
0´= samples that were grown in dark for 24 h (DD24); 15´= samples that were exposed to light for 15 min after growth in dark for 24 h.

Position (aa)	**aa +1**	**Peptide**	**Score**	**0´ (DD24) 15´ (LI15)**
T 138 or T 139	T T	IATPTTTTSGPSGGPSSGGGST	52	15´
S 331 or S 336 or T 339 or S 341	Q D P D	RMSQEGRSDVTPSDDTATQMGMTPFYIPMNA	14	15´
T 339 or S 341	P D	RMSQEGRSDVTPSDDTATQMGMTPFYIPMNA	32	0´
S 341	D	MSQEGRSDVTPSDDTATQMGMTPFYIPMNA	33	0´
S 390 and S 394	R I	IAGSRPDSIREKM	19	0´
S 394	I	IAGSRPDSIREKM	21	0´
		LTRENLEGIAGSRPDSIREKM	20	15´
S 433	P	ITTGNASPTL	58	0´
		ITTGNASPTLIKGDAG	70	0´
		SHGITTGNASPTLI	62	0´
		ITTGNASPTL	47	15´
		ITTGNASPTLIKGDAG	64	15´
		HGITTGNASPTLI	33	15´
S 433 or T 435	P L	ITTGNASPTLIKGDAGIAIP	51	0´
		HGITTGNASPTLIKGDAGIAIPL	37	0´
T 473 or S 476	L P	IKVAEEYVCTDCGTLDSPEWRKGPSGPKT	19	0´
		IKVAEEYVCTDCGTLDSPEWRKGPSGPKT	14	15´
T 523	P	AKKEKKKNANNNNNGGGIGGHNDIHTPMGDHMG	20	0´
		NANNNNNGGGIGGHNDIHTPMGDHMG	26	0´
		NDIHTPMGDHMG	20	0´
		AKKEKKKNANNNNNGGGIGGHNDIHTPMGDHMG	21	15´
		NDIHTPMGDHMG	17	15´

Table 5.5: Phosphorylated peptides of WC-2 purified by WC-2 Immunoprecipitation in January 2016.
0´= samples that were grown in dark for 24 h (DD24); 30´= samples that were exposed to light for 15 min after growth in dark for 24 h.

Position (aa)	**aa +1**	**Peptide**	Score	**0´ (DD24) 30´ (LI30)**
S80 or S82	M N	LDVGDSMSNPFTPVSVPPPLPAGNAGPSH	11	0´
S80 or S82	M N	LDVGDSpMSNPFTPVSVPPPLPAGNAGPSH	23	30´
S82		LDVGDSMSpNPFTPVSVPPPLPAGNAGPSH	28	30´
T86	P	LDVGDSMSNPFTpPVSVPPPLPAGNAGPSH	30	0´
		LDVGDSMSNPFTpPVSVPPPLPAGNAGPSH	38	30´
S118	P	VGVCGGHGAPDQLFSpPDDLIATSMSSAGPM	19	0´
		VGVCGGHGAPDQLFSpPDDLIATSMSSAGPM	35	30´
S128 or S129	S A	FSPDDLIATSMSpSAGPM	25	0´
T136	P	MSSAGPMIATpPTTTTSGPSGGPSSGGGSTLTEFT	30	0´
		FSPDDLIATSMSSAGPMIATpPTTTTSGPSGGPSSGGGST	50	30´
		IATpPTTTTSGPSGGPSSGGGST	81	30´
T138	T	IATPTpTTTSGPSGGPSSGGGST	23	30´
T136 or T138	P T	SMSSAGPMIATpPTTT	29	30´
T136 or T138	P T	SMSSAGPMIATpPTTT (second peptide)	29	30´
T136 or T138 or T139 or T140	P T T T	MSSAGPMIATpPTTTTSGPSGGPSSGGGSTLTEFT	30	0´
T136 or T138 or T139	P T T	IATpPTpTTTSGPSGGPSSGGGST	54	0´
T136 or T138 or T139	P T T	FSPDDLIATSMSSAGPMIATpPTTTTSGPSGGPSSGGGST	50	30´
T136 or T138 or T139 or T140 or T141	P T T T S	FSPDDLIATSMSSAGPMIATpPTTTTSGPSGGPSSGGGST	31	0´
T136 or T138 or T139 or T140 or T141	P T T T S	FSPDDLIATSMSSAGPMIATpPTTTTSGPSGGPSSGGGST	23	30´
T139 or T140 or T141 or S142	T T S G	TTTSpGPSGGPSSGGGSTLTEFT	25	30´
T141 or S 142	S G	TPTTTTSpGPSGGPSSGGGSTLTEFT	22	30´

S331 or S336 or T339	Q D P	MSQEGRSDVTpPSDDTATQMGMTPFYIPMNA	30	0´
T339	P	MSQEGRSDVTpPSDDTATQMGMTPFYIPMNA	30	0´
		MSQEGRSDVTpPSDDTATQMGMTPFYIPMNA	26	30´
		MSQEGRSDVTpPSDDTATQMGMTPFYIPMNAQADVMMPP PSQPASS	34	30´
T339 or S341	P D	MSQEGRSDVTPSpDDTATQMGMTPFYIPMNA	30	0´
T339 or S341	P D	MSQEGRSDVTpPSDDTATQMGMTPFYIPMN	11	0´
T339 or S341	P D	MSQEGRSDVTPSpDDTATQMGMTPFYIPMNAQADVMMPP PSQPASS	11	0´
S341	D	MSQEGRSDVTPSpDDTATQMGMTPFYIPMNA	30	0´
S341 or T344	D A	MSQEGRSDVTPSpDDTATQMGMTPFYIPMNA	30	0´
S390 or S394	R I	IAGSpRPDSIREKM	12	0´
S394	I	ENLEGIAGSRPDSpIREK	39	0´
		ENLEGIAGSRPDSpIREK	60	30´
S 433	P	SHGITTGNASpPTLIK	73	0´
		ITTGNASpPTL	58	0´
		SHGITTGNASpPTLIK	76	30´
		HGITTGNASpPTLI	47	30´
		ITTGNASpPT	53	30´
		ITTGNASpPTLIKGDAG	65	30´
T435	L	ITTGNASPTpLIKGDAG	36	30´
T523	P	NANNNNNGGGIGGHNDIHTpPMGDHMG	26	30´

5.6. Results of the pull-down experiment in January 2014

See figure 5.4 on the following pages.

Proteins of interest

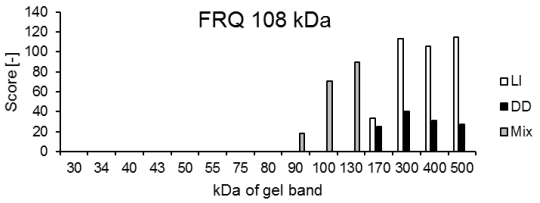

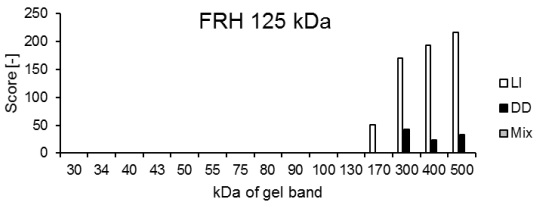

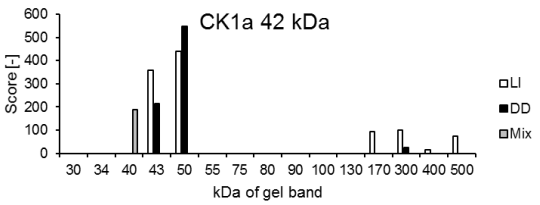

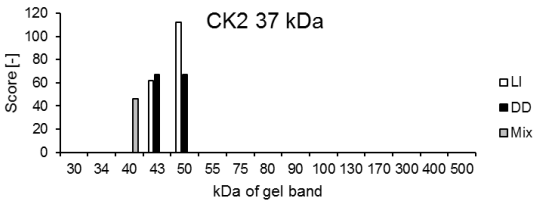

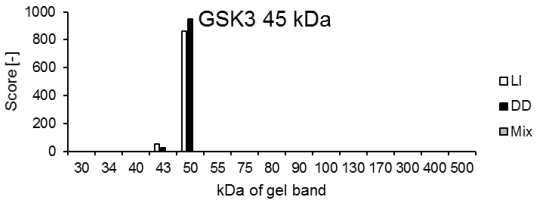

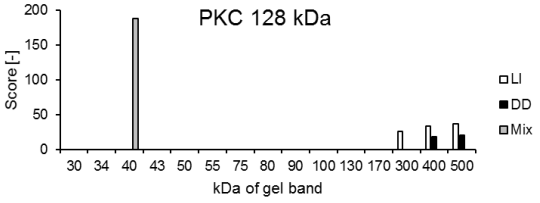

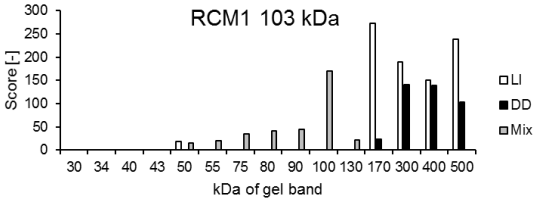

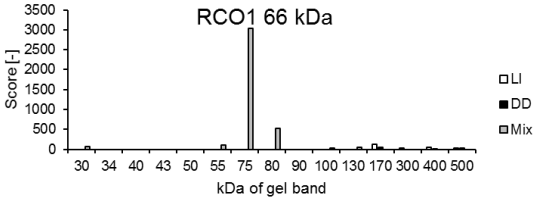

Proteins of control group

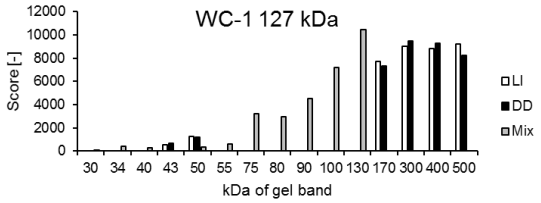

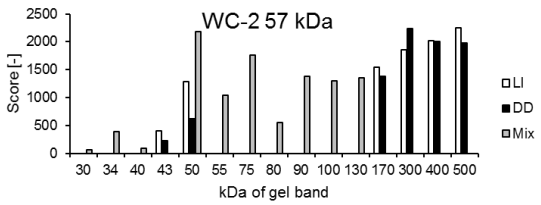

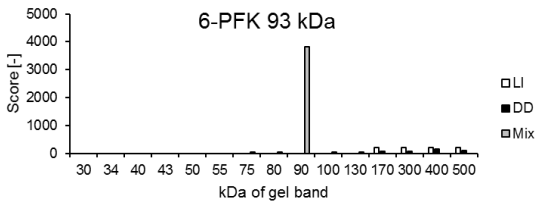

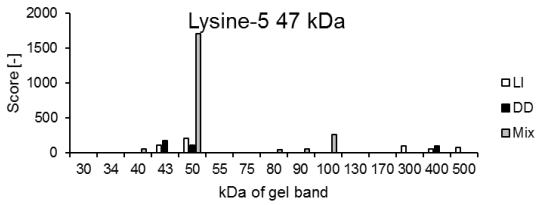

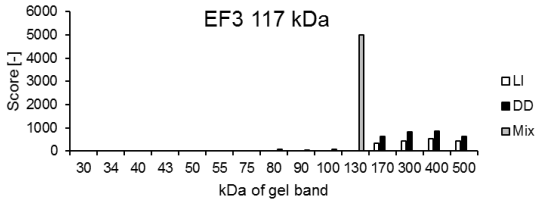

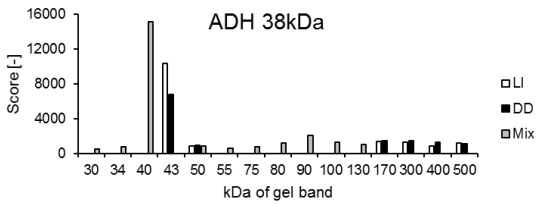

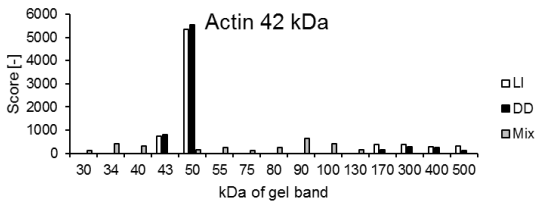

Figure 5.4: Selected proteins identified by mass spectrometry in the tandem affinity purification of tagged WC-2 in January 2014.
The light- and the dark-sample were separated by size in an SDS-gel. Tagged WC-2 and its very stable interaction partner WC-1 were pulled down at high concentrations and appeared as prominent bands in the gel. These bands were excised and analyzed for protein phosphorylation. The rest of the gel was cut into several bands that comprise a certain mass range. The intermediate mass of each band is indicated on the x-axis. The masses of 300, 400 and 500 kDa are only a very rough estimation since these bands were excised from the gel over the upper band of the molecular weight marker (170 kDa). For experimental reasons, some gel bands had to be pooled (mix, grey), others were analyzed independently (LI = light-sample; DD = dark-sample). Since the method used was not quantitative mass spectrometry, the protein score distribution over the whole mass range was analyzed for selected target proteins and for selected control proteins. Since the protein score contains some information about the abundance of the protein in the sample, the aim was to search for a light-induced enrichment of interaction partners of WCC. As control, WC-1 and WC-2 are shown. As outlined above, the actual WC-1 and WC-2 band are not part of the identification analysis shown here. The proteins scores of WC-1 and WC-2 shown here represent the smear of these proteins over the whole gel. As further controls, two very abundant proteins, ADH and actin, are shown. The metabolic enzymes 6-PFK and lysine-5 and the translation elongation factor 3 (EF3) represent unspecific protein hits of various size. As proteins of interest, FRQ, FRH, CK1a and CK2 are shown as known interactors of WCC. GSK3 and PKC were suggested to phosphorylate WCC previously. RCM1 and RCO1 were shown to also bind to LRE, the target sequence of WCC in light-inducible genes (Liu *et al.*, 2015; Olmedo *et al.*, 2010; Ruger-Herreros *et al.*, 2014).

Bibliography

Aronson, B.D., Johnson, K.A. and Dunlap, J.C. (1994) Circadian clock locus frequency. protein encoded by a single open reading frame defines period length and temperature compensation. *Proceedings of the National Academy of Sciences of the United States of America*, 91, 7683–7687.

Aryal, R.P., Kwak, P.B., Tamayo, A.G., Gebert, M., Chiu, P.L., Walz, T. and Weitz, C.J. (2017) Macromolecular Assemblies of the Mammalian Circadian Clock. *Molecular cell*, 67, 770-782.e6.

Aschoff, J. (1954) Zeitgeber der tierischen Tagesperiodik. *Naturwissenschaften*, 41, 49–56.

Aschoff, J. (1965) CIRCADIAN RHYTHMS IN MAN. *Science (New York, N.Y.)*, 148, 1427–1432.

Baker, C.L., Kettenbach, A.N., Loros, J.J., Gerber, S.A. and Dunlap, J.C. (2009) Quantitative proteomics reveals a dynamic interactome and phase-specific phosphorylation in the Neurospora circadian clock. *Molecular cell*, 34, 354–363.

Baker, C.L., Loros, J.J. and Dunlap, J.C. (2012) The circadian clock of Neurospora crassa. *FEMS Microbiol Rev*, 36, 95–110.

Ballario, P., Talora, C., Galli, D., Linden, H. and Macino, G. (1998) Roles in dimerization and blue light photoresponse of the PAS and LOV domains of Neurospora crassa white collar proteins. *Molecular microbiology*, 29, 719–729.

Ballario, P., Vittorioso, P., Magrelli, A., Talora, C., Cabibbo, A. and Macino, G. (1996) White collar-1, a central regulator of blue light responses in Neurospora, is a zinc finger protein. *The EMBO journal*, 15, 1650–1657.

Beadle, G.W. and Tatum, E.L. (1941) Genetic Control of Biochemical Reactions in Neurospora. *Proceedings of the National Academy of Sciences of the United States of America*, 27, 499–506.

Belden, W.J., Larrondo, L.F., Froehlich, A.C., Shi, M., Chen, C.H., Loros, J.J. and Dunlap, J.C. (2007) The band mutation in Neurospora crassa is a dominant allele of ras-1 implicating RAS signaling in circadian output. *Genes & development*, 21, 1494–1505.

Belden, W.J., Loros, J.J. and Dunlap, J.C. (2007) Execution of the circadian negative feedback loop in Neurospora requires the ATP-dependent chromatin-remodeling enzyme CLOCKSWITCH. *Molecular cell*, 25, 587–600.

Bobrowicz, P., Pawlak, R., Correa, A., Bell-Pedersen, D. and Ebbole, D.J. (2002) The Neurospora crassa pheromone precursor genes are regulated by the mating type locus and the circadian clock. *Molecular microbiology*, 45, 795–804.

Borkovich, K.A., Alex, L.A., Yarden, O., Freitag, M., Turner, G.E., Read, N.D., Seiler, S., Bell-Pedersen, D., Paietta, J., Plesofsky, N., Plamann, M., Goodrich-Tanrikulu, M., Schulte, U., Mannhaupt, G., Nargang, F.E., Radford, A., Selitrennikoff, C., Galagan, J.E., Dunlap, J.C., Loros, J.J., Catcheside, D., Inoue, H., Aramayo, R., Polymenis, M., Selker, E.U., Sachs, M.S., Marzluf, G.A., Paulsen, I., Davis, R., Ebbole, D.J., Zelter, A., Kalkman, E.R., O'Rourke, R., Bowring, F., Yeadon, J., Ishii, C., Suzuki, K., Sakai, W. and Pratt, R. (2004) Lessons from the Genome Sequence of Neurospora crassa. Tracing the Path from Genomic Blueprint to Multicellular Organism. *Microbiology and Molecular Biology Reviews*, 68, 1–108.

Bowman, E.A. and Kelly, W.G. (2014) RNA polymerase II transcription elongation and Pol II CTD Ser2 phosphorylation. A tail of two kinases. *Nucleus*, 5, 224–236.

Brockman, H.E. and Serres, F.J. de (1963) "Sorbose toxicity" in Neurospora. *Am. J. Bot.*, 709–714.

Buenning, E. (1935) Zur Kenntnis der erblichen Tagesperiodizität bei den Primärblättern von Phaseolus multiflorus. *Jb Wiss Bot*, 81, 411–418.

Castro, E. de, **Sigrist, C.J., Gattiker, A., Bulliard, V., Langendijk-Genevaux, P.S., Gasteiger, E., Bairoch, A. and Hulo, N.** (2006) ScanProsite. detection of PROSITE signature matches and ProRule-associated functional and structural residues in proteins. *Nucleic acids research*, 34, W362-5.

Cesbron, F., Oehler, M., Ha, N., Sancar, G. and Brunner, M. (2015) Transcriptional refractoriness is dependent on core promoter architecture. *Nature communications*, 6, 6753.

Cha, J., Chang, S.S., Huang, G., Cheng, P. and Liu, Y. (2008) Control of WHITE COLLAR localization by phosphorylation is a critical step in the circadian negative feedback process. *The EMBO journal*, 27, 3246–3255.

Chen, C.H., DeMay, B.S., Gladfelter, A.S., Dunlap, J.C. and Loros, J.J. (2010) Physical interaction between VIVID and white collar complex regulates photoadaptation in Neurospora. *Proceedings of the National Academy of Sciences of the United States of America*, 107, 16715–16720.

Chen, C.H., Ringelberg, C.S., Gross, R.H., Dunlap, J.C. and Loros, J.J. (2009) Genome-wide analysis of light-inducible responses reveals hierarchical light signalling in Neurospora. *The EMBO journal*, 28, 1029–1042.

Cheng, P., Yang, Y., Gardner, K.H. and Liu, Y. (2002) PAS Domain-Mediated WC-1/WC-2 Interaction Is Essential for Maintaining the Steady-State Level of WC-1 and the Function of Both Proteins in Circadian Clock and Light Responses of Neurospora. *Molecular and Cellular Biology*, 22, 517–524.

Cheng, P., Yang, Y., Wang, L., He, Q. and Liu, Y. (2003) WHITE COLLAR-1, a multifunctional neurospora protein involved in the circadian feedback loops, light sensing, and transcription repression of wc-2. *The Journal of biological chemistry*, 278, 3801–3808.

Chi, Y., Huddleston, M.J., Zhang, X., Young, R.A., Annan, R.S., Carr, S.A. and Deshaies, R.J. (2001) Negative regulation of Gcn4 and Msn2 transcription factors by Srb10 cyclin-dependent kinase. *Genes & development*, 15, 1078–1092.

Cho, E., Kwon, M., Jung, J., Kang, D.H., Jin, S., Choi, S.E., Kang, Y. and Kim, E.Y. (2019) AMP-Activated Protein Kinase Regulates Circadian Rhythm by Affecting CLOCK in Drosophila. *The Journal of neuroscience : the official journal of the Society for Neuroscience*, 39, 3537–3550.

Collett, M.A., Garceau, N., Dunlap, J.C. and Loros, J.J. (2002) Light and clock expression of the Neurospora clock gene frequency is differentially driven by but dependent on WHITE COLLAR-2. *Genetics*, 160, 149–158.

Corchnoy, S.B., Swartz, T.E., Lewis, J.W., Szundi, I., Briggs, W.R. and Bogomolni, R.A. (2003) Intramolecular proton transfers and structural changes during the photocycle of the LOV2 domain of phototropin 1. *The Journal of biological chemistry*, 278, 724–731.

Corpet, F. (1988) Multiple sequence alignment with hierarchical clustering. *Nucleic acids research*, 16, 10881–10890.

Crosthwaite, S.K., Dunlap, J.C. and Loros, J.J. (1997) Neurospora wc-1 and wc-2. transcription, photoresponses, and the origins of circadian rhythmicity. *Science (New York, N.Y.)*, 276, 763–769.

Dagan, Y. (2002) Circadian rhythm sleep disorders (CRSD). *Sleep medicine reviews*, 6, 45–54.

Dannappel, M.V., Sooraj, D., Loh, J.J. and Firestein, R. (2019) Molecular and in vivo Functions of the CDK8 and CDK19 Kinase Modules. *Frontiers in cell and developmental biology*, 6, 171.

Dasgupta, A., Chen, C.H., Lee, C., Gladfelter, A.S., Dunlap, J.C. and Loros, J.J. (2015) Biological Significance of Photoreceptor Photocycle Length. VIVID Photocycle Governs the Dynamic VIVID-White Collar Complex Pool Mediating Photo-adaptation and Response to Changes in Light Intensity. *PLoS genetics*, 11, e1005215.

Degli-Innocenti, F. and Russo, V.E. (1984) Isolation of new white collar mutants of Neurospora crassa and studies on their behavior in the blue light-induced formation of protoperithecia. *Journal of bacteriology*, 159, 757–761.

Diernfellner, A.C. and Schafmeier, T. (2011) Phosphorylations. Making the Neurosporacrassa circadian clock tick. *FEBS letters*, 585, 1461–1466.

Dunlap, J.C. and Loros, J.J. (2006) How fungi keep time. circadian system in Neurospora and other fungi. *Curr Opin Microbiol*, 9, 579–587.

El Khattabi, L., Zhao, H., Kalchschmidt, J., Young, N., Jung, S., van Blerkom, P., Kieffer-Kwon, P., Kieffer-Kwon, K.R., Park, S., Wang, X., Krebs, J., Tripathi, S., Sakabe, N., Sobreira, D.R., Huang, S.C., Rao, S.S.P., Pruett, N., Chauss, D., Sadler, E., Lopez, A., Nobrega, M.A., Aiden, E.L., Asturias, F.J. and Casellas, R. (2019) A Pliable Mediator Acts as a Functional Rather Than an Architectural Bridge between Promoters and Enhancers. *Cell*, 178, 1145-1158.e20.

Fant, C.B. and Taatjes, D.J. (2019) Regulatory functions of the Mediator kinases CDK8 and CDK19. *Transcription*, 10, 76–90.

Feldman, J.F. and Hoyle, M.N. (1973) Isolation of circadian clock mutants of Neurospora crassa. *Genetics*, 75, 605–613.

Filtz, T.M., Vogel, W.K. and Leid, M. (2014) Regulation of transcription factor activity by interconnected post-translational modifications. *Trends Pharmacol Sci*, 35, 76–85.

Flaus, A. and Owen-Hughes, T. (2011) Mechanisms for ATP-dependent chromatin remodelling. the means to the end. *The FEBS journal*, 278, 3579–3595.

Franchi, L., Fulci, V. and Macino, G. (2005) Protein kinase C modulates light responses in Neurospora by regulating the blue light photoreceptor WC-1. *Molecular microbiology*, 56, 334–345.

Froehlich, A.C., Liu, Y., Loros, J.J. and Dunlap, J.C. (2002) White Collar-1, a circadian blue light photoreceptor, binding to the frequency promoter. *Science (New York, N.Y.)*, 297, 815–819.

Froehlich, A.C., Loros, J.J. and Dunlap, J.C. (2003) Rhythmic binding of a WHITE COLLAR-containing complex to the frequency promoter is inhibited by FREQUENCY. *Proceedings of the National Academy of Sciences of the United States of America*, 100, 5914–5919.

Froehlich, A.C., Noh, B., Vierstra, R.D., Loros, J. and Dunlap, J.C. (2005) Genetic and molecular analysis of phytochromes from the filamentous fungus Neurospora crassa. *Eukaryotic cell*, 4, 2140–2152.

Funk, C., Schmeiser, V., Ortiz, J. and Lechner, J. (2014) A TOGL domain specifically targets yeast CLASP to kinetochores to stabilize kinetochore microtubules. *The Journal of cell biology*, 205, 555–571.

Galagan, J.E., Calvo, S.E., Borkovich, K.A., Selker, E.U., Read, N.D., Jaffe, D., FitzHugh, W., Ma, L.J., Smirnov, S., Purcell, S., Rehman, B., Elkins, T., Engels, R., Wang, S., Nielsen, C.B., Butler, J., Endrizzi, M., Qui, D., Ianakiev, P., Bell-

Pedersen, D., Nelson, M.A., Werner-Washburne, M., Selitrennikoff, C.P., Kinsey, J.A., Braun, E.L., Zelter, A., Schulte, U., Kothe, G.O., Jedd, G., Mewes, W., Staben, C., Marcotte, E., Greenberg, D., Roy, A., Foley, K., Naylor, J., Stange-Thomann, N., Barrett, R., Gnerre, S., Kamal, M., Kamvysselis, M., Mauceli, E., Bielke, C., Rudd, S., Frishman, D., Krystofova, S., Rasmussen, C., Metzenberg, R.L., Perkins, D.D., Kroken, S., Cogoni, C., Macino, G., Catcheside, D., Li, W., Pratt, R.J., Osmani, S.A., DeSouza, C.P., Glass, L., Orbach, M.J., Berglund, J.A., Voelker, R., Yarden, O., Plamann, M., Seiler, S., Dunlap, J., Radford, A., Aramayo, R., Natvig, D.O., Alex, L.A., Mannhaupt, G., Ebbole, D.J., Freitag, M., Paulsen, I., Sachs, M.S., Lander, E.S., Nusbaum, C. and Birren, B. (2003) The genome sequence of the filamentous fungus Neurospora crassa. *Nature*, 422, 859–868.

Gorl, M., Merrow, M., Huttner, B., Johnson, J., Roenneberg, T. and Brunner, M. (2001) A PEST-like element in FREQUENCY determines the length of the circadian period in Neurospora crassa. *The EMBO journal*, 20, 7074–7084.

Harding, R.W. and Turner, R.V. (1981) Photoregulation of the Carotenoid Biosynthetic Pathway in Albino and White Collar Mutants of Neurospora crassa. *Plant physiology*, 68, 745–749.

Harper, S.M., Neil, L.C. and Gardner, K.H. (2003) Structural basis of a phototropin light switch. *Science (New York, N.Y.)*, 301, 1541–1544.

Harper, T.M. and Taatjes, D.J. (2018) The complex structure and function of Mediator. *The Journal of biological chemistry*, 293, 13778–13785.

He, Q., Cha, J., Lee, H.C., Yang, Y. and Liu, Y. (2006) CKI and CKII mediate the FREQUENCY-dependent phosphorylation of the WHITE COLLAR complex to close the Neurospora circadian negative feedback loop. *Genes & development*, 20, 2552–2565.

He, Q., Cheng, P., Yang, Y., Wang, L., Gardner, K.H. and Liu, Y. (2002) White collar-1, a DNA binding transcription factor and a light sensor. *Science (New York, N.Y.)*, 297, 840–843.

He, Q. and Liu, Y. (2005) Molecular mechanism of light responses in Neurospora. from light-induced transcription to photoadaptation. *Genes & development*, 19, 2888–2899.

He, Q., Shu, H., Cheng, P., Chen, S., Wang, L. and Liu, Y. (2005) Light-independent phosphorylation of WHITE COLLAR-1 regulates its function in the Neurospora circadian negative feedback loop. *The Journal of biological chemistry*, 280, 17526–17532.

Heintzen, C., Loros, J.J. and Dunlap, J.C. (2001) The PAS protein VIVID defines a clock-associated feedback loop that represses light input, modulates gating, and regulates clock resetting. *Cell*, 104, 453–464.

Huang, G., Chen, S., Li, S., Cha, J., Long, C., Li, L., He, Q. and Liu, Y. (2007) Protein kinase A and casein kinases mediate sequential phosphorylation events in the circadian negative feedback loop. *Genes & development*, 21, 3283–3295.

Hurley, J.M., Dasgupta, A., Emerson, J.M., Zhou, X., Ringelberg, C.S., Knabe, N., Lipzen, A.M., Lindquist, E.A., Daum, C.G., Barry, K.W., Grigoriev, I.V., Smith, K.M., Galagan, J.E., Bell-Pedersen, D., Freitag, M., Cheng, C., Loros, J.J. and Dunlap, J.C. (2014) Analysis of clock-regulated genes in Neurospora reveals widespread posttranscriptional control of metabolic potential. *Proceedings of the National Academy of Sciences of the United States of America*, 111, 16995–17002.

Inamoto, S., Segil, N., Pan, Z.Q., Kimura, M. and Roeder, R.G. (1997) The cyclin-dependent kinase-activating kinase (CAK) assembly factor, MAT1, targets and enhances CAK activity on the POU domains of octamer transcription factors. *The Journal of biological chemistry*, 272, 29852–29858.

Kaldi, K., Gonzalez, B.H. and Brunner, M. (2006) Transcriptional regulation of the Neurospora circadian clock gene wc-1 affects the phase of circadian output. *EMBO reports*, 7, 199–204.

Keller, A., Nesvizhskii, A.I., Kolker, E. and Aebersold, R. (2002) Empirical statistical model to estimate the accuracy of peptide identifications made by MS/MS and database search. *Analytical chemistry*, 74, 5383–5392.

King, D.P., Zhao, Y., Sangoram, A.M., Wilsbacher, L.D., Tanaka, M., Antoch, M.P., Steeves, T.D., Vitaterna, M.H., Kornhauser, J.M., Lowrey, P.L., Turek, F.W. and Takahashi, J.S. (1997) Positional cloning of the mouse circadian clock gene. *Cell*, 89, 641–653.

Kishi, A., Yamaguchi, I., Togo, F. and Yamamoto, Y. (2018) Markov modeling of sleep stage transitions and ultradian REM sleep rhythm. *Physiological measurement*, 39, 84005.

Ko, L.J., Shieh, S.Y., Chen, X., Jayaraman, L., Tamai, K., Taya, Y., Prives, C. and Pan, Z.Q. (1997) p53 is phosphorylated by CDK7-cyclin H in a p36MAT1-dependent manner. *Molecular and cellular biology*, 17, 7220–7229.

Kondo, T., Strayer, C.A., Kulkarni, R.D., Taylor, W., Ishiura, M., Golden, S.S. and Johnson, C.H. (1993) Circadian rhythms in prokaryotes. luciferase as a reporter of circadian gene expression in cyanobacteria. *Proceedings of the National Academy of Sciences of the United States of America*, 90, 5672–5676.

Konopka, R.J. and Benzer, S. (1971) Clock mutants of Drosophila melanogaster. *Proceedings of the National Academy of Sciences of the United States of America*, 68, 2112–2116.

Laemmli, U.K. (1970) Cleavage of structural proteins during the assembly of the head of bacteriophage T4. *Nature*, 227, 680–685.

Lamb, T.M., Vickery, J. and Bell-Pedersen, D. (2013) Regulation of gene expression in Neurospora crassa with a copper responsive promoter. *G3 (Bethesda, Md.)*, 3, 2273–2280.

Larrondo, L.F., Olivares-Yanez, C., Baker, C.L., Loros, J.J. and Dunlap, J.C. (2015) Circadian rhythms. Decoupling circadian clock protein turnover from circadian period determination. *Science (New York, N.Y.)*, 347, 1257277.

Lauinger, L., Li, J., Shostak, A., Cemel, I.A., Ha, N., Zhang, Y., Merkl, P.E., Obermeyer, S., Stankovic-Valentin, N., Schafmeier, T., Wever, W.J., Bowers, A.A., Carter, K.P., Palmer, A.E., Tschochner, H., Melchior, F., Deshaies, R.J., Brunner, M. and Diernfellner, A. (2017) Thiolutin is a zinc chelator that inhibits the Rpn11 and other JAMM metalloproteases. *Nat Chem Biol*, 13, 709–714.

Lee, E., Jeong, E.H., Jeong, H.J., Yildirim, E., Vanselow, J.T., Ng, F., Liu, Y., Mahesh, G., Kramer, A., Hardin, P.E., Edery, I. and Kim, E.Y. (2014) Phosphorylation of a central clock transcription factor is required for thermal but not photic entrainment. *PLoS genetics*, 10, e1004545.

Linden, H. and Macino, G. (1997) White collar 2, a partner in blue-light signal transduction, controlling expression of light-regulated genes in Neurospora crassa. *Embo J*, 16, 98–109.

Liu, X., Li, H., Liu, Q., Niu, Y., Hu, Q., Deng, H., Cha, J., Wang, Y., Liu, Y. and He, Q. (2015) Role for Protein Kinase A in the Neurospora Circadian Clock by Regulating White Collar-Independent frequency Transcription through Phosphorylation of RCM-1. *Molecular and cellular biology*, 35, 2088–2102.

Liu, Y., He, Q. and Cheng, P. (2003) Photoreception in Neurospora. a tale of two White Collar proteins. *Cellular and molecular life sciences : CMLS*, 60, 2131–2138.

Loros, J.J., Denome, S.A. and Dunlap, J.C. (1989) Molecular cloning of genes under control of the circadian clock in Neurospora. *Science (New York, N.Y.)*, 243, 385–388.

Luciano, A.K., Zhou, W., Santana, J.M., Kyriakides, C., Velazquez, H. and Sessa, W.C. (2018) CLOCK phosphorylation by AKT regulates its nuclear accumulation and circadian gene expression in peripheral tissues. *The Journal of biological chemistry*, 293, 9126–9136.

Mahesh, G., Jeong, E., Ng, F.S., Liu, Y., Gunawardhana, K., Houl, J.H., Yildirim, E., Amunugama, R., Jones, R., Allen, D.L., Edery, I., Kim, E.Y. and Hardin, P.E. (2014) Phosphorylation of the transcription activator CLOCK regulates progression through a approximately 24-h feedback loop to influence the circadian period in Drosophila. *The Journal of biological chemistry*, 289, 19681–19693.

Malzahn, E., Ciprianidis, S., Kaldi, K., Schafmeier, T. and Brunner, M. (2010) Photoadaptation in Neurospora by competitive interaction of activating and inhibitory LOV domains. *Cell*, 142, 762–772.

Mehra, A., Baker, C.L., Loros, J.J. and Dunlap, J.C. (2009) Post-translational modifications in circadian rhythms. *Trends in biochemical sciences*, 34, 483–490.

Narlikar, G.J., Fan, H.Y. and Kingston, R.E. (2002) Cooperation between complexes that regulate chromatin structure and transcription. *Cell*, 108, 475–487.

Neiss, A., Schafmeier, T. and Brunner, M. (2008) Transcriptional regulation and function of the Neurospora clock gene white collar 2 and its isoforms. *EMBO reports*, 9, 788–794.

Nesvizhskii, A.I., Keller, A., Kolker, E. and Aebersold, R. (2003) A statistical model for identifying proteins by tandem mass spectrometry. *Analytical chemistry*, 75, 4646–4658.

Oehler, M. (28.02.2020) *Light-induced White Collar Complex has a dual function as combined transcriptional activator and repressor*, Dissertation, Heidelberg University.

Ohdo, S., Koyanagi, S., Matsunaga, N. and Hamdan, A. (2011) Molecular basis of chronopharmaceutics. *J Pharm Sci*, 100, 3560–3576.

Olmedo, M., Ruger-Herreros, C. and Corrochano, L.M. (2010) Regulation by blue light of the fluffy gene encoding a major regulator of conidiation in Neurospora crassa. *Genetics*, 184, 651–658.

Parry, B.L. (2002) Jet lag. minimizing it's effects with critically timed bright light and melatonin administration. *Journal of molecular microbiology and biotechnology*, 4, 463–466.

Perkins, D.D. (1992) Neurospora. the organism behind the molecular revolution. *Genetics*, 130, 687–701.

Pinna, L.A. and Ruzzene, M. (1996) How do protein kinases recognize their substrates? *Biochimica et biophysica acta*, 1314, 191–225.

Pittendrigh, C.S. (1960) Circadian rhythms and the circadian organization of living systems. *Cold Spring Harbor symposia on quantitative biology*, 25, 159–184.

Pittendrigh, C.S., Bruce, V.G., Rosensweig, N.S. and Rubin, M.L. (1959) Growth patterns in Neurospora crassa. *Nature*, 184, 169–170.

Poss, Z.C., Ebmeier, C.C. and Taatjes, D.J. (2013) The Mediator complex and transcription regulation. *Crit Rev Biochem Mol Biol*, 48, 575–608.

Querfurth, C., Diernfellner, A., Heise, F., Lauinger, L., Neiss, A., Tataroglu, O., Brunner, M. and Schafmeier, T. (2007) Posttranslational regulation of Neurospora

circadian clock by CK1a-dependent phosphorylation. *Cold Spring Harbor symposia on quantitative biology*, 72, 177–183.

Querfurth, C., Diernfellner, A.C., Gin, E., Malzahn, E., Hofer, T. and Brunner, M. (2011) Circadian conformational change of the Neurospora clock protein FREQUENCY triggered by clustered hyperphosphorylation of a basic domain. *Molecular cell*, 43, 713–722.

Reddy, P., Zehring, W.A., Wheeler, D.A., Pirrotta, V., Hadfield, C., Hall, J.C. and Rosbash, M. (1984) Molecular analysis of the period locus in Drosophila melanogaster and identification of a transcript involved in biological rhythms. *Cell*, 38, 701–710.

Rimel, J.K. and Taatjes, D.J. (2018) The essential and multifunctional TFIIH complex. *Protein science : a publication of the Protein Society*, 27, 1018–1037.

Robles, M.S., Boyault, C., Knutti, D., Padmanabhan, K. and Weitz, C.J. (2010) Identification of RACK1 and protein kinase Calpha as integral components of the mammalian circadian clock. *Science (New York, N.Y.)*, 327, 463–466.

Roche, C.M., Loros, J.J., McCluskey, K. and Glass, N.L. (2014) Neurospora crassa. looking back and looking forward at a model microbe. *Am J Bot*, 101, 2022–2035.

Rodriguez-Molina, J.B., Tseng, S.C., Simonett, S.P., Taunton, J. and Ansari, A.Z. (2016) Engineered Covalent Inactivation of TFIIH-Kinase Reveals an Elongation Checkpoint and Results in Widespread mRNA Stabilization. *Molecular cell*, 63, 433–444.

Roenneberg, T. and Merrow, M. (2016) The Circadian Clock and Human Health. *Current biology : CB*, 26, R432-43.

Ruger-Herreros, C., Gil-Sanchez Mdel, M., Sancar, G., Brunner, M. and Corrochano, L.M. (2014) Alteration of light-dependent gene regulation by the absence of the RCO-1/RCM-1 repressor complex in the fungus Neurospora crassa. *PloS one*, 9, e95069.

Ryan, F.J., Beadle, G.W. and Tatum, E.L. (1943) THE TUBE METHOD OF MEASURING THE GROWTH RATE OF NEUROSPORA. *American Journal of Botany*, 30, 784–799.

Salomon, M., Christie, J.M., Knieb, E., Lempert, U. and Briggs, W.R. (2000) Photochemical and mutational analysis of the FMN-binding domains of the plant blue light receptor, phototropin. *Biochemistry*, 39, 9401–9410.

Sancar, C., Sancar, G., Ha, N., Cesbron, F. and Brunner, M. (2015) Dawn- and dusk-phased circadian transcription rhythms coordinate anabolic and catabolic functions in Neurospora. *BMC biology*, 13, 17.

Sancar, G. and Brunner, M. (2014) Circadian clocks and energy metabolism. *Cellular and molecular life sciences : CMLS*, 71, 2667–2680.

Sancar, G., Sancar, C., Brunner, M. and Schafmeier, T. (2009) Activity of the circadian transcription factor White Collar Complex is modulated by phosphorylation of SP-motifs. *FEBS letters*, 583, 1833–1840.

Sargent, M.L. and Kaltenborn, S.H. (1972) Effects of medium composition and carbon dioxide on circadian conidiation in neurospora. *Plant physiology*, 50, 171–175.

Schafmeier, T., Diernfellner, A., Schafer, A., Dintsis, O., Neiss, A. and Brunner, M. (2008) Circadian activity and abundance rhythms of the Neurospora clock transcription factor WCC associated with rapid nucleo-cytoplasmic shuttling. *Genes & development*, 22, 3397–3402.

Schafmeier, T. and Diernfellner, A.C. (2011) Light input and processing in the circadian clock of Neurospora. *FEBS letters*, 585, 1467–1473.

Schafmeier, T., Haase, A., Kaldi, K., Scholz, J., Fuchs, M. and Brunner, M. (2005) Transcriptional feedback of Neurospora circadian clock gene by phosphorylation-dependent inactivation of its transcription factor. *Cell*, 122, 235–246.

Schilbach, S., Hantsche, M., Tegunov, D., Dienemann, C., Wigge, C., Urlaub, H. and Cramer, P. (2017) Structures of transcription pre-initiation complex with TFIIH and Mediator. *Nature*, 551, 204–209.

Schwerdtfeger, C. and Linden, H. (2000) Localization and light-dependent phosphorylation of white collar 1 and 2, the two central components of blue light signaling in Neurospora crassa. *European journal of biochemistry*, 267, 414–422.

Schwerdtfeger, C. and Linden, H. (2003) VIVID is a flavoprotein and serves as a fungal blue light photoreceptor for photoadaptation. *The EMBO journal*, 22, 4846–4855.

Shandilya, J. and Roberts, S.G. (2012) The transcription cycle in eukaryotes. from productive initiation to RNA polymerase II recycling. *Biochimica et biophysica acta*, 1819, 391–400.

Shim, H.S., Kim, H., Lee, J., Son, G.H., Cho, S., Oh, T.H., Kang, S.H., Seen, D.S., Lee, K.H. and Kim, K. (2007) Rapid activation of CLOCK by Ca2+-dependent protein kinase C mediates resetting of the mammalian circadian clock. *EMBO reports*, 8, 366–371.

Smith, K.M., Sancar, G., Dekhang, R., Sullivan, C.M., Li, S., Tag, A.G., Sancar, C., Bredeweg, E.L., Priest, H.D., McCormick, R.F., Thomas, T.L., Carrington, J.C., Stajich, J.E., Bell-Pedersen, D., Brunner, M. and Freitag, M. (2010) Transcription factors in light and circadian clock signaling networks revealed by genomewide mapping of direct targets for neurospora white collar complex. *Eukaryotic cell*, 9, 1549–1556.

Spengler, M.L., Kuropatwinski, K.K., Schumer, M. and Antoch, M.P. (2009) A serine cluster mediates BMAL1-dependent CLOCK phosphorylation and degradation. *Cell cycle (Georgetown, Tex.)*, 8, 4138–4146.

Stechmann, A. and Cavalier-Smith, T. (2003) Phylogenetic analysis of eukaryotes using heat-shock protein Hsp90. *Journal of molecular evolution*, 57, 408–419.

Swartz, T.E., Corchnoy, S.B., Christie, J.M., Lewis, J.W., Szundi, I., Briggs, W.R. and Bogomolni, R.A. (2001) The photocycle of a flavin-binding domain of the blue light photoreceptor phototropin. *The Journal of biological chemistry*, 276, 36493–36500.

Talora, C., Franchi, L., Linden, H., Ballario, P. and Macino, G. (1999) Role of a white collar-1-white collar-2 complex in blue-light signal transduction. *The EMBO journal*, 18, 4961–4968.

Tamaru, T., Hirayama, J., Isojima, Y., Nagai, K., Norioka, S., Takamatsu, K. and Sassone-Corsi, P. (2009) CK2alpha phosphorylates BMAL1 to regulate the mammalian clock. *Nature structural & molecular biology*, 16, 446–448.

Tang, C.T., Li, S., Long, C., Cha, J., Huang, G., Li, L., Chen, S. and Liu, Y. (2009) Setting the pace of the Neurospora circadian clock by multiple independent FRQ phosphorylation events. *Proceedings of the National Academy of Sciences of the United States of America*, 106, 10722–10727.

Tansey, W.P. (2001) Transcriptional activation. risky business. *Genes & development*, 15, 1045–1050.

Tataroglu, O., Lauinger, L., Sancar, G., Jakob, K., Brunner, M. and Diernfellner, A.C. (2012) Glycogen synthase kinase is a regulator of the circadian clock of Neurospora crassa. *The Journal of biological chemistry*, 287, 36936–36943.

Tischkau, S.A., Mitchell, J.W., Pace, L.A., Barnes, J.W., Barnes, J.A. and Gillette, M.U. (2004) Protein kinase G type II is required for night-to-day progression of the mammalian circadian clock. *Neuron*, 43, 539–549.

Vitaterna, M.H., King, D.P., Chang, A.M., Kornhauser, J.M., Lowrey, P.L., McDonald, J.D., Dove, W.F., Pinto, L.H., Turek, F.W. and Takahashi, J.S. (1994) Mutagenesis and mapping of a mouse gene, Clock, essential for circadian behavior. *Science (New York, N.Y.)*, 264, 719–725.

Vogel, H.J. (1956) A convenient growth medium for Neurospora (Medium N). *Microbial Genet. Bull.*, 42–43.

Wang, B., Kettenbach, A.N., Gerber, S.A., Loros, J.J. and Dunlap, J.C. (2014) Neurospora WC-1 recruits SWI/SNF to remodel frequency and initiate a circadian cycle. *PLoS genetics*, 10, e1004599.

Wang, B., Kettenbach, A.N., Zhou, X., Loros, J.J. and Dunlap, J.C. (2019) The Phospho-Code Determining Circadian Feedback Loop Closure and Output in Neurospora. *Molecular cell*, 74, 771-784.e3.

Wang, B., Zhou, X., Loros, J.J. and Dunlap, J.C. (2015) Alternative Use of DNA Binding Domains by the Neurospora White Collar Complex Dictates Circadian Regulation and Light Responses. *Molecular and cellular biology*, 36, 781–793.

Westergaard, M. and Mitchell, H.K. (1947) Neurospora. V. A synthetic medium favoring sexual reproduction. *Am. J. Bot.*, 573–577.

Xue, Z., Ye, Q., Anson, S.R., Yang, J., Xiao, G., Kowbel, D., Glass, N.L., Crosthwaite, S.K. and Liu, Y. (2014) Transcriptional interference by antisense RNA is required for circadian clock function. *Nature*, 514, 650–653.

Yoshitane, H., Takao, T., Satomi, Y., Du, N.H., Okano, T. and Fukada, Y. (2009) Roles of CLOCK phosphorylation in suppression of E-box-dependent transcription. *Molecular and cellular biology*, 29, 3675–3686.

Yu, W., Houl, J.H. and Hardin, P.E. (2011) NEMO kinase contributes to core period determination by slowing the pace of the Drosophila circadian oscillator. *Current biology : CB*, 21, 756–761.

Zoltowski, B.D., Schwerdtfeger, C., Widom, J., Loros, J.J., Bilwes, A.M., Dunlap, J.C. and Crane, B.R. (2007) Conformational switching in the fungal light sensor Vivid. *Science (New York, N.Y.)*, 316, 1054–1057.

Zoltowski, B.D., Vaccaro, B. and Crane, B.R. (2009) Mechanism-based tuning of a LOV domain photoreceptor. *Nat Chem Biol*, 5, 827–834.

Acknokwledgement / Danksagung

Michael Brunner
Thank you very much for this interesting and challenging project, for your supervision, inspiration, motivation and enormous support. Beyond science, I would like to thank you for so many great book, movie, recipe and restaurant tips.

The Brunner Lab
I would like to thank the whole team for immense support and making my PhD a great and memorable time. Thank you, Linda Lauinger and Julia Kaim, for your endless patience and answering, sharing experimental secrets, laughing and joking. Thanks to Michael Oehler, to the awesome Dani and Patrick, to Thomas, Sabine and Gabi for your support. Many thanks to Martina, the one and only tower of strength. Thank you, Anna Gatz for taking over and continuing the project. I wish you all the best both scientifically and beyond. Thank you, Axel, Erik, Geza, Francois, Bianca, Anton, Christoph P., Christoph S., Ibrahim, Carmen, Shu, Gencer, Cidgdem, Amit, Fidel, Nati, Merve, Kawira, Justus.

Irmi Sinning und Walter Nickel
Thank you very much for your continuous support and advice in my TAC meetings.

Mass spectrometry facilitiy of the ZMBH and of the BZH
I would like to thank Thomas Ruppert, Sabine Merker and all the others from the ZMBH MS facility and Johannes Lechner, Jürgen Reichert and Petra Ihrig from the BZH for their help and strong support.

HBIGS Graduate School
Many thanks to everyone from the HBIGS Graduate School team for offering a great program and for your support.

Lehre des BZH
Vielen lieben Dank an Cordula, Evelin, Alex, Gabi, Petra und alle anderen für so viele gute Erfahrungen und dafür, dass ich so viel bei euch lernen durfte.

Andrea Molt
Ohne dich hätte ich diese Arbeit nicht machen können. Du hast mir viel Motivation und Zuversicht gegeben.

FH IZI
Vielen Dank an Kati, Gerno und alle lieben Kollegen, ihr wart direkt und indirekt eine große Unterstützung.

Familie und Freunde
Vielen Dank für eure Unterstützung, eure Treue und euer grenzenloses Verständnis, ihr seid großartig. Selbstverständlich erwähne ich hier Mimi.

Meine lieben Eltern und mein Christian
Eure Bedeutung und Unterstützung für diese Arbeit und für mich ist nicht mit Worten zu fassen. Ihr seid mein größtes Glück.